THERMAL AND OPTICAL CHARACTERISTICS OF RADIATION INDUCED DEFECT CENTERS IN ALKALI HALIDE CRYSTALS (TLD-100)

Ph.D. Thesis

in

**Physics Engineering
University of Gaziantep**

**By
Ahmet Necmeddin YAZICI
October, 1996**

Approval of the Graduate School of Natural and Applied Science.

Prof.Dr.Mazhar ÜNSAL
Director

I certify that I have read this thesis and that in my opinion it is fully adequate, in scope and quality, as a dissertation for the degree of Doctor of Philosohy.

Assoc.Prof.Dr. Refik KAYALI
Chairman of the Department

We certify that We have read this thesis and that in our opinion it is fully adequate, in scope and quality, as a dissertation for the degree of Doctor of Philosophy.

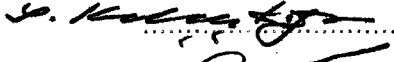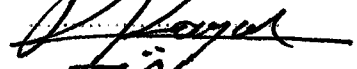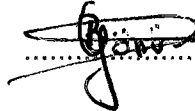Assist.Prof.Dr.Zihni ÖZTÜRK
Supervisor

Examining Committee in Charge

Prof.Dr.Selami KILINÇKAYA

Prof.Dr.Sadettin ÖZYAZICI

Assoc.Prof.Dr Refik KAYALI

Assist.Prof.Dr.Zihni ÖZTÜRK

Assist.Prof.Dr.Beşire GÖNÜL

Abstract

Thermal and Optical Characteristics of Radiation Induced Defect Centers in Alkali Halide Crystals (TLD-100) ˇ

YAZICI Ahmet Necmeddin

Ph.D. in P.E., University of Gaziantep

Supervisor: Asst.Prof.Dr. Zihni Öztürk

October 1996, 168 Pages

The exact cause of sensitivity loss in TLD LiF:Mg,Ti has not been completely understood yet. If a used TLD is not annealed at an elevated temperature prior to reuse, residual deep defect centers still present in dosimeter. These centers will interact with new incoming radiations and produce further centers. This will introduce significant errors in low dose measurements. If the structure, thermal and optical characteristics of these defects were better understood, then a better model could be proposed to overcome sensitivity loss.

Therefore, the samples were, firstly, irradiated by β-rays to produce sufficient concentration of defect centers, then optical absorption, phototransferred thermoluminescence, and thermoluminescence measurements were made to identify defect structures in LiF:Mg,Ti with appropriate heat treatments. The changes in the optical absorption band and

glow peak areas were determined as a function of various heat treatments using a computerised deconvolution program. The similarities in the variation of curves of glow peak 5 and OA band at 310 nm suggest that they may be belong to the same traps, namely Mg-trimer/Ti complex. The lack of correspondence between peak 2 and 380 nm band indicates that peak 2 is not related to Mg-dipoles as previously suggested, but related to Ti-related/F-center complex.

Deconvolution analysis of OA and glow curves produced by annealing at and above 125 ^{0}C for long times before irradiation permits the identification of a new peak at 175 ^{0}C and OA band at 282 nm. Due to their similar thermal decaying properties, it is thought that they may be belong to the Z_2-type centers.

The effects of pre-irradiation annealing on the values of trapping parameters of LiF:Mg,Ti were determined as a function of durations at 125 ^{0}C by computerized glow curve analysis. The application of pre-annealing with different durations made significant changes on the activation energies of peaks 1 to 5, especially of peak 4. These variations are due to the interactions of defects with each other during heat treatments.

A new simple model was developed to describe TL emission bands of luminescent centers in solids. TL emission spectra measurements of LiF:Mg.Ti showed one main emission band at 420 nm. The individual emission bands were separated using the developed model to investigate the success of the developed model. According to this model, the emission spectrum of whole glow peaks can be successfully fitted with two emission bands.

Keywords: Alkali halide, LiF:Mg,Ti, thermoluminescence, optical absorbance, emission spectra, trapping parameters.

Özet

Işınlanmış Alkali Halide Kristallerindeki (TLD-100) Hata Merkezlerinin Isısal ve Optiksel Karakteristikleri

YAZICI Ahmet Necmeddin

Ph.D. F.M. Gaziantep Üniversitesi

Tez Yöneticisi: Y.Doç.Dr.Zihni Öztürk

Ekim 1996, 168 sayfa

LiF:Mg,Ti termolüminesans dosimetresinde meydana gelen hassaslık kayıbının gerçek nedeni henüz tam olarak anlaşılamamıştır. Kullanılmış bir termolüminesans dosimetre eğer yeniden kullanma öncesi yüksek bir sıcaklıkta tavlanmazsa, dosimetrede hala derin hata merkezleri kalır. Bu merkezlerin ortamdaki radyasyon ile etkileşmesi malzeme içinde ilave merkezler oluşturmaktadır. Buda düşük dozlu radyasyon ölçümlerinde önemli hatalara neden olmaktadır. Eğer bu hataların yapısı, ısısal ve optiksel özellikleri iyi anlaşılırsa, hassaslık kayıbını gidermek için daha iyi bir model önerilebilir.

Bu nedenle yeterli yoğunlukta hata merkezleri oluşturmak için nümuneler önce beta ışınlamasına tabii tutuldular, sonra LiF:Mg,Ti'deki hataların yapılarını belirlemek için uygun ısısal işlemler altında optiksel soğurma, fototransfer termolüminesans ve termolüminesans ölçümleri yapıldı. Değişik ısısal işlemlerin bir fonksiyonu olarak optiksel soğurma bandlarındaki ve ışıldama tepe alanlarındaki değişimler bir bilğisayar proğramı kullanılarak hesaplandı. 310 nm'deki optiksel soğurma bandı ve 5'inci ışıldama tepe alanı eğrilerinde gözlenen benzerlikler onların aynı tipte bir hata merkezi ile (Mg-

trimer/Ti kompleksi) ilişkili olduğunu göstermektedir. Tepe 2 ve 380 nm bandı arasındaki uyum eksikliği daha önceleri farzedildiği gibi tepe 2'nin Mg-dipolleri ile değil, Ti-ilişkili/F-merkezi kompleksi ile ilğili olabileceğini işaret etmektedir.

Işınlama öncesi 125 ^{0}C ve üstünde uzun süre tavlatılarak üretilen optiksel soğurma ve ışıldama eğrileri ayırma analizleri 175 ^{0}C yeni bir tepe ve 282 nm'de yeni bir band belirtmektedir. Isısal bozulma özellikleri arasındaki benzerlikler sebebiyle bu yeni tepe ve bandın Z_2 tipli merkeze ait olabileceğini göstermektedir.

Işınlamadan önce 125 ^{0}C'de tavlamanın LiF:Mg,Ti'nin tuzaklarının parametre değerleri üzerindeki etkisi tavlama süresinin bir fonksiyonu olarak ışıldama eğrilerinin bilğisayar analizi ile belirlendi. Işıldama öncesi farklı sürelerde tavlama 1'den 5'e kadar tüm tepelerin, özellikle tepe 4'ün aktivasyon enerjileri üzerinde önemli değişiklikler meydana getirmektedir. Bu değişiklikler ısısal işlemler boyunca hata merkezlerinin birbirleri ile etkileşmeleri sonucu olmaktadır.

Katılardaki lüminesans merkezlerinin TL yayma bandlarını tanımlamak için yeni bir model geliştirildi. LiF:Mg,Ti'nin TL yayma ölçümleri 420 nm'de bir ana yayma bandı göstermektedir. Geliştirilen modelin başarısını görmek için bireysel yayma bandları geliştirilen modele uygulandı. Bu modele göre, tüm ışıldama tepelerinin yayma spektrumları iki yayma bandı ile başarılı bir şekilde ayrılabilmektedir.

Anahtar Kelimeler: Alkali Halide, LiF:Mg,Ti, termolüminesans, optiksel soğurma, yayma spektrası, tuzak parametreleri.

Acknowledgements

I would like to express my sincerest gratitude and thanks to my supervisor Assis.Prof.Dr. Zihni Ozturk for his guidance, suggestion, valuable criticism and the great help in the preparation of this study.

I would like to thank my gratitude to the research assistantes and other personnel of Department of Engineering Physics for their kind help and friendships.

I would like to extend my thanks and appreciation to my wife, girls, mother, father and brothers whose patience, love and continual encouragement were essential ingredients to complete this lengthy and time consuming work.

I am very grateful to the Resarch Fund of Gaziantep University for financial support to my work.

Table of Contents

List of Tables

List of Figures

List of Symbols

a : quantity of absorbance

A : transition coefficient for electrons in the conduction band

A_h: transition coefficient for holes in the valance band

A_r: recombination transition coefficient for electrons in the conduction band

α : probability of recombination

α_a : absorption coefficient

b : order of kinetic

β : heating rate

β_p : probability trapping

C_1: constant

d : lattice constant

D : concentration of thermally stable deep trap

E : activation energy (trap depth)

E_e: energy difference between ground and excited states

E_f: emitted photon energy

E_m: vibration excitation energy

E_0: photon energy at the band maximum

f : electron hole generation rate

f_s : oscillator strength

I: thermoluminescence intensity

$I(E)$: emission intensity at energy E

$I(E_0)$: emission intensity at the band maximum

k : Boltzmann's constant

k_e: force constant in the excited states

k_g: force constants in the ground states

λ : wavelength

m :slope

ν : frequency

n : concentration of electrons in the traps

n_c: concentration of electons in the conduction band

n_h: concentration holes in the recombination centers

n_i : index of refraction

n_v: concentration of holes in the valance band

n_0: initial concentration of trapped electrons

N : concentration of available electron traps

N_h: concentration of available hole centers

p : probability per unit time of the relase of an electron from the trap

p_1: probability of stimulation of an electron into the conduction band from deep traps

Q : configuration coordinate distance

R: concentration of holes in the recombination centers

δ : high temperature half width

s : frequecy factor or pre-exponential factor

S : Huang-Rhys factor

t : unit time

T : temperature

T_m: peak temperature

T_0: room temperature

τ : low temperature half width

τ_e :lifetime of an electron in the trap

U_e:potential energy of excited states

U_g:potential energy of ground states

X : ptical path length

w=effective vibrational frequency (s^{-1})

ω=full width at half maximum (^0C)

W=full width at half maximum (eV)

CHAPTER 1

Literature Survey

1.1 Introduction

Today LiF is one of the most important thermoluminescence material which is used for radiation dosimetry. Because of its approximately tissue equivalent response LiF finds wide application in personel dosimetry and health physics. LiF is also one of the most important alkali halide crystals which gives a good thermoluminescence properties when doped with appropriate impurities. Application of thermoluminescence is found in scientific disciplines like dosimetry (for measuring irradiation dose), archaeology (for dating ancient pottery using the accumulation of background dose in thermoluminescence within the clay which the pottery is made of) and solid state research as a tool to investigate defect structures and some trap and recombination center parameters in insulator and semiconductor.

If a used thermoluminescent dosimeter (TLD) is not annealed at an elevated temperature prior to reuse, there will be residual deep defect centers still present in the dosimeter. These defect centers could make a significant contribution to the TL response after subsequent exposure. This could introduce a significant error in low dose measurements such as required for environmental monitoring around nuclear power plants. The exact cause of

the loss of sensitivity of dosimeter is not yet understood. If the defect model of radiation induced defects, their optical and thermal properties, process leading to thermal luminescence were better understood, then it could propose a better process for used dosimeters to maintain their sensitivity.

1.2 Literature Survey

LiF was found by Daniel and co-workers to be a particularly good material for use in radiation dosimetry due to its high sensitivity [1]. However, a commercial dosimeter has been manufactured over the forthy years by Harshaw Chemical Co. [2] and about last ten years by Teledyne Isotopes. Harshaw developed this material (the special name TLD-100) after their earlier LiF crystals (manufactured before 1955) had been studied for their application to dosimetry [3]. Both kinds of Harshaw LiF contain Mg concentration of the order of 200 ppm, in addition to other metallic impurities.

Many investigations have been done to understand the structure of certain defects present in the TLD-100 responsible for the complex behaviour of the thermoluminescence glow curve of this material and to explain the behaviour of the glow peaks as a function of thermal annealing treatments, different dose levels, read-out, cooling, and heating rates. In these studies, optical absorption, dielectric loss, ionic conductivity, electron spin resonance, and TL emission methods have been employed in order to understand the nature of centers in this material [4]. Despite of an overwhelming amount of data on this subject, a satisfactory description is still lacking.

The first attempt at correlating thermoluminescence glow peaks to specific crystals defects in LiF:Mg,Ti was made by Grant and Cameron (1966)[5]. They measured the thermoluminescence emitted by LiF containing approximately 100 ppm of Mg^{+2} as a function of pre-irradiation anneal time at 67, 81 and 95 ^0C after a quench from 400 ^0C, 1 hour anneal and rapid cool.

2

They used dielectric loss method for measuring dipole concentrations and TL measurements and found that at a storage temperature of 67 ^{0}C, the Mg^{+2}-positive ion vacancy distributed in the lattice decays at the same rate of peak 2 height. Following this close similarity between the two decay curves, they suggested that Mg^{+2}-V_c^- dipole pairs were the traps responsible for peak 2. Although, Dryden and Shutter (1973) [6] used the same method to confirm the relation between Mg^{+2}-V_c^- dipole concentration and the intensity of peak 2, they concluded that the intensity of peak 2 is not proportional to the dipole concentration. In some cases at higher pre-irradiation annealing temperature the height of peak 2 actually increases while the dipole concentration decreases. At low annealing temperature the peak 2 is proportional to dipole concentration during the earlier part of the decay curve. On the other hand, they pointed out that the dipoles and trimers both contributed to the heights of peaks 4 and 5, but aggregates containing more than three Mg^{+2}-V_c^- pair made no contribution to the height of these peaks and there was a competition between traps, particularly between the traps responsible for peaks 2 and 5.

A further was study made in order to observe the effect of cooling rate and the Mg^{+2}-V_c^- associated pair concentration on the height of peaks by Bradbury et al. (1976a,b-1977) [7-10]. They showed that (i) peaks 2 and 3 increase at low and high cooling rates and have a minimum at about 2 ^{0}C/min and at the high quench rate peaks 2 and 3 appear to level off and become constant, (ii) peak 4 exhibits a broad maximum at a cooling rate of 100 ^{0}C/min and at lower cooling rates (<100 ^{0}C/min) peaks 4 and 5 drop rather sharply, (iii) the dipole concentration coincides with the peak 2 curve in the intermediate cooling rate region but there is a large difference at low and high cooling rates. Additionally, Barsis et al. (1967) [11] showed that if crystals were held above 210 ^{0}C for several hours, the response of glow peaks had no revealed effect but below this temperature precipitates do occur, thus the thermoluminescence response strongly reduces.

These works illustrate that by annealing the LiF crystals at or above the solubility limit of the precipitate phase (250 ^{0}C) the Mg^{+2} ions are all in solid solution; but below this temperature due to the columbic interactions, there is a tendency for the Mg^{+2} ions and cation vacancies to form pairs (dipoles) which can then cluster to form dimers, trimers and precipitate phase (Suziki phase) ($6LiF.MgF_2$) and also with increasing temperature the clusters partially dissociate, i.e., precipitate $\Leftrightarrow$ trimers $\Leftrightarrow$ pairs $\Leftrightarrow$ free Mg^{+2} ions and free cation vacancies, whereas on cooling the reverse direction is predicted. Thus different temperatures should lead to different cluster concentrations. These ideas are also supported by the work of Rao (1974) [12]. However, recently Gavartin et al. (1991) [13] showed that the aggregation of impurity-vacancy dipoles can lead to formation of a phase with a periodic structure differing from the traditional Suziki phase. They have shown that the formation of tetramers was taken place after the formation of trimers.

Heat treatments were studied in further detail by Taylor and Lilley (1982) [14-16]. Some of the important features of these measurements can be seen that association of TL peak 2 with Mg^{+2}-V_c^- pairs and peak 5 with (Mg^{+2}-V_c^-)$_3$ trimers is unacceptable. They have proposed a new model in which some impurity other than Mg^{+2} is the peak 2 trap. They suggested that Ti^{+4} associated with cation vacancies, or OH^-,or O_2^- ions or with a combination of vacancies, OH^- and O_2^- ions represented by Ti^*, is the peak 2 trap and that the peak 5 trap is a combination of (Mg^{+2}-V_c^-) pairs and the peak 2 trap which they labelled as $Ti^*(Mg^{+2}$-$V_c^-)_n$. This suggestion, however, is not favoured by a detail work on LiF:Ti crystals (Mieke and Nink 1980) [17]. They have shown that LiF:Ti exhibits just two glow peaks, both of which exhibit completely different behaviour from peak 2 in TLD-100.

Additionally, the results of Taylor and Lilley have been criticised by some other authors in the latter years using emission spectra, x-ray luminescence and photoluminescence measurement methods. In addition to the glow curves, if an emission spectrum (TL intensity versus wavelength) is

4

also recorded, then the nature and characteristics of luminescent centers and some trapping centers can also be understood. The emission spectrum of nominally pure LiF exhibits a main emission band at ≈415 nm for all the glow peaks up to ≈525 K when irradiated at room temperature (Sagastibelza and Alverez Rivas 1981) [18]. The 415 nm emission is in the same spectral range as that observed for other alkali halides that this emission may be resulted from interstitial-vacancy recombination. They also suggested that the complex emission in LiF is dependent upon background impurities. The perturbation in the emission is suggested in LiF with divalent doped impurities. However, Miller and Bube (1970) [19] observed that the F-center is not directly involved in the production of the visible luminescence emission, either under x-ray irradiation or during TSL.

The main emission spectrum for TLD-100 has been reported by several authors. Harris and Jackson (1970) [20] found that the spectrum varied markedly with temperature and also the peak emission energy varied with temperature. The variation of peak emission with temperature is the sum of the variation of at least two and probably three peaks at approximately 3.2, 3.0, and 2.5 eV at room temperature by means of a series of Gaussian curves. At low temperatures the emission spectrum 2.5 eV and at high temperatures the emission spectrum 3.1 eV are dominant. Podgorsok et al. (1971) [21] measured the emission spectra of dosimetry peaks 1-5, which showed only one maximum (at 400 nm) in the range from 190 to 510 nm. For very high irradiation doses of 10^6 Gy and irradiations performed with particles of high ionising density, Jain et al. (1973) [22] recorded a more complex spectrum near 540 and 640 nm. Following Crittenden et al. (1974) [23], Ti impurity ions influence both the 420 nm and 650 nm emission bands. They recorded that the emission at 300 nm is characteristic of both pure and doped LiF and is only affected below 100 ^{0}C. They pointed out that the glow peaks 1 and 6 behave differently from those associated with Mg impurities and they may be intrinsic defects. At low temperatures (<200 ^{0}K), Cooke and colleagues (1978-1981) [24-25] suggested that shallow trapped electrons may recombine

5

directly with V_k centers and produce emission in the UV ($\approx$270 nm). At approximately 150 K, the V_k centers may be thermally annealed and produce emission near 400 nm by direct recombination at an activator F-center complex. It is also shown that it is possible to produce both UV and visible emission over this limited temperature range solely by the release of electrons. These results are confirmed by detail spectral measurements of Fairchild et al. (1978) [26] and Townsend et al. (1983) [27]. Fairchild et al. measured the emission spectrum of TLD-100 as a function of sample temperature and found out that below 10^3 Gy the thermoluminescence emission can be described by a single Gaussian shaped band whose peak energy and full width vary irregularly with temperature. Townsend et al. also performed emission spectra measurements on the TLD-100. They arrived to a conclusion that the dominant emission was related to large defect complex associated with Ti. They observed a gradual shift in the emission maximum to lower wavelengths with increasing peak temperature. They also noted that emission in LiF:Ti occurs as a result of interstitial-vacancy recombinations, whereas in LiF:Mg,Ti; Mg forms defect complexes which include Ti and thus perturb the emission, depending on the exact form of the Mg within the lattice. Additionally, on the basis of x-ray induced luminescence, TL spectral emission measurements and photoluminescence measurements, in unannealed and annealed LiF:Mg,Ti and also in Mg free LiF:Ti samples, McKeever (1984) [28], Yuan and McKeever (1988) [29] come to conclusion that a Mg dipole/Ti complex is responsible for TL peak 2 and a Mg-trimer/Ti complex is involved in the production of TL peak 5. However, recently, Jain (1986-1987) [30-31] challenged these assertions and presented data on the peaks below room temperature which he took to be evidence that the TL peaks above room temperature (peak 2) can not in fact be caused by Mg^{+2}-V_c^- /Ti complexes. According to his results, up to about 150 K, three emission bands at $\approx$250, $\approx$305 and $\approx$420 nm were observed. The 250 nm band then gradually disappeared and the 420 nm band gained in prominence. At temperatures above 200 K, the emission spectrum contained only the 420 nm band. Kos and Nink (1980) [32] also pointed out that natural defects such

(Mg^{+2}-V_c^-) dipoles and Mg^{+2}-V_c^- trimers would not be expected from electrostatic considerations, to act as traps for electrons and holes. They suggested that the cation vacancies in the dipoles are converted during irradiation into anion vacancies. Thus the dipoles in the unirradiated LiF:Mg,Ti are converted to another type of centers (possibly Z-type centers) during irradiations.

The role and structure of Ti-impurity in the alkali halide crystals have been studied in detail over the thirty years [33]. It is found that Ti impurities influence the efficiency of luminescence in all crystals.

The first investigations on the role of Ti impurities in LiF crystals was done by Rossitter et al. (1971-1972) [34-35]. They found that the addition of Ti impurities increased the thermoluminescence near 200 ^{0}C and also the magnitude of the absorption near 200 nm. That is, the absorption band is directly related to the Ti content and to the luminescent output, indicating process as a photon emission center in this material. They also pointed out that the optimum value of Ti in LiF crystal is about 8 ppm. The case of Ti in LiF is particularly stimulating since it can enter the crystal either as trivalent or as tetravalent. Because Ti plays a key role in the thermoluminescence mechanism of LiF:Mg,Ti, hence a better knowledge of the lattice defects induced by Ti is also of technological interest. Ti^{3+} exhibits a $3d^1$ electron configuration, hence it can be monitored by means of ESR measurements and by crystal field optical spectra. Davies (1974) [36] using the electron spin resonance method found that Ti enters LiF lattice substantially for Li^+ in either the Ti^{+3} or Ti^{+4} state. He also suggested that some of Ti^{+4} ions in the lattice become Ti^{+3} after irradiation and revert to Ti^{+4} by 300 ^{0}C. He proposed two possible structures of the Ti-related centers: (i) [$Ti^{+3}F_6$] with the Ti^{+3} off-center or (ii) [$Ti^{+3}F_3^-O_3^-$], but he pointed out that latter is partially charge compensated and seems to be more likely. In the later years, Stobe et al. (1980) [37] used the electron spin resonance and ionic conductivity and Capelletti et al. (1991) [38] used ITC measurements, optical absorption spectra,

7

microspectrophotometry, photoluminescence spectra, optical and electron microscopy and x-ray diffraction to define the possible defect states of Ti in LiF. The ESR spectrum lines were found to be due to the specific equilibrium defect, Ti^{+3} and F center. They found a broad ESR line spectra due to Ti^{+3} in a precipate phase and there was no trace of Ti^{+2} ions in LiF. They suggested that Ti^{+3} defect was produced by absorbing an electron possibly from Ti^{+4}-related centers during irradiations. The possible defect structure proposed by Stobe et al. is that (i) before irradiation Ti^{+4} can be bound to three cation vacancies at near-neighbour positions $(Ti^{+4}\text{-}3V_c^-)$ or to three OH^- $(Ti^{+4}\text{-}3OH^-)$, or three O_2^- ions $(Ti^{+4}\text{-}3O_2^-)$, or to a combination of vacancies, O_2^- and OH^-, (ii) after irradiation the defect structure is $(Ti^{+3}F_3^-O_3^-)$. Additionally, Wintersgil et al. (1980) [39] pointed out the structure and the role of Ti-related centers in LiF by the electron spin resonance in the form of $(Ti^{+4}\text{-}3O_2^-)$. On the other hand, Watterich et al. (1983) [40], using a different measurement technique, found that in double doped LiF:Mg,Ti the Ti^{+3} ions appear to be in the aggregated form which gives rise to a broad absorption band at ≈ 660 nm and also at ≈ 137 nm band. They also observed two infrared bands at 3525 cm^{-1} and 3662 cm^{-1}. Finally, Vergara et al. (1991) [41] applied the optical absorption measurement technique to Ti doped LiF crystals to investigate the structure of Ti-related defects and observed that Ti^{+3} ions give rise to an absorption band at 5.65 eV in LiF:Ti while the Ti^{+4} ions are responsible for the absorption band at 6.2 eV, which is a result of charge transfer absorption. More recently He et al. (1994) [42] observed that the absorption band at 5.7 eV are due to Ti^{+3} ion and the 5.3 eV band is mostly likely a result of the formation of Ti^{+2} ion centers. Delgado and Delgado (1984) [43] investigated the photoluminescence properties of Ti-centers in the TLD-100 and suggested that the Ti-related 200 nm absorbing center is the recombination center associated with the dosimetric glow peak 5.

Another important impurity which is generally present in the alkali halides is the hydroxide ion (OH^-). OH^- ion impurities have been shown to

influence TL behaviour because they are involved in the luminescent recombination process.

Vora et al. (1975) [44] suggested that the OH$^-$ ions are present as a background impurities in TLD-100. They concluded that the 200 nm absorption band in MgF$_2$ and Li$_2$TiF$_6$ doped LiF crystals is caused by titanium-hydroxyl complexes and also OH$^-$ ions are involved in the recombination process. Further evidence for the formation of Ti-OH complexes comes from the ionic conductivity work of Jain and Sootha (1967) [45].

Wachter et al. (1980) [46] and Wachter (1982) [47] studied the influence of OH$^-$ ions on the thermoluminescence properties of LiF:Mg,Ti, the correlation between glow curve structure existence of certain TL peak and the OH$^-$ concentration. They found that, (i) to each Ti concentration an optimum Mg concentration at which the ratio of the main dosimetric peaks 4,5 to the low temperature peaks 2,3 show a maximum, (ii) a Ti related center (Ti alone or a Ti-O complex) acts as emission center, (iii) certain Ti-hydroxyl complexes Ti(OH$^-$)$_n$ can act as traps for a TL peak at 120 ^{0}C, (iv) if the hydroxyl content is raised the peaks 4 and 5 are reduced. (v) if OH$^-$ ions are bound to the Mg ions, the resulting complex is assumed to be inefficient as an electron trap.

During irradiation, OH$^-$ impurities decompose to substitutional oxygen ions, U centers and F centers. A similar behaviour was observed by Kamikawa (1975) [48] when hydroxyl ions which have nearly the same mass and atomic radii as F$^-$ ions were diffused into the LiF lattice by annealing in air at elevated temperature. The oxygen ion remains in the anion site previously occupied by the OH$^-$ ion, yielding Mg and Ti ion complexes containing oxygen ions and cation vacancies.

Recent investigation indicates that (Stobe et al. (1985) [49]) the Ti-OH$^-$ complexes act as the luminescent centers in TL grade LiF and Mg-OH$^-$ complexes act as competitors.

A different explanation for the situation of OH⁻ ions in LiF crystals was made by Watterich et al. (1980) [50]. They found two types of H^0 and one H^- center by ESR and vacuum UV absorption measurements in the X-ray irradiated LiF:Mg. They suggested that the band at ≈124 nm in a non-irradiated LiF:Mg may be due to OH⁻ impurities. After irradiation a band at 127.3 nm was identified as a H^- ion and also the band at ≈222 nm may be connected to the OH⁻ impurity, not a Z-type center as previously suggested. The X-ray irradiation probably breaks OH⁻ ions to the H^0 and H^- centers.

In order to describe the nature of trapping centers in LiF many models have been developed. The first model called as the dipole related model mentioned in the previous paragraphs is formed by Mg^{+2}-cation vacancies or dipoles plus Ti and/or OH⁻ impurities as trapping centers. The other model is the famous Z-center model.

The Z-centers are normally only formed in alkali halides, when doped with divalent cation impurities and followed by bleaching the irradiated crystal with F-band light [51-52]. In general, five types of Z-centers have been found in the alkali halides but still there is controversy about their individual structure. There are close relationship between Z-centers and thermoluminescence glow peaks in some alkali halides, which have been discussed in literature [53-55].

The Z-center model is based upon the identification of an optical absorption bands. The qualitative agreement between some bands in the absorption spectrum and the peaks in the thermoluminescence glow curve with suitable pre- and post-irradiation heat treatment has been used by some workers to understand the nature of defects. The optical and thermal bleaching behaviour of Mg impurity and TL related optical absorption bands in irradiated LiF:Mg,Ti have also been studied by a number of workers in order to explain the nature of the centers responsible for TL in this material.

The origin of the absorption bands in TLD-100 is still uncertain but some of them are well known to be related to Mg-impurity and some experimenters have suggested that they might be the Z-type centers.

The optical absorption spectrum of irradiated pure LiF shows a prominent peak at 5.0 eV, which is due to F-centers and F-aggregate M, R_1, and R_2 centers [56-57]. McLaughin et al. (1980) [58] measured the color centers formed by irradiation of pure LiF in the dose range from 10^2 to 10^7 Gy. The irradiation of relatively pure LiF induces discrete optical absorption bands representing a series of color due to the filling of anionic lattice vacancies by electrons and it can be shown that the wavelengths of absorption maxima are F,247; F,620; M,443; R_1,315; R_2,374; N_1,517 and N_2,547 nm.

The strength of the absorption band at 5.5 eV in the Mg doped samples was studied by Mort (1965) [59-60], who found that this band is enhanced by quenching the crystals prior to irradiation. It was concluded that this absorption arises from a trapped electron center of the Z_3 type for which there is a number of models.

Christy et al. (1967) [61] and Klick et al. (1967) [62] measured a variety of optical absorption bands in the 300-400 nm region into two peaks centered on 380 nm (3.26 eV) and 310 nm (4.0 eV) in the commercial LiF:Mg and all of them concluded that they are hole traps associated with the glow peaks. Clafy (1967) [63] found that pre-irradiation quenching of the crystal after heating to 400 ^{0}C enhanced the 380 nm absorption band. Slow cooling before irradiation enhanced the 310 nm band, and bleaching with F-band light preferentially destroyed a band at 340 nm. A correlation was established between the 210 ^{0}C TL peak and the 340 nm band, the 285 ^{0}C TL peak and the 310 nm band. However, Christy et al. suggested that the bands 380 nm and 310 nm are associated with the 115 ^{0}C and 210 ^{0}C glow peaks, respectively. On the contrary the results of Mort, Klick et al. suggested that the 220 nm band arises from Mg^{+2}-vacancy complexes which have captured two holes.

Further evidence to the result of Christy et al. has been made by Harris and Jackson (1970) [20]. They observed the changes in the optical absorption and TL as a function of various pre and post-irradiation heat treatments and found an apparent correlation between the decay of TL peaks 2 and 3 and the absorption band at 380 nm, and between peaks 4 and 5 and the band at 310 nm. On the other hand, Crittenden et al. (1974) [64] made a detail analysis of optical absorption using thermal annealing and optical bleaching and declared that there are at least seven optical absorption bands in the near ultraviolet spectrum between 200 and 400 nm. The presence of a new band at 280 nm in addition to previous results is linked to Mg and changes in this band are related to the changes in peak 4 and 5 of the glow curve.

The earlier trap structure has been suggested to be due to the hole traps. However, in a series of papers about the trapping mechanism of LiF, Mayhung et al. (1970a,b,c -1972) [65-68] suggested that the 380 and 310 nm band are probably due to trapped electrons. In particular, the traps for 4 and 5 centers may be anion vacancies altered by nearly Mg-related defects. Additionally, they also studied the optical absorption bands over the wavelength range 105-750 nm and showed that an optical absorption band was produced at 113 nm in both pure and Mg-doped LiF and at 137 nm in Mg-doped LiF by irradiation with the x-rays at room temperature. This band at 113 nm is identified as the V_3 band. The TL process intimately involves V_3 centers.

Another investigation on the optical absorption of LiF crystals between 450 nm to 180 nm at room temperature after the irradiation followed by various thermal treatments was done by Nink and Kos (1976) [69-71]. They suggested that there are close correlations between the 310 nm and 225 nm absorption bands based on Z-centers. They developed a simple model for the trapping process in LiF:Mg,Ti. The Z_2 center turns out to be the electron trap responsible for the main glow peak 5 which is produced by irradiation via Z_0

and Z_3 centers in a two step process. Additionally, they reported another absorption peak at 280 nm which is said to be due to Z_1 centers [72]. In their another paper (1977) [73] the principal role of F-centers in LiF:Mg,Ti is discussed and it is thought that F-centers act as electron source for refilling of empty shallow traps. But during F-band bleaching they may also form additionally Z_1 and Z_2 centers. Further evidences to the results of Nink and Kos come from the studies of Rao (1980) [74] and Battaglia et al. (1982) [75]. A glow peak at 250 ^{0}C (peak 6) is then identified with the thermal annealing of Z_3 (5.5 eV) centers [76-77]. But the main flaw in the identification of the Z_3 (225 nm) band with a TL peak in LiF at peak 6 is that the Z_3 band is quite stable even after peak 6 or 7 is removed by 300 ^{0}C post-irradiation annealing. The only TL peak which correlates with the Z_3 band is peak 10 ($\approx$400 ^{0}C) [78-81]. In another investigation on optical absorption, phototransfer thermoluminescence (PTTL) and TL measurements are performed on LiF:Mg,Ti after γ-irradiation and thermal annealing in order to explain radiation induced sensitization and a model was proposed by Jain et al. (1974) [82] in which a complex center TCLC breaks upon irradiation into traps centers (TC) and luminescent center (LC). The trap centers have been identified with the absorption bands at 220 nm and coplex centers TCLC at 137 nm, respectively.

Mehta et al. (1977) [83] extended the Z-center model to suggest that the 380 nm band is caused by a Z_2'-center (i.e., Z_2-center with an extra trapped electron). Peak 2 is then said to result from the thermal release of this additional electron (converting the center to a Z_2-center). An apparent relationship between the intensity of peak 2 and the concentration of Mg^{+2}-vacancy dipoles (e.g., Grant and Cameron, 1966 [5]) is explained by Kos and Nink (1980) [32] in terms of a dipole $\rightarrow$Z-center conversion mechanism during irradiations.

By using dichroism method, the authors Jen and Merklin (1978) [84] reported the effect of bleaching on the irradiated LiF:Mg,Ti with polarized light

at 313 nm and they proposed a different center model in which a defect center is an interstitial magnesium ion in a next-nearest neighbour site adjacent to a negative ion vacancy with two electrons [85].

However, recently, strong criticism of the Z-center model has been accumulated. Moharil (1980) [86] pointed out that the Z-centers can be obtained only under specific conditions. In as-irradiated crystals only F-centers and a small number of Z_1-centers can be present [87-88]. If the previously Z-center model is correct, then Mg doped LiF has some peculiar properties from other alkali halides [89-90]. The all optical absorption bands in LiF:Mg,Ti grow linearly and then sublinearly with dose in the dose range 0 to 10^3 Gy. In the terminology the Z_2-center is formed by a two-hit process (capture of two electrons) and the Z_3 is formed by a one-hit process (capture of one electron). But in the glow curve peaks 5 and 6 grow supralinearily. Thus Horowitz (1982) [91] raised very serious doubts as to the validity of Z-center model.

It should also be mentioned that the peak at 5.5 eV has never conclusively been proved to be related to Z_3-centers. The identification of this absorption band with these defects was made by Mort (1966) who suggested an empirical Mollwo-Ivey relationship between the Z_3-centers in alkali halides. According to the empirical Mollwo-Ivey relationship, the energy positions of the Z_3 and Z_2 bands are calculated to be 5.5 eV and 4.4 eV respectively [92-93]. Watterich et al. (1984) [94], Nepomnyashchikh et al. (1980) [95], Radyabov et al. (1981) [96-97], Landreth and McKeever (1985) [98], Caldas et al. (1983) [99], McKeever (1990) [100], Kathuria et al. (1985) [101], however, pointed out the dangers of this assignment. Watterich et al. point out that the existence of a Mollwo-Ivey type relationship alone does not seem to be satisfactory in a center identification, especially not in those cases when the crystal is uncontrolled for impurities like OH⁻ or Ti which seems to be very effective in many respects, even in a very low concentration. They suggested that the centers peaking at 5.5 eV seem to recombine simply with the H⁻ ions

14

during X-ray irradiation. Nepomnyachikh and Radyabov suggested that the 225 nm band is caused by a Mg atom at anion site associated with cation vacancies, whilst Radyabov and Nepomnyachikh assert that centers at 310 nm are Mg^+-cation vacancy-anion vacancy centers (Mg^+-V_a^+-V_c^-).

On the other hand, Kathuria et al. (1985) [101] investigated the role of the impurities (Mg, Ti, Mn, Al) on the glow curves,absorption spectra and TL emission spectra of the laboratory grown crystals. They found that all the impurity doped crystals showed three absorption bands at 245, 310 and 375 nm after 400 ^0C annealing. Another absorption band at 222 nm is observed in all the impurity doped crystals after 350 ^0C, 15 min thermal annealing. Their results show that these bands are not only produced when the crystal doped with Mg and Ti impurities, they also produced when the crystal doped with other impurities. Therefore, they suggested that cation vacancies V_c^- in the crystal lattice perturbed by the impurities provide the trapping center for holes which are responsible for various glow peaks in lithium flouride. F-center act as the luminescent center.

The main ideas in the identification of the Z_2-center were its conversion by thermal and photo-ionization to the Z_3-center. McKeever (1990) suggested that the expected reconversion of Z_3-centers to Z_2-centers by repeated X-ray irradiation does not occur.

However,a modified Z-center model is proposed by Lakshmanan and colleagues (1980a,b,-1982a,b-1983) [102-106], in which Z_2 and Z_3 centers correspond to TL peaks 7 (260 ^0C) and 10 (400 ^0C) respectively. More recently, Lakshmanan (1993,1994) [107-108] confirm, their previous ideas . They studied the optical absorption and TL of LiF:Mg,Ti single crystals as a function of irradiation temperature and they suggested that the optical absorption of peak 7 centers occurs at 250 nm or two different centers; (i) one centers giving rise to peak 7 and (ii) isolated F centers not related to any of the

TL peaks above room temperature give rise to optical absorption at the same or two position close to 250 nm.

Finally, He (1994) [109] proposed a trap structure for 4.0 eV band which is most likely due to Mg^{+1}-vacancy complex centers while the absorption band between 5.0 and 6.0 eV is probably due to Ti related bands in addition to the possible Mg^{+2} ion related Z_3-centers.

A radically different trap structure model was proposed by Alveraz Rivas and co-workers (1981) [18,110-111]. According to this model (mobile interstitial model), the mobile entity is neither hole nor electron but instead of these entities the thermoluminescence process in many alkali halides irradiated at any temperature is related to the recombination of radiation induced lattice defects such as interstitial halogen atoms and vacancy centers. The attractive feature of the model is that it gives general explanation about TL in alkali halides (pure and doped). However, this model was critized by Moharil and Kathuria (1982,1984) [112-113]. They showed that although the TL glow curves are better described by this model, PTTL is not explained with this model.

The glow curves obtained after UV exposure (254 nm) of previously irradiated and partially annealed TLD-100 present some difference with respect to these induced by ionising radiation. Perhaps the most remarkable difference is the absence of glow peak 4 in the UV-induced glow curves. This fact noticed from the beginning of the work in this field was reported explicitly by several authors (Sunta and Wattanable, (1976) [114]) and interpreted as an indication that peak 4 is produced by a hole trap, so that, the release of electrons from deep traps by the action of the UV light will not refill trap 4 as occurs with electron-type traps. Nevertheless, Moharil and Kathuria (1985, 1988a,b) [115-117] in recent works on the TL and PTTL glow curves in TLD-100, reported that peak 4 can be found in the PTTL curves when this material is annealed for 23 h at 150 ^{0}C. This fact would question the whole character of

this peak, as it is difficult to assume that only by the action of these thermal treatments would change the nature of the trapped entity.

On the other hand, Delgado and colleagues (1987, 1988, 1992) [118-121] expressed some doubt about the correct identification of the peak produced by annealing for 23 h at 150 ^{0}C. These doubts were based on the relatively important difference in temperature between the peak produced by the heavy annealing. They also suggested that the 23 h, 150 ^{0}C treatment could produce not only a change in the relative intensities of peaks IV and V, but create a new glow peak different from the pre-existing one. It is caused by the creation of a new trap by modifications of normal peak V trap structure, due to impurity aggregation process, which are very active at the relatively high treatment temperature (150 ^{0}C). The new trap presents the same electron character as the original peak V and thus it is repopulated by the usual phototransfer techniques. At the same time, Delgado (1992) [120] observed that peak IV trap is certainly present in unirradiated sample, therefore, he suggested that it is an intrinsic trap.

When a specific lattice defect traps electrons, which are released on heating to give rise to a glow peak, the electrons may be described by a trapping depth below the conduction band E (activation energy), and a frequency factor s (pre-exponential factor). The trapping parameters of LiF TLD-100 have been investigated by a number of groups. There are many methods available for analyzing glow peaks; however, there are widely differing values of the trap parameters reported in literature. Published values of activation energy E, and the frequency factor s, for TLD-100 glow peaks and the methods used to obtain them, are summarized in Table 1.

Taylor and Lilley (1978) [122] determined these trapping parameters E and s for the glow peaks 2 to 5 in TLD-100 with three different methods and found good agreement. Fairchild et al. (1978) [123], using a computerized best fit procedure, obtained trapping parameters which are independent of

Author(s)	Analysis	Peak 2			Peak 3			Peak 4			Peak 5		
		E	s	T_m	E	s	T_m	E	s	T_m	E	s	T_m
Blak et al (1974)	Isothermal annealing							1.10	10^{10} to 10^{11}		1.24	10^{11} to 10^{12}	
Johnson (1974)	Isothermal annealing	0.97	4×10^{10}		0.84	3×10^7					1.31	$.6 \times 10^{12}$	
Zimmerman et al (1974)	Isothermal annealing							1.19	10^{11} to 1.5×10^{12}		1.25	5×10^{10} to 1.4×10^{12}	
Miller and Bube (1970)	Initial rise	1.07		86							1.59		177
Grant et al (1968)	Computer fit first-order	1.08	2×10^{13}		1.13	5×10^{12}		1.15	1.2×10^{12}		1.36	2.2×10^{13}	220
Ziniker et al (1973)	Peak shape	1.10	10^{13}	97	1.21	10^{13}	137				1.97	10^{20}	197
Moran and Podgors (1971)	Peak shape	1.47	10^{18}	102	1.77	10^{21}	137				2.20	10^{23}	183
Fairchild et (1978)	Computer fit first- order	1.07	10^{13}	94	1.05	10^{11}	137	1.55	4×10^{15}		2.20	10^{22}	190
Gorbics et al (1969)	Variable heating										2.40	1.7×10^{24}	
Pohlt (1969)	Variable heating	1.77	5×10^{23}		2.26	10^{29}							

exposure in the range of 800 to 3×10^7 R. Similar results were found by de Vries et al. (1988) [124] for photon doses in the range from 0.5 mGy to 1 Gy and irradiation photon energies in the range from 29 keV to 1.25 MeV. Moreover, there is a lack of correspondence between observed fading rates of the TL peaks and those predicted from E and s values (Horowitz (1990) [125]). One explanation for these observations may be found in the non-uniformity between different production batches. Bos et al. (1990) [126] indeed showed significant difference in the values of trapping parameters for different production batches of TLD-100. Another evidence largely arises from observation that the trapping parameters are strongly dependent on the experimental parameters (e.g. cooling rate following the high-temperature (400 ^{0}C) pre-irradiation anneal and glow curve heating rate and also aging effect before irradiations) [127-128] as well as from observations that these parameters are also strongly dependent on the method of measurement (e.g. peak shape analysis, isothermal decay) [129]. In addition, it has been demonstrated that mean lives deduced from isothermal decay measurements at elevated temperatures cannot be extrapolated using first-order kinetic theory to predict room-temperature mean lives (fading) [130]. Therefore, over the years there has been large controversy on the order of kinetics of peaks IV and V. It is well known that all the glow peaks of TLD-100 (in a five-glow peak) can be fitted with first-order kinetics. However, the computerized curve-fitting measurements have indicated that the glow curves of TLD-100 are well described by first-order kinetic. On the other hand, by using this method, Fairchild et al. [123] pointed out that the presence of an additional peak between the peak III and IV (a peak IIIa) is necessary for a better fit. But, the results of Fairchild et al. [123] were also critized by McKeever (1980) [131] that there is no evidence of the additional peak between peak III and IV. He explained that the glow curves of TLD-100 between room temperature and dosimetric peak V is well described by just five glow peaks. However, in the past a number of experimental evidences using peak shape analysis or isothermal decay has indicated that the peaks IV and V of TLD-100 do not follow first order kinetics [132-135]. In a subsequent paper Sunta et al. (1983)

19

[136] argued that their non-first-order kinetic model has been supported by the unpublished results of Levy (Brookhaven National Laboratory USA) and Fleming (Monash University, Australia). Survey of the literature, which by no means can be called exhaustive, shows that the non-first-order kinetic model of TLD-100 has been severely criticized by a number of workers (Lilley and Taylor (1981) [137], Lilley and McKeever (1983) [138], Delgado and Gomez Ros (1988, 1990, 1991) [139-141]).

An instructive article which summarized (but does not begin to resolve) some of the controversy concerning peak 5 has recently been published by Gartia and Sing (1993) [142]. The trapping parameters for peak 5 which can arise from some of the various models are shown in Table 2 [142]. Gartia and Singh conclude that the exact model for peak 5 of LiF TLD-100 remains unsolved but in their another paper (Singh and Gartia (1993) [143]), they conclude that peaks 4 and 5 of TLD-100 do not follow either the Randal and Wilkins (1945) [144] first-order kinetics or the general order kinetics model of Chen (1969a,b) [145-146] as debated by a number of workers and they proposed that the continuous uniform distribution of trapping levels may be one of the candidates to explain mystery on the kinetic order of peak 4 and 5.

Table 2. Trapping parameters of peak V of LiF TLD-100.

Model	activation energy E (eV)	frequency factor s (s^{-1})	order of kinet. b
Randall-Wilkins model	2.53	2.54×10^{26}	1
general-order kinetic model	3.18	2.25×10^{32}	1.5
continuous uniform trap distribution model	2.6 DE=0.05	1.30×10^{26}	1

It is an experimental fact that in most cases a TL peak is not completely clean, which limits the applicability of the analysis by curve fitting. If the peak is contaminated by a satellite at the low-temperature side, it can be thermally cleaned. A similar technique was followed by Delgado and Barreiro (1986) [147] to obtain the fairly isolated peak V of TLD-100. They used relatively low heating rate (0.4167 ^{0}C/sec.) to minimize the thermal gradient across the sample and found that the symmetry factor is equal to 0.474 at half intensity, which clearly shows that it does not follow first-order kinetic. Finally a further evidence comes to the result of the non-first order peaks from the observation of Yossian and Horowitz (1995) [148]. They studied the kinetic parameters of peak 5 in TLD-100 as a function of the duration of post-irradiation annealing at 165 ^{0}C. They concluded that a post-annealing at 165 ^{0}C for 20 min reduces the intensity of the lower temperature satellite, peak 4, to negligible levels. The shape of isolated peak 5 changes as a function of the duration of the post-irradiation annealing. All three trapping parameters show important changes as the duration of the anneal increases. Computerized peak shape analysis shows that the order of kinetics of peak 5 increases from 1.2 following a 5 min anneal to 1.72 following a 30 min anneal. The activation energy increases from 1.75 eV after annealing for 5 min to 2 eV after annealing for 15 min and then remains constant for longer annealing times.

CHAPTER 2

Theory

2.1 Crystal structures and Crystal Defects

2.1.1 Alkali Halides:

The alkali halides are typical ionic compounds, and their physical properties are in general well known. The majority of the alkali halides crystallize in the rock salt structure, as shown in figure 1. In this structure each cation (alkali metal ion M^+) is surrounded by six nearest-neighbour anions (halogen ions X^-) and each by six nearest neighbour cations. The cations and anions are each situated on the points of separate face-centered cubic lattices, and these two lattices are inter-leaved with each other.
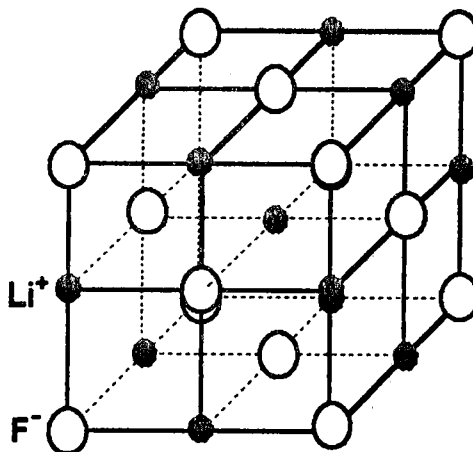
Figure 1. The structure of the rock salt (NaCl) type alkali halides.

These materials, of the type M^+X^-, where M=Group I alkali metal and X=Group VII halogen, are possibly the best known of all ionic compounds. Research into alkali halides was initiated in the early 1920s in the hope that it would aid our understanding of the behaviour of solids as a whole.

At normal temperatures the alkali halides are highly insulating solids. The difference in energy between the valance band and the conduction band in pure alkali halides varies from 5.38 eV (229 nm) for sodium iodide (NaI) to 13.6 eV (105 nm) for lithium fluoride (LiF).

The alkali halides are transparent to light in the visible, far infrared and near ultraviolet. The ultraviolet absorption corresponds to electronic transitions, while the infrared absorption is related to the vibrations of the ions composing the solids. Many chemical impurities, when incorporated in the alkali halides even in parts-per-million (ppm), affect the physical and chemical properties of alkali halides. When the temperature is raised, the electrical conductivity increases very rapidly. The carriers of electric charge are ionic in nature, not electronic.

2.1.2 Band Model and Electronic Transitions in the Alkali Halides

An insulator, like an alkali halide, can be described quantum mechanically by the band model. The conduction band is separated from the valance band by the forbidden region. Figure 2 shows schematically the energy band models of an alkali halide, the electronic energy levels within the forbidden energy gap, and the common electronic transitions in these levels.

For a crystal without lattice defects there are no energy levels between the valance and conduction bands. The energy levels introduced may be discrete, or may be distributed depending upon the exact nature of the defect and of the host lattice. In general terms, it is believed that the lattice

imperfections, impurities, intrinsic and extrinsic defects give rise to the localized energy levels (metastable state) within the forbidden energy gap and they may be well understood using the example of an alkali halide crystal of the type M^+X^-. A free electron in these crystals may become attracted by columbic field of a vacant anion site and become trapped. The energy required to release the electron from the trap is less than that required to free a valance electron from an X^- ion and thus anion vacancy has associated with it an energy level which lies somewhere between the valance and the conduction bands. A similar situation is satisfied for hole which is trapped with cation vacancies and once again they give localized energy levels within the band gap. Similar arguments apply to the incorporation of impurity ions (cation or anion) within the crystal lattice, either in substitutional or interstitial positions.
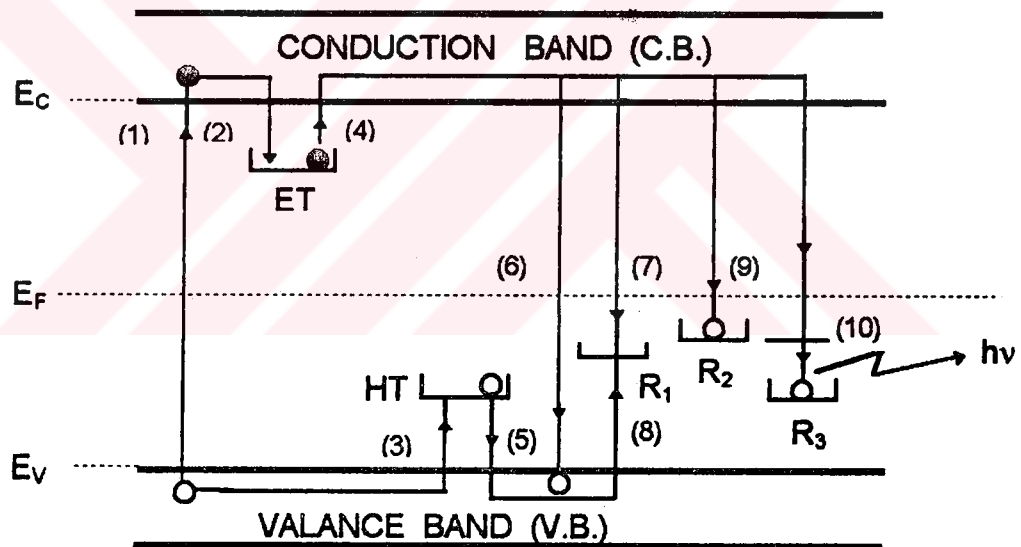
Figure 2. Common electronic transitions in crystalline solids: (1) ionization; (2) and (3) electron and hole trapping respectively; (4) and (5) electron and hole release; (6) direct recombination; (7), (8), (9), (10) indirect recombination. (ET: Electron Trap; HT=Hole Trap; R_1, R_2, and R_3 Recombination Centers)

During absorption of light in the far ultraviolet or irradiations with α, β and γ correspond to the liberation of an electron from the valance band into

the conduction band leaving a hole in the valance band (transition (1)). Thus, transition (1) corresponds to the process of ionization. The free electron in the conduction band and free hole in the valance band wander through the crystal until they become trapped at the lattice defects. The electron may be trapped by a transition to the lowest available energy level at the defect (transition (2)). The hole may be also be trapped at a lattice defect above the valance band (transition (3)). The trapped electrons and holes may be released from the traps when the crystal is heated or under the optical excitation (transition (4) and (5)).

The probability of a charge carrier being thermally released from its trap is exponentially related to -E/kT (see Section 2.2.2), where E is called as "trap depth" which is the energy difference between the trap and conduction band (for electrons) or the valance band (for holes), T is the temperature at which charge carriers are being excited from their corresponding delocalized band.

When the charge carriers are released to their corresponding band, they are once again free to move through the crystal and may recombine with a charge carrier of opposite sign, either directly (transition (6)), or indirectly (transitions (7), (8) and (9)). The band-to-band recombination may be termed as "direct", whilst recombination involving localized levels, i.e. band to center or center-to-center, may be termed as "indirect". If either of these recombination mechanism is accompanied by the emission of light then luminescence results (radiative transitions). When the free electron transits to an excited state from conduction band due to the relaxation of the lattice around the defect according to new situation, no photon is emitted (non-radiative transitions). But the new situation is not stable, the excited electron transits to the ground state via emitting a photon (transition (10)).

Thus, localized energy levels can act either as traps or as recombination centers. The defect where the electron is released is called trapping center or trap. The defect where the electron and hole recombine is

called recombination center or luminescent center if this recombination produces a photon. In principle it is believed that recombination centers are located towards the middle of the forbidden gap and traps are located towards the edges of corresponding bands. However, a center becomes trap at high temperatures, but may become recombination center at low temperatures.

2.1.3 Imperfections in the Alkali Halide Crystals

The crystal lattice is formed by a repeated arrangement of atoms. The detail of this arrangement can be determined by analyzing the diffraction effects which are produced when a beam of some appropriate radiation (x-rays, electrons, or neutrons) is incident on the crystal.

In reality, crystals are never perfect and contain various types of imperfections and defects. There are two types of geometrical defect in a crystal. These are; point defects and dislocations. In this work, we only consider point defects because of their very easy formation in the alkali halide crystals by irradiations or impurities. The elemental impurities which can be incorporated into alkali halide crystals can be divided into the following 7-groups which give point defects in these crystals: (1) hydrogen and alkali metals; (2) monovalent metals; (3) metals of group IIA of the periodic table; (4) metals of group IIB of the periodic table; (5) rare earths; (6) halogens; (7) transition metal impurities.

A two-dimensional representation of a polar crystal containing no defect is shown in figure 3a. This type of crystal is well known as ionic crystal. The simplest defect configuration arises when an atom is missing from its site in the crystal lattice. Sometimes a foreign atom in a crystal occupies an interstitial site between surrounding atoms in normal atom site. This type of point defect is called as interstitialcy.
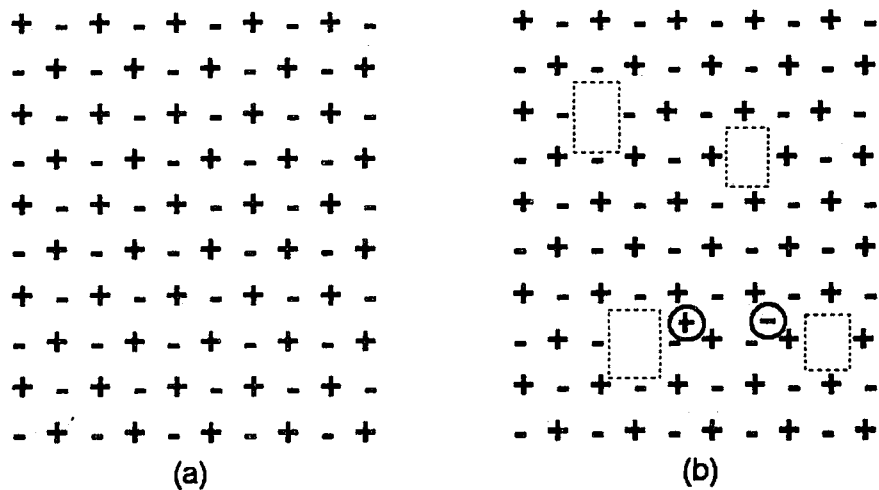
Figure 3. (a) Two-dimensional perfect crystal. (b) Schottky defect (cation and anion vacancies) and Frenkel defect (interstitial cations and anions with corresponding vacancies).

In ionic crystals point defects are more complex due to the necessity to maintain electrical neutrality. When two oppositely charged ions are missing from an ionic crystal, a cation-anion divacancy is created which is known as a Schottky defect. Therefore, the dual imperfection consisting of a cation vacancy and an anion vacancy is shown in figure 3b. If a cation M^+ is removed from its normal lattice site by some process and placed in an inter-lattice position; an anion X^- also similarly moves and replaced in an interstitials site. As one removes either the cation or the anion to an interstitials position one creates a corresponding vacant lattice site either a cation vacancy or an anion vacancy. This type of dual imperfection the interstitials ion together with the vacancy, is known as a Frenkel defect shown in figure 3b.

2.1.4 Production Techniques of Defects in the Alkali Halide Crystal

Defect centers can be generated in a crystal by a variety of techniques. These are simply (1) additive coloration, (2) electrolytic coloration and (3) exposure to ionizing radiation. The first two techniques are extremely difficult

and require a high technology to produce defect centers in the alkali halide crystals. Since we are going to utilize the ionizing radiation to produce defects, we will be interested in the third type of defect production techniques in this work.

The term ionizing radiation includes all sources that can generate free electrons and holes in the materials. The energies range from ultraviolet photons of about 10 eV, through soft x-rays of 10-60 keV and ^{60}Co gamma rays of 1.25 MeV, ^{90}Sr/^{90}Yb β-rays of 2.25 MeV, up to high energy protons or neutrons of 100 MeV.

Exposure of the alkali halides to ionizing radiation produces many types of color centers. Since the sample must remain electrically neutral, it is an inherent characteristic of this type of coloration that both excess electron centers and excess hole centers are formed. In contrast to additive coloration or electrolytic coloration, irradiation normally does not change the stoichiometry of the crystals. The types of defects that can be generated by ionizing radiation at room temperature are additively colored crystals. The main differences between additively colored crystals and colored by ionizing radiation are found if the irradiation is done at low temperatures, i.e., some centers are formed at liquid helium temperatures that are unstable at liquid nitrogen temperatures, and some centers formed at liquid nitrogen temperatures are unstable at room temperatures. It is impossible to produce many of these centers by additive coloration, which necessarily involves elevated temperatures. Thus one of the great advantages of ionizing radiation is its ability to generate color centers at these low temperatures.

The amount of centers that is produced under the irradiations depends on the irradiation temperature and irradiation time for a given sample.

2.1.5 The Structure of Defect Centers in the Alkali Halide Crystals

2.1.5.1 Impurity Defects

The vacancies or interstitial ions can not only be produced by irradiation or thermal means, but also by the incorporation of another type of imperfection, namely chemical impurities. An example of this effect is shown in figure 4a for a two dimensional polar crystal in which the substitution of a divalent cation for a monovalent one places an extra positive charge in the crystal. In order to preserve the electrical neutrality of a crystal as a whole, either an extra negative ion must be incorporated interstitially or a positive-ion vacancy must be formed at a lattice point. It is clear that vacancies and interstitial ions are local regions of unbalanced charge in the crystal. Thus a cation vacancy bears an effective negative charge and an anion vacancy bears an effective positive charge. This causes an electrostatic attraction between the two defects, leading to the formation of a double vacancy or "pair", with the cation and anion vacancies residing on two adjacent sites as shown in figure 4a. By similar considerations, in divalent doped crystals at room temperature and above, one would also expect that a divalent impurity would tend to associate with a cation vacancy ($M^{++}V_c^-$). This type of defect is called as dipole defect (figure 4b). There is also a tendency for the associated dipoles to form higher order clusters such as dimers and trimers (figure 4b) and even precipitate particles. The reaction sequence might be written as

free M^{++} ions + cation vacancies $\Leftrightarrow$ dipoles $\Leftrightarrow$ dimers $\Leftrightarrow$ trimers $\Leftrightarrow$ precipitates.
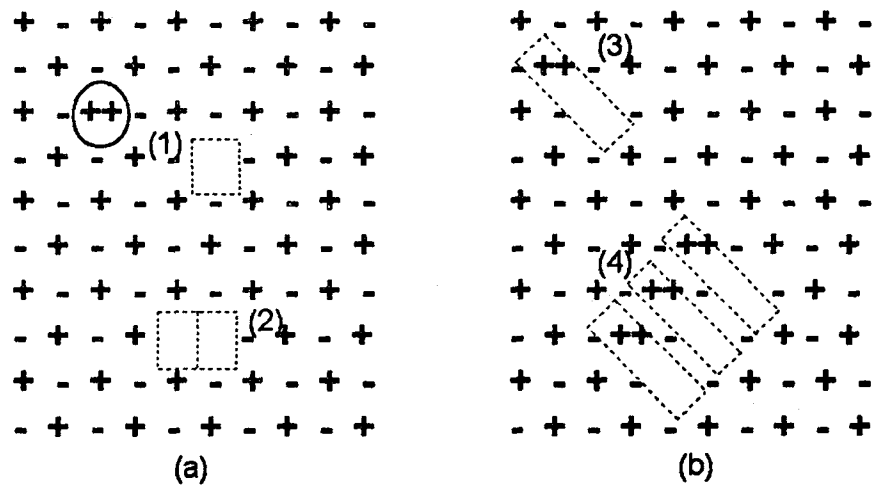
Figure 4. Models of cationic defects in alkali halides. (a) (1) A divalent impurity ion with a dissociated extrinsic cation vacancy; (2) vacancy pair. (b) (3) An associated impurity-vacancy pair, called a dipole; (4) a simple complex containing three dipoles :a trimer.

2.1.5.2 Color Centers

The system comprising an electron trapped at a halogen ion vacancy (anion vacancy) can be described quantum mechanically as a hydrogen atom, in which an electron bound by the positive mechanical description is the particle in the box model. Like a hydrogen atom, the electron-vacancy system has discrete energy levels. The electron can make transitions between these levels by absorption or emission of light. The absorption of a photon of the proper energy can raise the electron from the ground state of the system to one of its higher excited states, and a sufficiently energetic photon can even promote the electron from its ground state into the conduction band. The possibility of absorbing light of energy less than the band gap energy makes the crystal colored and the imperfections which give rise to these absorption are called "color centers".

A-) Trapped Electron Centers in Pure Crystals

F-Center

A particularly well-studied color center is the F-center (from the German Farbe-color). The structure of the F-center is described as an electron trapped in an anion vacancy. A representation of F-center structure is shown in figure 5. The F-center has two different energetic states: the electronic ground state and the relaxed excited state. These states are combined by optical absorption, fluorescence emission and lattice relaxations. Therefore, the F-center can absorb light in a region of the spectrum where the alkali halide crystal is normally transparent.

Figure 5. Representation of important color centers in the alkali halides.

Careful experiments have shown that in pure LiF the F-center optical absorption band has a I_{max} at 250 nm and a full width at half-maximum (FWHM)=0.85 eV at room temperature.

The F-center formed initially by irradiation can be transformed into other centers or again reform F center by the appropriate treatment, principally by illumination with light absorbed by the original centers (F-centers) and thermal treatment. This is satisfied as the absorption of a photon by the center that the electron is promoted to an electronically excited state below the conduction band. This electron can be thermally promoted into the conduction band from the electronically excited state and the alkali halide crystal is now said to be conductive. The ejected electron can wander through the crystal and recombine with a trapped hole, giving out the energy of recombination in the form of a photon (fluorescence) or heat. Therefore, the concentration of the centers decreases and, consequently, the absorbance of the center decreases. If this process is satisfied by optical treatment, it can be called as "optical bleaching", if it is satisfied by heat, this process called as "thermal bleaching".

F'-Center

Other trapped electron center which is produced in the pure alkali halide crystals is the F'-center. Its structure can be described as two electrons trapped at one anion vacancy (figure 5) and it can be produced at low temperature (200 K) by the optical bleaching in the F-band region. At high temperatures the F'-center decays and reforms F centers.

F-Aggregate Centers

When the alkali halides are subjected to prolonged irradiation near room temperature, F-centers combine to form F-aggregate centers in addition to F-centers. These centers are formed also by the appropriate thermal or optical treatment.

The F_2 center, originally called M-center, is composed of two F centers which are aligned along one of the <110> directions of the crystal as shown in figure 5.

The second product of F-center aggregation is the F_3 center which was called R-center. The atomic structure of the F_3-center can be described as the three F-center associated in the <111> plane.

The F_4-center which is called as N-center is a planar combination of four F-center with different symmetry. They are both obtained by adding one F-center to an F_3-center.

The thermal stability of F-aggregate centers can be described as: at approximately 50^0C the F_3 centers decay into F_2 centers and F centers, at $T>100\ ^0C$ F_4 centers decay into F_2 centers and at $T>130\ ^0C$ F_2 centers decay into F centers.

If free electrons are trapped by F-aggregate center (F_2, F_3 and F_4), F_2^-, F_3^- and F_4^- centers are formed respectively, but the thermal stability of these centers seem to be smaller than that of the F^--center. Besides negatively charged centers, if these centers are ionized, then F_2^+, F_3^+ and F_4^+ centers can be created. However the ionization of F center produces another type center, which called α-center as shown in figure 5.

B-) Trapped Electron Centers with Foreign Ions

When an alkali halide doped with a monovalent or divalent foreign alkali ions is irradiated, the electrons and holes can be trapped by the dopants, the defects produced by the irradiations, or dopant-vacancy complexes. In the case of F_A centers these are monovalent foreign alkali ions, in the case of F_z centers these are divalent ions which are nearest neighbours to the anion vacancy. The atomic structure of F_A-centers is shown in figure 5.

F_z-Centers

If the alkali halides doped with alkaline earth impurities (Mg, Ca, Sr and Ba) are exposed to high energetic radiation and subsequent thermal and optical treatment, it may lead to the formation of the Z (F_z) type centers. Six type of color centers can be observed. These are called Z-centers and are labelled with subscripts 0 to 5.

The Z-centers can be generated by the following treatment. When alkali halide is doped with divalent alkaline earth impurities and coloured additively, it will contain only F-centers. Z-centers are introduced on optical or thermal bleaching. F-light bleaching at room temperature generates Z_1 center. If this crystal is then heated to approximately 110 ^{0}C, the Z_1 centers are destroyed, Z_2 centers and some F centers are formed. F-light irradiation at -90 ^{0}C generates the Z_3 centers and heavy irradiation with F light at room temperature produces Z_4 centers.

Different sets of models for the Z-centers were proposed by several authors. The model of the Z_1, Z_2 and Z_3 centers suggested by Pick, is shown in figure 6. According to Pick the Z_1 center is the impurity-cation vacancy pair which has captured an electron. On warming the crystals, Pick argued that the vacancy migrates away from the center and a singly charged divalent impurity M^+ (M stands for Mg, Ca, Sr or Ba) left over forms the Z_2 centers. The Z_3center was assumed to be a Z_2 center which has captured another electron at a substitutional divalent ion. Later in 1951, Seitz revised the model, in which the Z_1 center is a singly charged divalent ion which is the identical to Pick's model for the Z_2 center. He suggested that the Z_2 and Z_3 centers consist of one and two electrons respectively trapped at a vacancy pair adjacent to a substitutional divalent ion. These models together with other models proposed by different workers are also shown in figure 6. Okhura made a very through

34
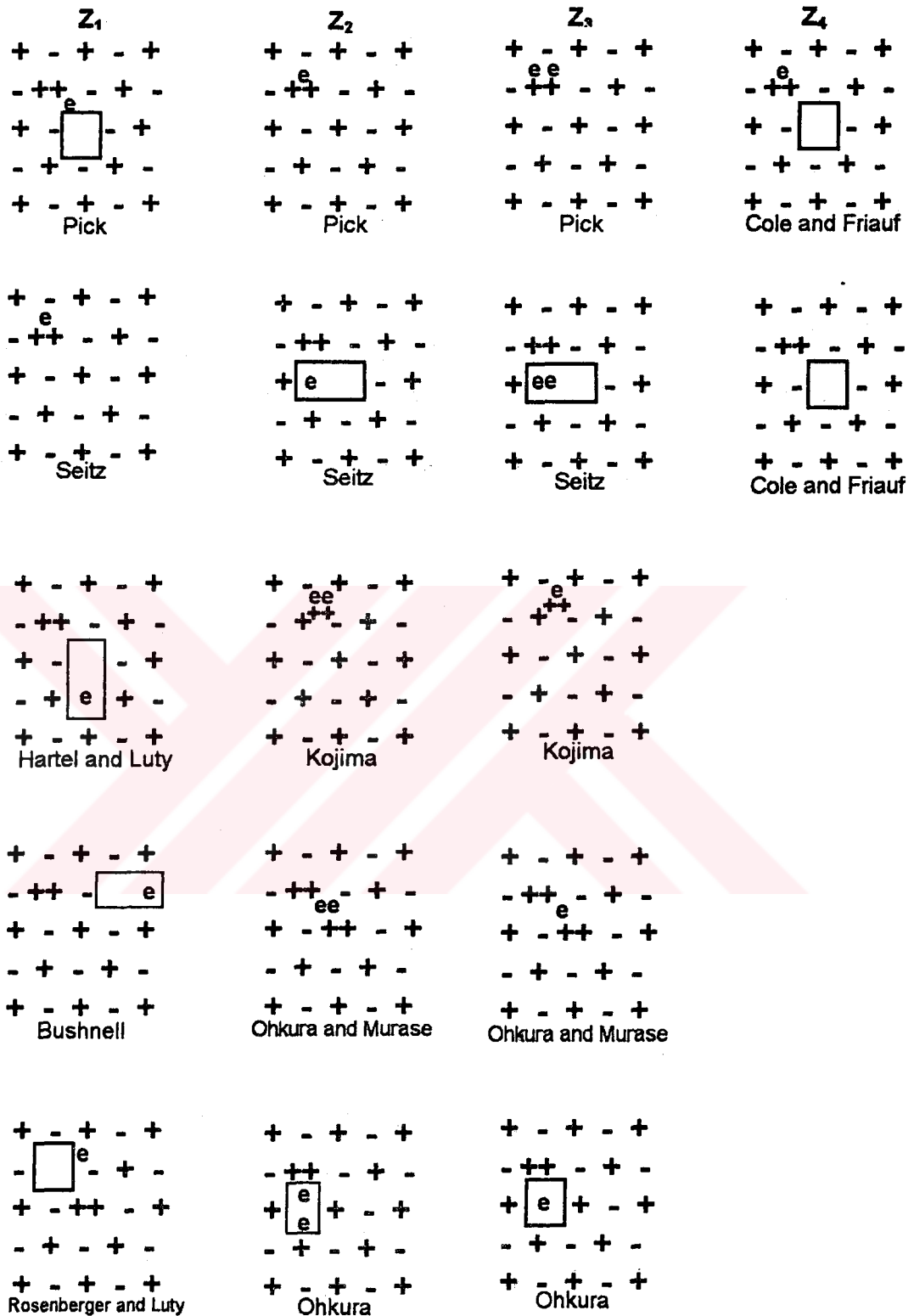
Figure 6. Different models proposed for the Z centers.

ESR study of the Z_2 and Z_3 centers and came to the conclusion that the Z_2 center is not paramagnetic but the Z_3 center is paramagnetic. He suggests that the Z_3 center is formed by the removal of one of the two electrons from the Z_2 centers. The Z_0 center is the divalent impurity ion associated with an anion vacancy.

As mentioned previously, the Z-centers are produced only under appropriate optical and thermal treatment after irradiations. However, some authors have suggested that they have been obtained immediately after irradiation.

C-) Trapped Hole Centers

Trapped hole centers, usually called "V-centers", are produced by similar techniques to trapped electron centers. High-energy radiation produces both electrons and holes so it is reasonable to expect bands associated with trapped positive charges. V centers can also be produced by an excess of halogen. V_k centers are produced at temperatures below 80 ^{0}K by irradiation of alkali halide crystals with irradiations. Its structure can be considered as a hole localized between two adjacent halide ions. To a good approximation it is simply an X_2^- molecule ion, where X is a halogen, created from two X^- ions and the hole as shown in figure 7.
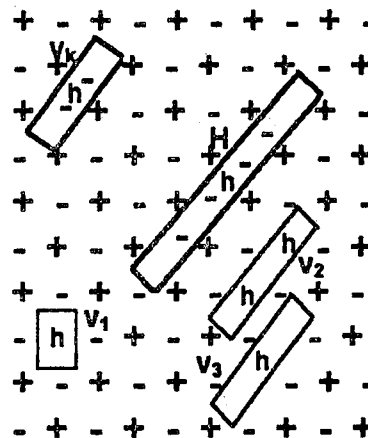
Figure 7. Models of the trapped hole color centers in alkali halide crystals.

If an alkali halide is irradiated with x, α, γ or β rays at room temperature, or if it is irradiated at low temperature and warmed to room temperature, the V_2 and V_3 bands are observed. If the crystals is irradiated at -180 ^{0}C and measured at this temperature without warming up, the V_1 band is observed. The models of the V centers have been the cause of much speculation. Their structure are shown in figure 7.

Another hole-type center produced by irradiation at liquid helium temperature has been discovered optically and positively, and identified by electron spin resonance. The structure of the H center is shown in figure 7. The H center is known to be a hole trapped at an interstitial halide ion and it has <110> symmetry as V_k center.

D-) Chemical Defects

Alkali halides as well as other materials are normally impure. They have to be purified and doped to be suitable for investigation of chemical defects.

OH⁻ ions

Another important impurity which is generally present in the alkali halide is the hydroxide ion (OH⁻). Hydroxyl ion impurities have been shown to influence some properties of the alkali halides such as TL, optical absorption and etc. It can be suggested that the OH⁻ ions are present as a background impurity in the alkali halide crystals. But, determination of OH⁻ ion concentrations in the crystals is a problem. In some cases, the optical absorption technique can be used to determine the OH⁻ contents. However, optical absorption, in particular, is influenced by the combined state of the OH⁻ in the sample, and the values obtained can thus only be regarded as estimates. The free OH⁻ ions also cause infrared absorption due to stretching vibration and ultraviolet absorption due to charge transfer. During irradiation,

OH⁻ impurities decompose to substitutional oxygen ions, U centers and F centers. The oxygen ion remains in the anion site previously occupied by the OH⁻ ion.

Hydrogen Centers

The atomic hydrogen is found in the alkali halides in three different modifications (figure 8). The U band is due to substitutional H_s^- ions, the U_1 belongs to interstitial H_i^- ions, and the U_2 center stands for atomic hydrogen in an interstitial position H_i^0. They can be produced probably by breaking of OH⁻ ions or by heating an additively colored crystals in hydrogen gas or by growing a crystal with an addition of an alkali hydride. They have been identified with the aid of optical experiments and electron spin resonance techniques.
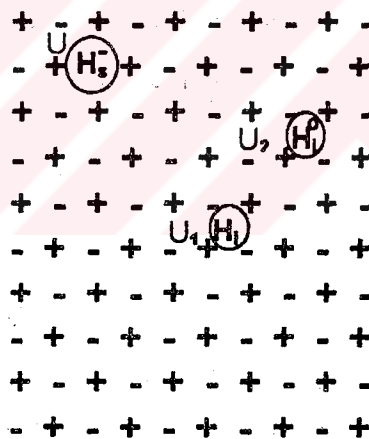
Figure 8. Atomic structure of U centers in the alkali halide crystals.

2.1.6 Transition Metal Impurities in the Alkali Halide Crystals

When an alkali halide doped with transition metal impurity ions, new energy levels are formed by the mixing of the wave functions of the impurity and the surrounding ions of the host lattice, and the transitions which are forbidden in the free ions become partially allowed inside the crystal. The interaction of transition metal impurity with the lattice defects, phonons and the crystal field removes some of the degeneracy of the impurity ions and splits the energy levels.

The transition metals are those from the three series in the periodic table with incomplete inner shells: the iron group ($3d^n$), the rare earths ($4f^n$) and the actinides ($5f^n$). Many of their properties are governed by the partly filled shell of inner electron orbits. Therefore, the energy level structure of d^n and f^n ions, which are called magnetic ions in the ionic compound crystals, can be explained, to a large extent, by crystal field theory. The $3d^n$ transition metals occupy a zone of the periodic table with atomic numbers 21-30. When they enter in an ionic crystal as impurities, they lose the electrons of the 3d shell. The partly empty 3d shell, responsible for the magnetic properties of the ions, is the outermost shell which is strongly exposed to the action of the neighbouring ions. This fact is the cause of the greatest difference between the energy levels of the ions in crystals and the energy levels of the free ions.

In an ionic crystal, each electron feels the influence of the electrons belonging to the other ions (a repulsion) and of the nuclei belonging to the ions (an attraction). This influence is known as crystalline field action. The electronic transition between the inner electron shells of the transition metal ions is called as crystalline field spectra. In addition to the crystal field spectra, the magnetic ions in crystals may present charge transfer spectra. According to this model, the electron is removed from the ligand and transferred to the metal ion or, more correctly, transferred to a molecular orbital, which is largely concentrated on the metal. The intensity of charge transfer spectra is hundred or thousand of times greater than crystal field spectra.

2.1.7 Measurement Techniques of Defect Centers in the Alkali Halide Crystals

The nature of crystal defects have been studied over the past 60 years. Some properties such as defect concentrations, energies of formation, activation energies, frequency factor, charge nature, defect models, defect interactions and relevant parameters are generally investigated by using optical absorption, electron spin resonance, x-ray diffraction, photoconductivity, thermoluminescence, phototransfer, ionic conductivity, dielectric loss, photoluminescence, emission spectra and many more techniques. In this thesis we utilize thermoluminescence, phototransfer, emission spectra and optical absorption techniques to investigate the model (structure), activation energies, frequency factor and charge nature of defects in LiF:Mg,Ti (TLD-100). Therefore, in the next sections we will only explain the theories of these models.

2.2 THERMOLUMINESCENCE KINETICS

2.2.1 Introduction

Thermoluminescence (TL) method is a relatively complex process since it involves traps and luminescence centers. When an insulator or semiconductor is exposed to ionizing radiation at room or at low temperature, electrons are released from the valance band to the conduction band. This leaves a hole in the valance band. Both types of carriers become mobile in their respective bands until they recombine or until they are trapped in lattice imperfections in the crystalline solids. These lattice imperfections play very crucial role in the TL process. The trapped electrons may remain in the traps for a long period when the crystals are stored at room temperature. They can be released due to the sufficient energy given to the electron when the crystal is heated. These electrons may move in the crystalline solid until they recombine with suitable recombination centers that contain holes with the emission of TL light. This process of light emission by thermal stimulation from a crystalline solid after irradiations is called as "thermally stimulated process" or simply "thermoluminescence".

The nature of crystal defects has been investigated over the past 60 years. In principle, TL measurements provide a very sensitive indication of complex defects in insulators and some semiconductors. But the study of defect structure (model) in solids using only this method is perhaps the most difficult. In fact, this technique has only limited value in arriving at a true characterization of the defect structure of the solid under study. Therefore, this type of measurement has been supplemented by many other experimental techniques. The analysis of the TL glow curves also provides different kinds of basic information in a large variety of crystal such as charge trap concentrations, trap depths, frequency factor, carrier mobility, capture cross section of traps and other details of the light-emission kinetics.

41

2.2.2 Simple Models for Thermoluminescence

The simplest model for TL consists of a single type of electron defect level and a single type of hole defect level in the forbidden gap, as depicted in figure 9. It is required to remember here that the two energy level band model is the minimum number needed in order to describe the thermoluminescence mechanism. But, the band model of an actual specimen may be much more complex than this simple model. However, this simple model is enough to explain the fundamental features of TL production. If the electron level is relatively shallow in the forbidden gap, the hole center is thermally stable during the heating while electrons are thermally released and move to the
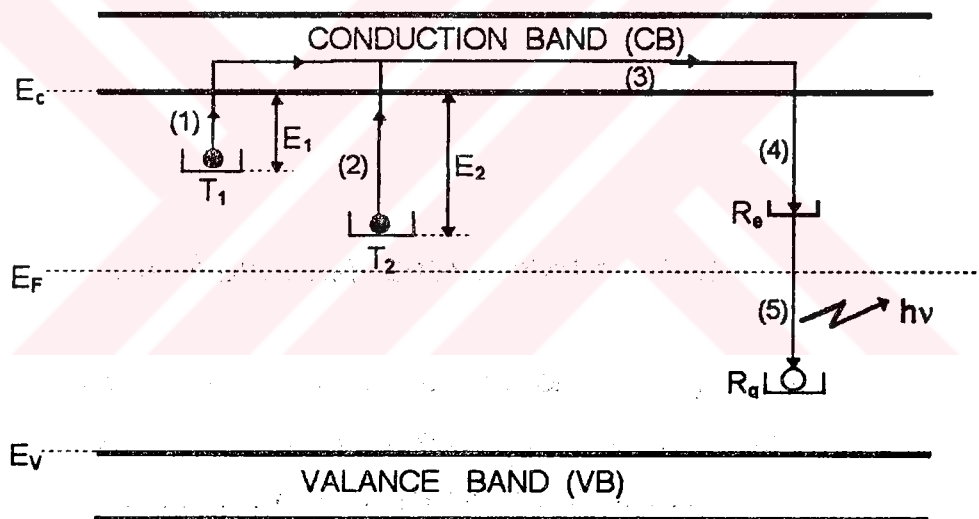
Figure 9. Simple band model for TL emission. T_1 and T_2 are electron traps, R_e and R_g are the excited and ground state of a recombination (luminescent) center, E_1 and E_2 are the energy difference between the band edge of the conduction band and electron trap T_1 and T_2, respectively. Allowed transitions: (1) and (2) thermal release, (3) migration, (4) non-radiative recombination, (5) radiative recombination.

conduction band. Eventually they recombine with the hole centers to produce TL. The shallower level is called "trap" and the other one "recombination center" or "luminescent center".

The probability p per unit time of the release of an electron from the trap to the conduction band can be calculated by the Arrhenius equation

$$p = \tau_e^{-1} = s\exp(-\frac{E}{kT})$$ (1)

where τ_e is defined as the lifetime of an electron in the trap, E (activation energy) is the vertical energy separation between the trap and the conduction band which is frequently called as the trap depth (eV), s (sec^{-1}) is the attempt to escape frequency from the trap which is frequently called as "frequency factor" or "pre-exponential factor", k is the Boltzmann's constant and T is the temperature.

As can be understood from Arhenius equation, if the trap depth E is greater than kT_0, where T_0 is the irradiation temperature, then any electron which has been trapped will remain there for a long period of time. If the temperature of the specimen is raised above T_0 such that $E \leq kT$, this will increase the probability p and the electron will now be released from the trap into the conduction band. Therefore, the recombination rate increases at first because more trapped charge carriers are released per second. As the electron traps are progressively emptied, then, after reaching a maximum, the rate of recombination decreases and thus the TL intensity decreases accordingly. Thus, it can be said that TL is highly depend on the trap depth E (eV) and frequency factor s (sec^{-1}).

2.2.3 Trap Filling Process

The trap filling process during the irradiation is described by the Chen, McKeever and Durrani (1981) [149] by the following four equations:

43

$$\frac{dn_c}{dt} = f - n_c A_r n_h - n_c (N - n)A \qquad (2)$$

$$\frac{dn}{dt} = n_c (N - n)A \qquad (3)$$

$$\frac{dn_v}{dt} = f - n_v (N_h - n_h) A_h \qquad (4)$$

$$\frac{dn_h}{dt} = n_v (N_h - n_h) A_h - n_c n_h A_r \qquad (5)$$

where f is the electron hole generation rate, n_c is the concentration of electrons in the conduction band (per unit volume, m^{-3}), n_v is the concentration of holes in the valance band, n is the concentration of electrons in traps, N is the concentration of available electron traps (of depth E below the conduction band), n_h is the concentration of holes in the recombination centers, N_h is the concentration of available hole centers, A is the transition coefficient for electrons in the conduction band becoming trapped volume per unit time ($m^3 sec^{-1}$), A_h is the transition coefficient for holes in the valance band becoming trapped in the hole centers and A_r is recombination transition coefficient for electrons in the conduction band with holes in centers.

2.2.4 Trap Emptying Process

Assuming a single electron trap and a single hole center, the rate equations describing the flow of charge between various energy levels and bands during trap emptying have been described by Adirovitch (1956) [150], Haering and Adams (1960) [151], and Halperin and Braner (1960) [152] as

$$\frac{dn_c}{dt} = ns\exp(-\frac{E}{kT}) - n_c(N-n)A - n_c n_h A_r \qquad (6)$$

$$\frac{dn}{dt} = n_c(N-n)A - ns\exp(-\frac{E}{kT}) \qquad (7)$$

$$I_{TL} = -\frac{dn_h}{dt} = n_c n_h A_r \qquad (8)$$

where I_{TL} is the TL intensity (photons/sec).

According to Eq. 8, I_{TL} is equal to the rate of recombinations, which is proportional to the number of recombination centers and the number of free electrons. Unfortunately, there is no general analytical solution of these Eqs.6, 7 and 8, however, an approximate solution can be achieved by making some assumptions. Alternatively, numerical solutions can be found for a given set of the parameters E, s, A_r, A, N, N_c, n_c, n and n_h [153-155]. These numerical solutions are quite useful for studying the dependence of the TL curve on various parameters.

In order to obtain an analytical solution of Eqs. 6-8, the following two assumptions may be used

$$n_c \ll n, \qquad \frac{dn_c}{dt} \ll \frac{dn}{dt} \qquad (9)$$

It was also assumed that the charge neutrality condition becomes

$$n_c + n = n_h \qquad (10)$$

which for $n_c \approx 0$ means $n = n_h$ and $dn/dt \approx dn_h/dt$. Since $dn_c/dt \approx 0$, one gets from Eqs.6-8;

$$I = -\frac{dn_h}{dt} = \frac{ns\exp(-\frac{E}{kT})}{1 + \frac{(N-n)A}{nA_r}} \qquad (11)$$

45

Although Eq.11 is simpler than Eqs.6-8, it cannot be solved analytically without additional assumptions. When retrapping can be neglected, i.e., $(N-n)A<<nA_r$, one gets (by substituting $n_h=n$) the famous first-order kinetics (Randal & Wilkins 1945a,b) [144,156]

$$I = -\frac{dn}{dt} = ns\exp(-\frac{E}{kT}) \tag{12}$$

if the coefficients for retrapping and recombination are equal i.e., $A=A_r$ and the assumptions $n<<N$ and $n=n_h$, the Eq. 11 yields the second-order kinetics (Garlick and Gibson 1948) [157]

$$I = -\frac{dn}{dt} = n^2 s'\exp(-\frac{E}{kT}) \tag{13}$$

where $s'=sA/NA_r$, the power of n in Eqs.12 and 13 indicates the order of kinetics. When the simplifying assumptions do not hold, the TL peak will fit neither the first- nor the second-order equation. The general-order kinetic equation is given as

$$I = -\frac{dn}{dt} = n^b s'' \exp(-\frac{E}{kT}) \tag{14}$$

where b is the kinetic order, s" has a dimension of $(sec^{-1}m^{3b-3})$. Equation 14 is called the general-order kinetics which was first proposed by May and Patridge (1964) [158]. Equations 12 and 13 are known as the special cases of the general order kinetic with b=1 and b=2, respectively.

The solution of Eq.12, assuming a linear heating rate programme β (^{0}C/sec), gives the famous first-order equation of Randal & Wilkins,

$$I(T) = n_0 s\exp(-\frac{E}{kT})\exp(-\frac{s}{\beta}\int_{T_0}^{T}\exp(-\frac{E}{kT'})dT') \tag{15}$$

The solution of Eq.13 gives the second-order equation of Garlick & Gibson (1948) as

$$I(T) = n_0^2 s'\exp(-\frac{E}{kT})[1+\frac{n_0 s'}{\beta}\int_{T_0}^{T}\exp(-\frac{E}{kT'})dT']^{-2} \tag{16}$$

and the solution of Eq.14 for b $\neq$1 is

$$I(T) = n_0 s'' \exp(-\frac{E}{kT})[1 + \frac{(b-1)s''}{\beta} \int_{T_0}^{T} \exp(-\frac{E}{kT'})dT']^{\frac{b}{b-1}} \qquad (17)$$

where T_0 and n_0 are the initial temperature and initial concentration of trapped electrons, respectively, and $s'=s/N$, $s''=s'n_0^{(b-1)}$. The values of b lies in general between 1 and 2 but, in principle, values of b outside this range are also possible.

2.2.5 Methods For Determining The Trapping Parameters

There are various methods for evaluating the trapping parameters namely; activation energies E (trap depth), frequency factor s (attempt-to-escape frequency or pre-exponential factor), kinetic order b, and the number of trapped electron concentrations n_0. Some of the various methods are listed below:

(1) Initial rise method,

(2) Heating rate method,

(3) Peak shape method,

(4) Isothermal decay method, and

(5) Computer curve fitting method

In addition to these methods, there are also more methods to evaluate the trapping parameters from TL glow curves.

2.2.5.1 The Computation of s

The second exponential term in Eqs.15, 16 and 17 become more important than first exponential term at high temperatures. Thus a maximum T_m temperature is always observed at a certain temperature in glow curves. At the maximum intensity I_m, by equating the derivative of I with respect to T to

47

zero (dI/dT=0) when $T=T_m$ or the derivative of ln(I) (dln(I)/dT=1/I(dI/dt)=0 at $T=T_m$), Eq.15 yields

$$s = \frac{\beta E}{kT_m^2} \cdot \exp(\frac{E}{kT_M})$$ (18)

Similarly, from Eq.17 for the general order kinetics, one gets

$$s = \frac{\beta E}{kT_m^2}[\exp(-\frac{E}{kT_m})(1+(b-1)\frac{2kT_m}{E})]^{-1}$$ (19)

Once the value of E is determined, the frequency factor s can be obtained from the Eq.18 for first order glow peaks. However, for other kinetics, the values of b are required to be known previously. Therefore, the value of b must be obtained by other methods previously. Then using the Eq.19, one can obtain the value of s.

2.2.5.2 Calculation of Activation Energy E

i-) Initial Rise Method

At first, the trap depths of the glow peaks were obtained by the initial-rise method (Garlick & Gibson 1948 [157]) for the glow peak intensity I(T). In the region, where $T<<T_m$ (up to 10 to 15 % of I_m) all factors other than exp(-E/kT) in the Eqs.15, 16 and 17 do not show an appreciable variation with T and therefore the intensity is proportional to exp(-E/kT) according to the expression for either type of kinetics

$$I \alpha \exp(-\frac{E}{kT})$$ (20)

Thus, plotting ln(I) as a function of 1/T produces a straight line with a slope equal to -E/k from which the value of E can be found.

When s depends on the temperature with $s = s_0 T^a$, a correction factor comes to the activation energy with $E = E_{ir} - akT_m$, where E is the true activation energy and E_{ir} is the value measured by the initial rise method and the value of a usually ranges from -2 to +2. If ignoring this correction factor, the true activation energy may distort from the real value by 5 to 10 %.

The initial rise method does not give any information on b. Actually the low temperature side of the peak is not very sensitive to the kinetic order b.

ii-) Heating Rate Method

Another important method to determine E is the heating rate methods. Bohun (1954) [159] and Booth (1954) [160] suggested that T_m in a first order peak depends on the heating rate β according to Eq.18. Therefore, if a sample is heated at two different linear heating rates, β_1 and β_2, the peak temperatures will be different. Equation 18 can, therefore, be written for each heating rate and dividing the equation 18 with β_1 (and T_{m1}) by the equation with β_2 (and T_{m2}) and rearranging, one gets an explicit equation for the calculation of E

$$E = k \frac{T_{m1} T_{m2}}{T_{m1} - T_{m2}} \ln[\frac{\beta_1}{\beta_2}(\frac{T_{m2}}{T_{m1}})^2] \qquad (21)$$

Similarly, another way was suggested by Hoogenstraaten (1958) [161]. When various heating rates for the first-order kinetics are used, the following expression is obtained:

$$\ln(\frac{T_m^2}{\beta}) = (\frac{E}{k})(\frac{1}{T_m}) + \text{constant} \qquad (22)$$

A plot of $\ln(T_m^2/\beta)$ versus $1/T_m$ should yield a straight line with a slope E/k, then E is found. Additionally, extrapolating to $1/T_m = 0$, a value for $\ln(sk/E)$ is obtained from which s can be calculated by inserting the value of E/k found from the slope.

Chen & Winer (1970) [162] proved that the same method is also applicable to general order peaks. They showed that for the general order case, one can plot $\ln[I_m^{b-1}(T_m^2/\beta)^b]$ versus $1/T_m$, whose slope is equal to E/k.

iii-) Peak Shape Method

This method based on the shape of the peak utilizes just two or three points from the glow-curve. Usually, these are the maximum of the peak T_m and either or both, the low and high-temperature half-heights at T_1 and T_2 (see figure 10).
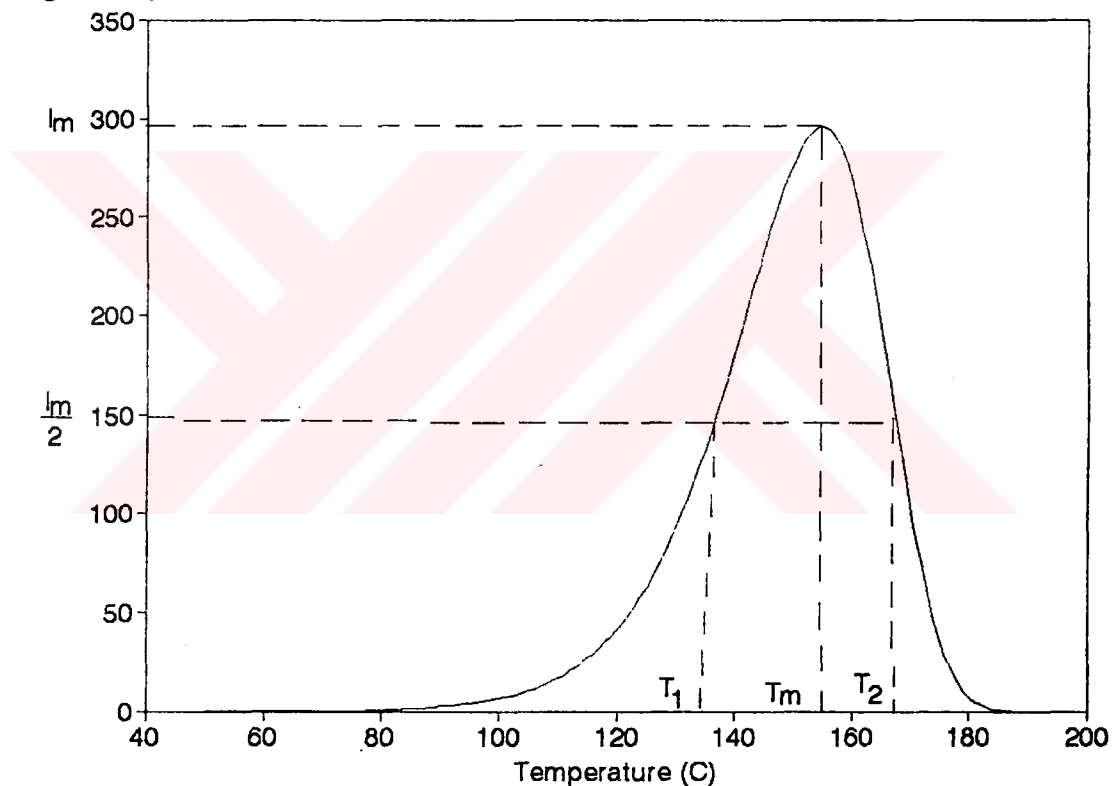
Figure 10. A typical glow curve shape. $\tau=T_m-T_1$, $\delta=T_2-T_m$, $w=T_2-T_1$. The ordinate shows TL intensity.

The peak shape method explained in this thesis were those of Grossweiner (1953) [163], Lushchik (1956) [164], Halperin & Braner (1960) [152] and Chen (1969a,b).

Grossweiner [163] has suggested the following approximate equation to calculate the activation energy by means of τ

$$E = a\frac{kT_1 T_m}{\tau} \qquad (23)$$

where $\tau = T_m - T_1$, $a = 1.41$ and 1.68 for first and second-order kinetics, respectively.

Lushichik [164] obtained two different expression for the first and second order kinetics based on the measurement of $\delta = T_2 - T_m$. For the first and second order kinetics, the Eq.(23) was modified by Chen (1969b) [146] as

$$\begin{aligned} E &= 0.976\frac{kT_m^2}{\delta} \quad (b = 1) \\ E &= 1.706\frac{kT_m^2}{\delta} \quad (b = 2) \end{aligned} \qquad (24)$$

Halperin & Braner [152] suggested a method based on the measurement of T_1 and T_m for the both first and second order cases. Considering τ and the correction by Chen [146], the expressions were as follows:

$$\begin{aligned} E &= 1.52\frac{kT_m^2}{\tau} - 3.16kT_m \quad (b = 1) \\ E &= 1.813\frac{kT_m^2}{\tau} - 4.0kT_m \quad (b = 2) \end{aligned} \qquad (25)$$

In addition to these formulas, Chen (1969a,b) also analyzed these methods to their fullest extent. Chen (1969a) gives three equations each for first and second order peaks, using total-half width $w = T_2 - T_1$, low-temperature half-width $\tau = T_2 - T_1$ and high-temperature half-width $\delta = T_2 - T_m$. A general formula for E was given as:

$$E_\alpha = c_\alpha\frac{kT_m^2}{\alpha} - b_\alpha(2kT_m) \qquad (26)$$

where α stands for δ, τ or w and the values of coefficients c_α and b_α for the three methods are:

$$c_\tau = 1.51 + 3.0(\mu_g - 0.42)$$
$$c_\delta = 0.976 + 7.3(\mu_g - 0.42)$$
$$c_w = 2.52 + 10.2(\mu_g - 0.42)$$
$$b_\tau = 1.58 + 4.2(\mu_g - 0.42) \tag{27}$$
$$b_\delta = 0$$
$$b_w = 1$$

If the temperature dependence of the frequency factor of the type $s = s_0 T^a$ is suspected, then a term $a/2$ must be added to the constants b_a. Chen has also discussed the determination of the geometrical factor $\mu_g = \delta/w$ for different values of b. The resultant variation of μ_g with b has been used to determine the value of kinetic order b from the experimental glow curve.

iv-) Isothermal Decay Method

Another method for determining trapping parameters is the isothermal decay method, which is not exactly a TL method. It deals with phosphorescence rather than TL. According to this method, if a TL material is hold at a constant temperature, the luminescence emission can be recorded as a function of time while the TL material is held at a constant temperature, rather than being heated up. For the first order kinetic, by solving Eq.16 for constant T, the decay in intensity is given by

$$I(t) = ns\exp(-\frac{E}{kT})\exp[-st\exp(-\frac{E}{kT})] \tag{28}$$

A plot of ln(I) against time is linear and the slope m is given by

$$m = s\exp(-\frac{E}{kT}) \tag{29}$$

If the experiment is carried out at two different constant temperatures T_1 and T_2, two different slopes, m_1 and m_2, are obtained and from these two slopes one obtains

$$\ln\left(\frac{m_1}{m_2}\right) = \left(-\frac{E}{k}\right)\left(\frac{1}{T_1} - \frac{1}{T_2}\right) \qquad (30)$$

v-) Computerized Curve Fitting Method

The trapping parameters E, s, n_0, b for the individual peaks can be calculated by a method of computerized curve fitting. In this method, a theoretical curve is computed using the initial values of the trap parameters which are based on the first or second or general-order kinetics and compared with the experimental curve. The computer program uses a least square minimization procedure to determine the peak area, activation energy and frequency factor for first-order kinetics. The trapping parameters of each peak in the experimental glow curve can be set independently. Then the values of the parameters are then sequentially varied until a "best-fit" between the computed and experimental curves is obtained, (i.e.,the rms (root mean square) deviation is minimized).

2.3 PHOTOTRANSFERRED THERMOLUMINESCENCE (PTTL)

2.3.1 Introduction

After incomplete annealing of an irradiated thermoluminescence (TL) sample, the residual trapped charge carriers remain in the deep traps. In the phototransfer (PT) process, during the illumination of the sample with ultraviolet light, the residual electrons from the deep traps can be transferred into empty shallow trapping sites and this process can induce regeneration of the filled shallow traps. Then the filled shallow traps give regenerated lower-temperature glow peaks during the second heating cycle. The phenomenon is called phototransfer thermoluminescence (PTTL). The deep traps in the phototransfer process act as donors and the shallow traps as acceptors of carriers.

Often the illumination with ultraviolet light induce low-temperature glow peaks but it is also seen to diminish high-temperature glow peaks (residual deep traps). This can be interpreted as the release of charge from the deep traps. This increase in lower temperature glow peaks at the expense of a decrease in the high-temperature glow peaks is appearance of a transfer of charge between centers. Therefore, the phototransfer thermoluminescence technique can be used to understand the electronic charge nature of defect centers in the crystalline solid. If the lower-temperature glow peak is regenerated and the size of high-temperature peak is decreased, they can be considered that they are electron type defect centers otherwise they can be considered as hole centers.

PTTL technique has been used over the years for ultra-violet dosimeter (Oberhofer & Scharmann 1981) [165] and more importantly, in the dating of geological and archaeological samples (Aitken 1978) [166]. It has been also investigated in various materials. Sunta & Watanable (1976) [114] studied PTTL in LiF (TLD-100) as a function of the residual glow curve intensity, the

photon energy of the incident light and the temperature of the sample during light exposure. They find that the PTTL glow peaks have the same temperatures in the original glow curves and their relative intensities depend considerably on the residual glow curve and the energy of photons causing the charge transfer. They plot the UV induced glow peak intensity as a function of UV energy. The maxima in the plot occurring at an energy E_{opt} is known as the optical trap depth or optical activation energy of the donor traps and they showed only one clear maximum at 5.25 eV photon energy in addition to two humps at 4.27 eV and 4.66 eV in TLD-100.

2.3.2 Band Model of Phototransferred Thermoluminescence

The energy band model of a crystal phosphor showing transfer of electron from deep trap to shallow trap is shown in figure 11.
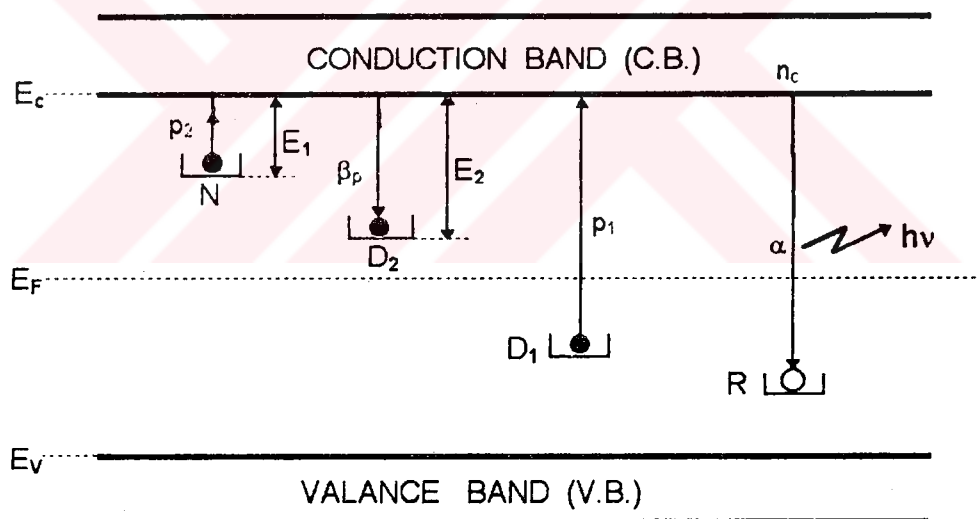
Figure 11. Energy band model of phototransfer thermoluminescence (PTTL).

The D_1 is the concentration of thermally stable deep trap level, D_2 is the concentration of shallower trap levels, then carrier transitions from deeper to

shallower traps under the influence of photo-excitation will be governed by the following equations:

$$\frac{dn_c}{dt} = p_1 D_1 + p_2 n - \beta_p n_c (D_2 - n) - \alpha n_c R$$

$$\frac{dn}{dt} = \beta_p n_c (D_2 - n) - p_2 n \qquad (31)$$

$$\frac{dR}{dt} = -\alpha n_c R$$

where n_c is the concentration of electrons in the conduction band, α is the probability of recombination, β_p is the probability of trapping, p_1 is the probability of stimulation of an electron into the conduction band from the deep traps, p_2 is the probability of stimulation of an electron into the conduction band from shallow electron level, R is the concentration of holes in the recombination centers, n_1 is the concentration of electrons in the shallower trap levels and n_2 is the concentration of electrons in the shallower trap levels D_2.

2.4 THERMOLUMINESCENCE EMISSION SPECTRA

2.4.1 Introduction

The simultaneous measurement of the light emission during heating of the TL materials as a function of sample temperature and in terms of emitted photon energy gives the information on the TL mechanism, trapping parameters for the individual defects and the influence on the reactions. For example, in order to obtain information on the position (in terms of energy) of the recombination (luminescent) center, it is necessary to revert to measurements of the spectra of the emitted thermoluminescence. The energy of the emitted light is governed by the energy difference between the excited state (or conduction band) and the ground state of the recombination center. Then usual procedure is to perform a wavelength scan at a given glow-curve temperature (or over a narrow range of temperatures). In addition, it gives an idea about the structure of defects within the insulator and semiconductor when this type of measurement has been supplemented by many other techniques such as optical absorption and ESR measurements.

The fundamentals of models for emission and absorption spectra of luminescent centers in crystalline solid derived from the theory of molecule spectra, although there are many sophisticated models for emission originating from solids in literature [167].

2.4.2 Line Shape of a TL Emission Spectra

The shape of an emission band of a recombination center in the crystalline solid can be explained by the use of a configuration coordinate model which is drawn in the Section 2.5.3. According to this model, the TL and PL emission spectra have been fitted to Gaussian components using the general expression for Gaussian bands:

$$I(E) = I(E_0) \exp[\frac{-4\ln(2)}{W^2}(E - E_0)^2]\qquad(32)$$

where I(E) is the intensity at the energy E, I(E_0) is the intensity at the band maximum, E_0 is the photon energy at the band maximum, W is the full-width at half-maximum.

It is usual for alkali halide color center absorption bands and emission spectra to be slightly asymmetric

$$E_0(T) = C_1 - C_2\coth(\frac{\hbar w}{2kT})\qquad(33)$$

where C_1 and C_2 are constants, $w/2\pi$ is the effective vibrational frequency in sec^{-1}. This expression predicts that the emission band maximum should decrease slowly and monotonically with increasing temperature.

The data for the full-width at half-maximum W, behaves in an analogous non physical manner. For a single emission band, the full-width is given by

$$W^2 = 8\ln(2)(\hbar w)^2 S\coth(\frac{\hbar w}{2kT})\qquad(34)$$

where S, the only underfined symbol, is the Huang-Rhys factor. This expression indicates that the full-width should increase monotonically with increasing temperature.

2.5 OPTICAL ABSORPTION

2.5.1 Introduction:

It is clear that the colorations produced by various techniques in normally transparent crystals are due to centers formed by the trapping of electrons or holes at lattice defects. Therefore, a large number of absorption bands can be shown when investigating optical absorption measurement, corresponding to the large number of defects, or combinations of defects, that can act as electron traps or hole traps. The investigation of optical absorption bands in the alkali halides will be very helpful to understand the properties of these centers. The optical absorption spectrum of lattice defects provides the most direct information about electronic properties of these centers and also presents the most direct information on the electronic defect structure. The optical absorption bands in the alkali halide, in general, have been designated as the F-center absorption band, F'-center absorption bands and etc. corresponding to the their defect model.

2.5.2 Measurement of the Absorption Coefficient

The terms of the absorption coefficient in crystals explain the fraction of the light transmitted through the crystal at a particular wavelength.

In the optical absorption measurement, the absorption of an irradiated crystal which contains defect centers is compared with an unirradiated crystal that contains no defect centers. This comparison is made as a function of the wavelength of the measured light. If I_0 is the intensity of light transmitted by the unirradiated crystal and I is the intensity transmitted by the irradiated crystal, the quantity of absorbance A can be described as

$$a = \log_{10}(\frac{I_0}{I})$$

$$= \alpha_a X$$

(35)

where I_0/I is the ratio of incident to transmitted photon intensity, X is the optical path length in cm, and α_a is the absorption coefficient related to trap center concentration. Therefore, the absorbance (optical density) is directly proportional to the number of absorbing centers per cm^2 of the sample and is independent of the distribution of these centers along the direction of the light path. If the concentration of centers does not vary with depth, the number of centers per cm^3 can be calculated from the absorption constant α_a.

If the centers giving rise to the absorption band do not interact with one another, the area under the optical absorption curve is directly proportional to the concentration of the absorbing centers by the relation [168]

$$Nf_s = 0.87 * 10^{17} \frac{n_i}{(n_i^2 + 2)^2} \alpha_{max} W_{1/2}$$

(36)

Where N is the concentration of defects per cubic centimetres, f_s is the oscillator strength of an absorption band, a factor which is related to the probability of the optical transition producing absorption, n_i is the index of refraction of the crystal at the wavelength of the absorption band peak I_{max}, $W_{1/2}$ is the full-width at half maximum of the band in eV and α_{max} is the absorption coefficient in cm^{-1} at the peak of the absorption band. In order to determine N, the values of oscillator strength and the refractive index of the crystal at the peak wavelength must be known.

2.5.3 Line Shape of Absorption Band

Optical absorptions at a lattice defect are determined by the ground and excited energy states of the defect center. This results in an absorption

spectrum with lines at a certain energy and a certain line shape. It is clear that the most obvious difference between various types of defects is the energy of a specific absorption line.

However, to understand the shape of optical absorption of lattice defects requires a knowledge of the basic elements of its electronic structure in relation to the band structure of the surrounding lattice. The electronic energy levels of a center is affected with its lattice surrounding ions.

A convenient way to describe the shape of optical absorption and emission curves is by a configuration co-ordinate diagram as shown in figure 12. A configuration coordinate diagram consists of a potential energy curve of the ground state of a center and a potential energy curve of the excited state of this center. In this diagram x-axis represents the configuration coordinate Q and y-axis represents the total potential energy. The potential energy of the system varies quadratically with the magnitude of the coordinate position Q. The system can be treated as a harmonic oscillator.
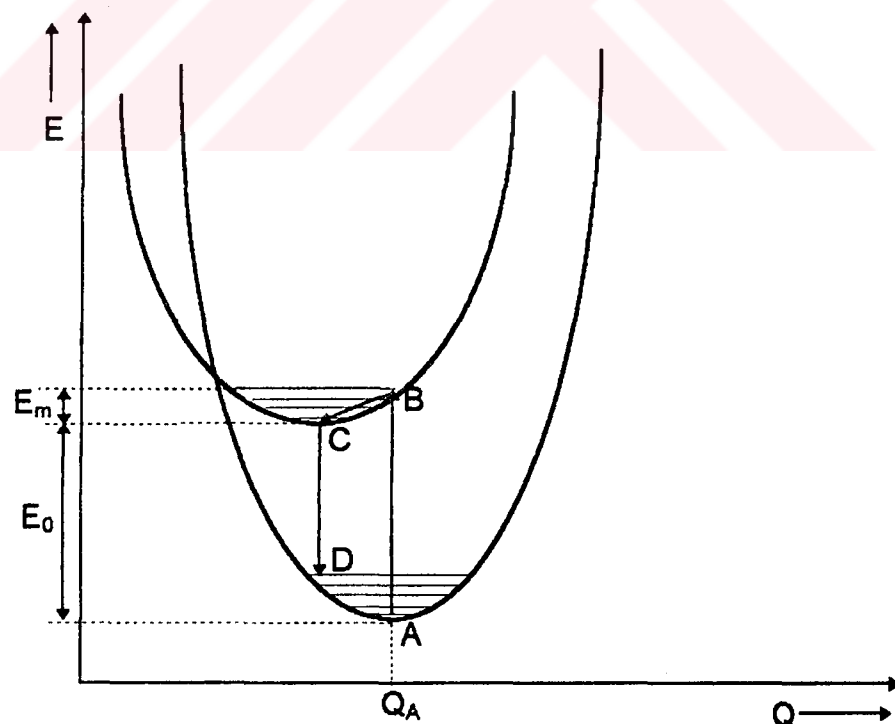

Figure 12. The configuration coordinate diagram of a defect center in crystalline solid.

61

When the center is excited by a light, the electronic transitions between the ground state and excited state is described by the Franck-Condon principle. According to this principle, only vertical transition allowed and during the transitions there is no change in the configuration coordinate. In figure 12 absorption will occur between point A, the ground state equilibrium position and point B, the point on the excited state curve with the same configuration coordinate Q_A. A photon must have the energy E_B-E_A to produce this excitation, The equilibrium energy state of the excited state is the E_C, then the excited electron move its equilibrium position by loss its excess energy E_B-E_C. This energy appears as heat, i.e., as lattice vibrations. The electron from point C can jump to D on the ground state with the emission of a photon of energy (E_C-E_D). There is a wavelength shift between the absorption and emission wavelength. This shift is called as Stokes shift.

According to the quantum mechanics, the system in the ground state will have $hw_g/2$ zero point energy and a distribution of vibrational levels in coordinates is Gaussian. If the excited state curve at B is approximated by a straight line, the configuration coordinate model predicts that the absorption band is also approximately Gaussian the same as emission band with different half-width and peak wavelength value.

The Gaussian line shape frequently is used to explain the optical absorption spectra of a deep center. The line shape function for a Gaussian line is given by

$$F_{(\nu-\nu_0)} = \frac{1}{\sqrt{2\pi}\sigma} \exp[-(\frac{\nu-\nu_0}{2\sigma})^2]$$
(37)

with a line width at half of its maximum strength

$$W_{1/2} = 2\sqrt{2\ln 2}\sigma = 2.355\sigma$$
(38)

There is another typical line shape, the Lorentzian line shape, which is observed for shallower center semiconductor. It is given by the line-shape function

$$F_{(v-v_0)} = \frac{\sigma}{2\pi} \frac{1}{(v-v_0)^2 + (\frac{\sigma}{2})^2} \qquad (39)$$

which yields a line width at half of its maximum strength

$$W_{1/2} = \sigma \qquad (40)$$

Both line shapes are distinguished by their tails which the Gaussian line wider than the Lorentzian line shape. The damping factor in Eqs.37 and 39 can be related to the lifetime of the excited state, and in simple cases given by $\sigma \cong 1/\tau$.

Although the Eqs.37 and 38 did not considered a temperature dependent factor, the half-width of the absorption band depends on the temperature. The band becomes narrower with deacresing temperature and its peak position shifts to shorter wavelengths. At higher temperatures the band width varies as $T^{1/2}$, but at low temperatures the width approaches a limiting value of a few tenths of an electron volt. The half-width $W_{1/2}$ should be proportional to $A[coth(hv_g/2kT)]^{1/2}$, where A is a constant and the quantity v_g is a vibrational frequency, which was found to be $4.1*10^{12}$ s^{-1} for LiF.

2.5.4 The Characteristics of the Defect Center Absorption

The spectral position and width of an absorption band depend on the nature of the alkali halide and the temperature. For an alkali halide with the NaCl structure the positions of the peaks of the optical absorption band λ_{max} of the F center at room temperature are given by the empiricall Mollwo-Ivey relation

$$\lambda_{max} = 703 d^{1.84} \qquad (41)$$

63

where d is the lattice constant of the alkali halide. Table 3 lists the wavelengths of the peaks of the various trapped- electron and trapped-hole

Table 3. Wavelengths of the absorption peaks arising from various trapped-electron and trapped-hole centers in the alkali halides [168].

Center	K	F	F'	R_1	R_2	M	α	V_k	V_3
Temperature of observation (K)	93	300	170	300	300	300	90	77	300
LiF		250		313	380	444		348	
LiCl		385		580	650				
NaF		341		415	505	131			
NaCl		458	510	545	596	725	174	210	
NaBr		540			199				
NaI		588							
KF		455		570					
KCl	457	556	750	658	727	825	177	365	212
KBr	525	625	700	735	790	918	201	385	265
KI	585	689			238	404			
RbCl	523	609							
RbBr	593	694		805	859	957	205		
RbI	646	756			240				
CsCl		605							
CsBr		680							

centers in several alkali halides. The centers have been designated as the F,F',M, etc., whose defect models are discussed in the section 2.1.5.

The F-band shape is mainly Gaussian [4]. If the absorption band has a shape of Gaussian, then it must have a symmetric shape for which $W=W_H$ for $E>E_m$ and $W=W_L$ for $E<E_m$, where E_m is the absorption band peak energy.

64

However, in LiF, Davson and Pooley [169] have shown that the shape of the absorption band of the F-center has an asymmetric shape and high energy width W_H becomes larger than the low energy width W_L. But it can be noted that the inaccuracies introduced by assuming a normal Gaussian shape are minor compared to the height of the peak and that the value of E_m is approximately the same in both cases.

Careful measurements have shown that on the short wavelength side of the F-band there are small addition bands K, L_1, L_2, L_3. These bands belong to transition to higher excited bound (K,1s-3p) and conductive (L) states.

In addition to these bands, also there are other absorption bands on the high energy side of F-band closer to the fundamental lattice absorption when an alkali halide crystal is colored with F-centers. These have been named as α and β bands. Their absorption corresponds to the production of exciton states and these exciton states give rise to discrete absorption bands near the fundamental absorption edge.

If an additively colored crystal is illuminated in its F band at low temperature, the F absorption is reduced in intensity. Simultaneously a new broad absorption band, poorly resolved from the F band, appears at longer wavelengths. This new absorption is called the F'-band. It is not stable at high temperatures and fades below room temperature even in the dark.

When the alkali halides are subjected to prolonged irradiation near room temperature, in addition to the F-band, several new absorption bands situated at longer wavelengths than the F absorption are formed. These bands, therefore, are due to the electron-trapped centers. An empirical relations between the wavelength of the absorption maximum of these bands and the lattice constant of the alkali halide are given as:

$$\lambda_{max} = 816 d^{1.84} \quad \text{(for } R_1 \text{)}$$
$$\lambda_{max} = 884 d^{1.84} \quad \text{(for } R_2 \text{)} \quad \quad (42)$$
$$\lambda_{max} = 1400 d^{1.58} \quad \text{(for } M \text{)}$$

Trapped hole centers, usually called "V-centers", are produced by similar techniques to trapped electron centers. Irradiation of the alkali halides can produce V-bands in the ultraviolet region of the spectrum. However, it is found experimentally that unlike the trapped-electron bands, the V-bands do not follow a Mollwo-Ivey relation. Some of these bands are produced only at very low temperature and are not stable at or above room temperature, i.e., V_1 band is observed only below -180 ^{0}C. Its absorption band, in general, is situated at longer wavelength than the V_2 and V_3 bands. In the irradiated crystal an absorption is also produced in the short-wave ultraviolet region, i.e., V_2 and V_4 absorption band. Similarly, these bands again are not stable near room temperature. Finally, it can be represented that only V_3 center is stable near or above room temperature and its absorption band is situated near to the fundamental lattice absorption. The other hole-trapped centers are the V_K and H centers which are produced at temperatures below 80 ^{0}K by irradiation of the alkali halide crystal with high energetic radiation.

In the previous paragraphs, we introduced the characteristics of absorption bands in the pure crystal. In contrast to this, if the crystals contain foreign impurities, the new absorption bands are produced which can also affect the color center absorption band that occurs when there are no impurities.

As an example of impurity centers in alkali halides, the U centers are formed by the addition of hydrogen to the lattice. The absorption band of an U band is in the ultraviolet region whose magnitude is proportional to the amount of the hydrogen impurities. Its location in various alkali halide crystals follows a Mollwo-Ivey relation of the form

$$\lambda_{max} = 615 d^{1.10} \tag{43}$$

The fundamental optical absorption of the U-centers may be viewed as the transfer of an electron from the hydrogen ion to an alkali halide ion. Since the electron affinity of hydrogen is appreciably less than that of the halogens, it is reasonable to associate the U band with the transfer of an electron from the

hydrogen ion to a neighbouring alkali ion. The U band bleaches with light absorbed in the band. During the U band bleaching, the hydrogen ion may lose its electron or ion may escape from it place. The high temperature bleaching follows a reaction

$$U + h\nu \rightarrow U_2 + F$$
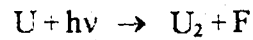
where U_2 center is a natural hydrogen atom in an interstitial site. At low temperatures a different reaction is produced by the bleaching light and the entire hydrogen ion becomes interstial and does not thermally dissociate. The final defects are the U_1 center and an empty halogen vacancy, i.e.,

$$U + h\nu \rightarrow U_1 + \alpha$$
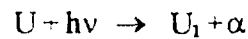
All synthetic crystals of alkali halides contain OH⁻ ions. OH⁻ centers give rise to optical absorption bands in the different spectral regions. The electronic absorption consists of a broad band in the UV region, The peak position of the OH⁻ absorption band in the UV region satisfies an Ivey relation in the form

$$\lambda_{max} = 691 d^{0.90} \tag{44}$$

The vibrational absorption in the infrared region has a small absorption strength due to the stretching vibrations.

The influence of divalent cation impurities on the electrical and optical properties of alkali halides have been studied for many years. With the proper thermal and optical treatments of the alkaline earth doped crystals, it is possible to produce color centers that are characteristics of the divalent impurity. The location of Z-bands have always controversy but in principle, it has been suggested that Z_0, Z_1, and Z_2 bands lies on the high -wavelength side of F-band and Z_3 band lies on the short wavelength side of the F-band.

CHAPTER 3

Experimental Procedure

The experimental procedure, equipments and materials utilized in this work are described below.

3.1 Materials

The samples used in this work were LiF:Mg.Ti (TLD-100) single crystalline chips with dimensions of 3x3x0.9 mm^3 obtained from Harshaw Chemical Company.

The concentration of Mg and Ti impurities in these specimens have been found by different workers to vary from 150 to 250 ppm and 10 to 20 ppm, respectively [28]. In addition to these impurities, recent studies indicate that TLD-100 also contains considerable amount of hydroxyl ions (OH⁻) which combine with Ti and Mg impurities [49]. It is well known that their presence in the LiF:Mg,Ti (TLD-100) influences the TL glow curves, emission and absorption spectra.

3.2 Annealing Ovens and General Heat Treatment

The experiments were carried out to observe the effect of the pre- and post-irradiation heat treatment on the glow curves and absorption bands. The annealing procedures were done at different temperatures with a microprocessor controlled Nuve FN 501 type electrical oven for different intervals ranging between 1 min to 36 hours. The temperature is measured with a Chromel-Alumel thermocouple placed in close proximity to the samples. Temperature of the electrical oven was continuously monitored during the annealing period. The temperature sensitivity of the oven was estimated to ± 1 ^{0}C for the whole temperature range employed from room temperature to 350 ^{0}C.

The standart annealing process was done for all samples to remove any trapped defect centers which can interfere with subsequent emission and absorption measurement prior to every irradiation. In this case, the samples were held at 410 ^{0}C for 30 minutes in a microprocessor controlled Nuve MF 120 type electrical oven. This oven is used for the high temperature annealing between 400 ^{0}C and 1200 ^{0}C with a relatively low sensitivity such as ± 10 ^{0}C. The samples were quenched to room temperature by a rapid cooling rate at approximately 50 ^{0}C per second following every annealing process by withdrawing the samples from the oven onto a cold glass (≈ 0 ^{0}C).

3.3 Radiation Source and Irradiation Procedure

The samples were irradiated at room temperature immediately after quenching. All irradiations were carried out with ^{90}Sr-^{90}Y β-source. The activity of β-source is about 100 mCi. It is calibrated by manufacturer on March, 10 1994. The recommended working life-time is about 15 years. Stronium-90 emit high energy beta particles from their daughter products (^{90}Sr β-0.546 MeV together with ^{90}Y β-2.27 MeV). Beta radiation is absorbed by air, so its

intensity declines with distance much more rapidly than inverse square law calculations would indicate. The maximum range of Y-90 beta particles in air is approximately 9 meter. The typical strength of a 100 mCi Sr-90 β-source installed in a 9010 Optical Dating System is 2.64 Gy/minute=0.0438 Gy/Sec for fine grains on aluminium, or 3.3 Gy/min=0.055 Gy/sec for 100 m quartz on stainless still. The irradiation equipment is an additional part of the 9010 Optical Dating System which is purchased from Little More Scientific Engineering, UK [170]. The irradiation source equipment interfaced to a PC computer using a serial RS-232 port. During the investigation of pre-irradiation effects on the TLD-100, the irradiation durations were adjusted to 3 minutes for TL spectra and 24 hours for absorption spectra measurements.

3.4 TL Analyzer and TL Measurements

The glow curve measurements were made using a Harshaw TLD System 3500 Manual TL Reader [171]. It economically provides high reliability. The technical architecture of the system includes both the Reader and a DOS-based IBM-compatible computer connected through a standard RS-232 serial communication port to control the 3500 Reader. The basic block diagram of reader is shown in figure 13. All functions are divided between the reader and the specialized TLDShell software that runs on the PC. All data storage, instrument control, and operator inputs are performed on the PC. Signal acquisition and conditioning are performed in the reader. In this way, each glow curve can be analyzed using a best-fit computer program based on a Marquardt algorithm minimisation procedure, associated to first-order and general-order kinetic expressions. The program resolves the individual peaks present in the curve, giving the best values for the different peak parameters.

The instrument includes a sample change drawer for inserting and removing the TLD elements. The reader uses contact heating with a closed
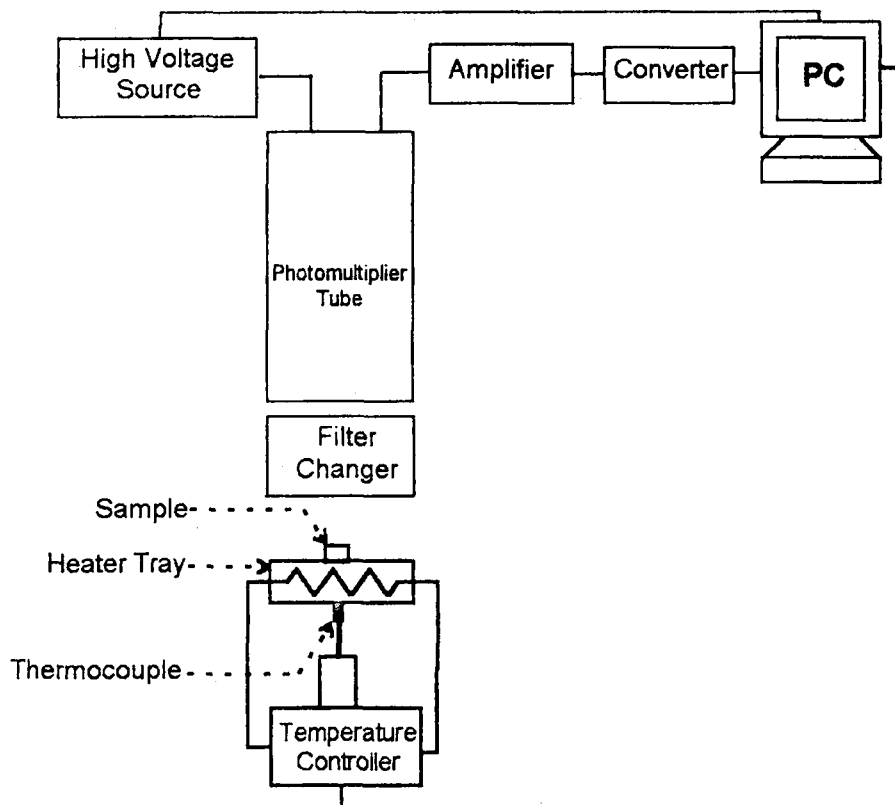
Figure 13. Basic block diagram of TL reader.

loop feedback system that produces adjustable linearly ramped temperatures from 1^0C to 50^0C per second accurate to within $\pm$ 1 ^0C to 400 ^0C in the standard reader. The Time Temperature Profile (TTP) is user defined in three segments: Preheat, Acquire, and Anneal, each with independent times (Pre-read anneal: adjustable 0 to 1000 sec, Linear ramp: adjustable from 1 ^{0} to 50 ^{0} per second, Post-read anneal: 0 to 1000 sec) and temperature (Pre-read anneal:room temperature to 200 ^0C, Post-read anneal: up to 400 ^0C). The typical time temperature profile is shown in figure 14.

To improve the accuracy of low-exposure readings and to extend planchet life, the 3500 provides for nitrogen to flow around the planchet. By eliminating oxygen in the planchet area, the nitrogen flow eliminates the unwanted oxygen-induced TL signal. Nitrogen is also routed through the photo-multiplier tube (PMT) chamber to eliminate moisture caused by condensation.
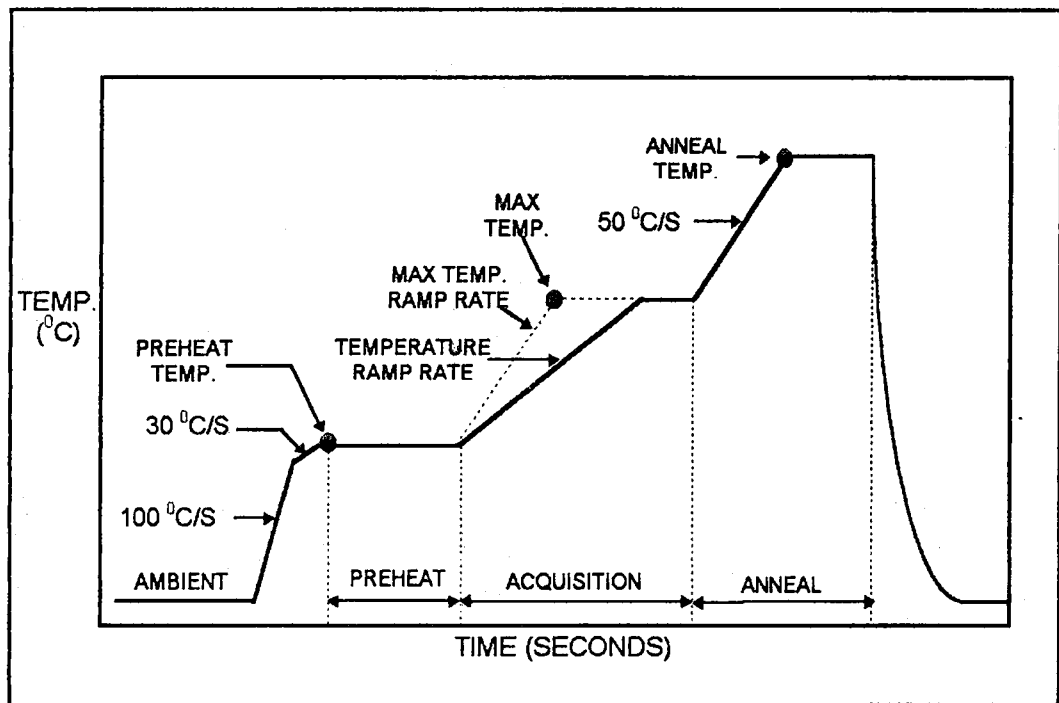
Figure 14. Typical time temperature profile (TTP).

Glow curve readout procedures in the investigation of pre-irradiation heat treatment were carried out using a linear heating rate 2 ^{0}C/sec^{-1} up to 400 ^{0}C. This particular condition was chosen to correspond to the heating rate used by Bradbury et al. [8] in their study of the effect of cooling rate on the precipitation of 6LiF:MgF$_2$. A heating rate of 2 ^{0}C per sec is also a convenient compromise between the requirements of adequate glow curve resolution and speed of readout. At high heating rates, peak 4 tends to merge into peak 5 and its deconvolution from peak 5 becomes very problematic [140-141]. The time duration between irradiation and TL readout was always kept constant about 45 sec.

For PTTL measurements, the irradiated sample was annealed at 280 ^{0}C for 30 sec in the annealing oven to remove the low-temperature glow peaks, and then cooled quickly to room temperature. During this process, the all glow peaks except peak XII disappear. It was then exposed to UV light

72

(254.7 nm) using a spectrophotometer and then the PTTL glow curve was recorded.

Additionally, the emission spectra was recorded using the above explained TL reader. The bandwidth and I_{max} of employed filters in this reader was measured by using a Jasko 7800 Model spectrohotometer. We only used those filters that have less than 10 nm bandwith. The measurements were performed between 300 and 1000 nm. All the spectra were recorded at a heating rate 1 ^{0}C/sec.

3.5 Spectrophotometer and Optical Absorption Measurements

The Jasko (Model 7800) spectrophotometer was used to measure the optical absorption spectra [172]. This instrument measures the absorption of a sample in the ultraviolet/visible/near infrared region of 200 to 1100 nm wavelengths. Figure 15 shows the optical system of this instrument. It uses a deuterium lamp in the ultraviolet region and a tungsten iodine lamp in the visible-to-near infrared region as the light source. The light from the light source, after passing through a high order light cut-off filter, goes to the monochromator that uses a concave diffraction grating. The light is monochromated by the monochromator and is split into two beams by the beam splitter. One of the beams passes through the reference sample and the other passes through the sample and is incident on the silicon photocell detector. After the light signal is converted into an electrical signal by detector and amplified, the logarithm of the ratio of reference intensity to transmitted sample intensity, $\log(I_0/I)$, is plotted as the absorbance versus wavelength.

Prior to any optical absorption measurements, the blank absorbance (air vs. air) at 520 nm was set to zero and the absorption spectrum was measured at room temperature from 200 nm to 520 nm. After each general

thermal treatment, as explained earlier, the crystal background absorption was performed and subtracted from the irradiated crystal absorption spectra.

W₁=Tungsten iodine lamp

D₂=Deuterium lamp

M₁ to M₄=Mirror

F=Filter

G=Concave diffraction grating

BS=Beam splitter

D=Dedector

S₁, S₂=Slit
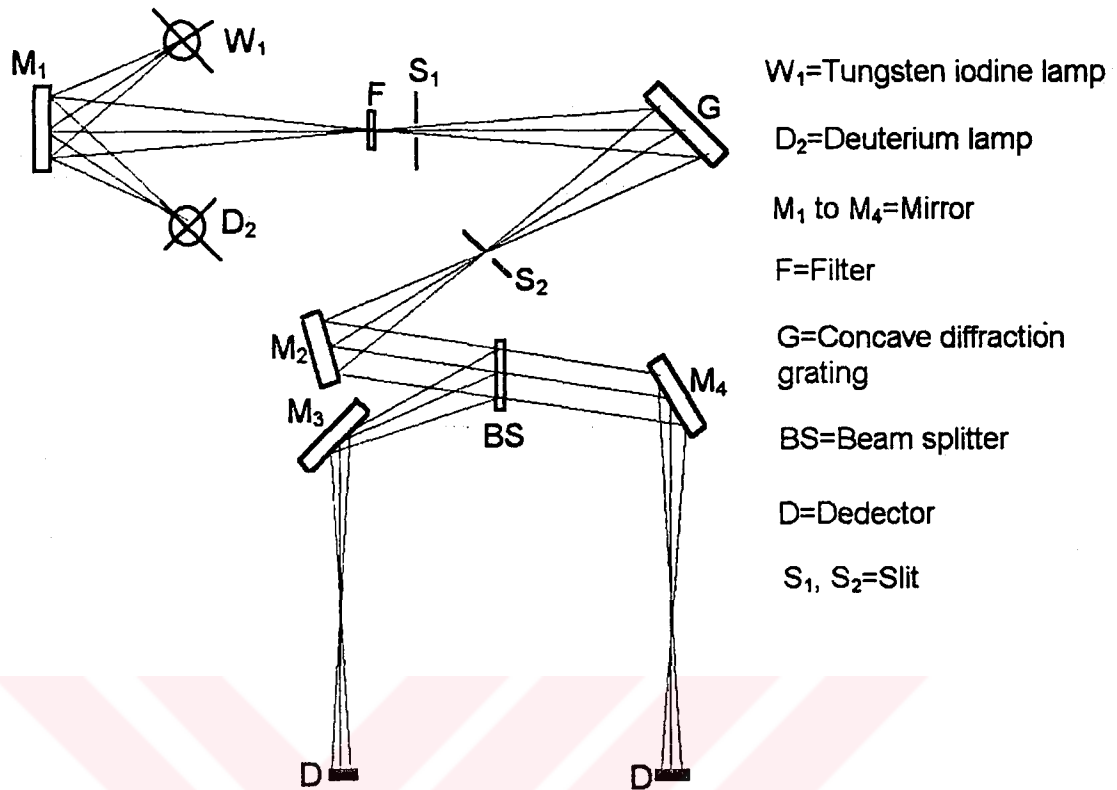
Figure 15. The block diagram of the optical absorption spectrophotometer system.

3.6 Glow curve and Optical Absorption Deconvolution Procedure

The studies of thermally stimulated processes like thermoluminescence (TL) and optical absorption bands yield information on defect centers in solids. TL has been recognized that information about the trapping levels can be extracted from the glow curve [173-176] and absorption spectra gives the models about the defect structure in the crystalline solids [168]. Computerized glow curve analysis is now used not only for extraction of physical parameters but also for dosimetric purposes. Since the avability of the personal computer the decomposition of the glow curve in its individual glow peaks has become very popular [177-183]. However, it can be noted that

different models, approximations and minimization procedures are used for the glow curve analysis. As a consequence one may wonder whether the results of the glow curve analysis reflect properties of the TL material and/or irradiation conditions or should be ascribed to artifacts of the analysis procedure used in the computerized glow curve fitting.

In this study, the TL glow curves and also optical absorption spectra were analyzed using a computerized glow curve and absorption spectra deconvolution technique (CGCD-CASD) developed at the IRI, Delft, Netherlands [184]. Each peak in the glow curve is fitted to the first-order Randal-Wilkins model. Additionally, each band in the absorption spectra is fitted to the Gaussian function given in Eq.37. The computer program is based on the Marquardt algorithm to obtain minimum chi-squared. A computerized curve fitting program constructs an absorption spectra or glow curve using the initial values of the input parameters and compares the computed curve with the experimental curve. The values of parameters are then sequentially varied until a best fit is obtained.

As a measure of the 'goodness-of-fit' the figure of merit (FOM) has been used. This quantity is defined as [185-186]:

$$FOM = \sum_{J_{start}}^{J_{stop}} \frac{|y_j - y(x_j)|}{A} \times 100$$

where FOM=figure of merit in per cent, j_{start}=first channel in fitting region, j_{stop}=last channel in fitting region, y_j=content of channel j, $y(x_j)$=value of fitting function in the middle of channel j, and A=the integral of the fitted glow curve. The reason for taking this value instead of the well known chi squared is that the standard deviation σ_j of the TL intensity in channel j is not a priori known. It is worthwhile noting that all programs in the intercomparision used a 'chi squared' in which the factor $(1/\sigma_j)^2$ was set equal to one. This means that the value of this chi squared will vary with the intensity and that its value in

general will not be equal to one for a good fit. As the FOM value is expressed in per cent it is a more suitable measure for comparing the fit results of different glow curves.

CHAPTER 4

The Investigation of Defect Structures in LiF:Mg,Ti (TLD-100) after β-irradiations

4.1 Introduction

LiF:Mg,Ti (TLD-100) is a thermoluminescence (TL) material developed by Harshaw Chemical Company for use in dosimetry. Pure LiF is a poor TL emitter, but the addition of Mg and Ti impurities makes it an efficient TL phosphor. Owing to its application in TL dosimetry, TL studies on LiF:Mg, Ti have received a wide attention. In the last years many efforts have been made to understand the basic mechanism of TL. These studies are expected to provide guideline for understanding the TL process in other alkali halide as well.

The knowledge of the authentic structure of defects in the LiF:Mg,Ti thermoluminescence dosimetry material would promote the understanding of the TL process, but incorrect structure identification can be misleading. Therefore, in the last years, numerous investigations have been carried out concerning the nature of the trapping centers and as a result two distinct models have been developed, both based on Mg^{+2} impurity ions as part of centers acting as electron traps. The detail informations about these models

77

were given in the literature survey and in the theory sections of this thesis. However, suffice it to say that, one models interprets dipoles formed by Mg^{+2}-cation vacancies [5-16] as acting trapping centers, and the other model is based on Z-centers formed by pairs of Mg^{+2}-electron occupied anion vacancies [69-85].

In determining the nature of the trapping centers in LiF:Mg,Ti, there are two problems. One is the atomic nature of the trap, and the other is whether it is an electron or hole that is trapped. To understand the mechanism of TL and nature of the trapping centers in LiF:Mg,Ti, a correlation is often attempted between TL and optical absorption bands. However, the interpretation of the data has not proved to be straightforward owing to extreme complexity of both the optical absorption and the thermoluminescence data of this material. On the other hand, unambigous correlations between given TL peaks and given absorption peaks have rarely proved possible [20, 28-29,107-108].

It has become well established that post and pre-irradiation thermal annealing of TLD-100 drastically alters both the optical absorption and TL curves. In a post-irradiation isothermal (65 ^{0}C) ageing study of the optical absorption and TL, Jackson and Harris [56] found an apparent correlation between the decay of TL peaks 2 and 3 and the absorption band at 380 nm and between peak 4 and 5 and the band at 310 nm. In an earlier study, Grant and Cameron [5] monitored the pre-irradiation isothermal (67 ^{0}C) decay of Mg^{+2}-cation vacancy pairs using dielectric loss and TL measurements and found a correlation between TL peak 2 and the Mg^{+2}-cation vacancy pair concentration. The close similarity between the two decay curves promoted Grant and Cameron to suggest that peak 2 (and peak 3) and the 380 nm band were directly related to free Mg^{+2}-cation vacancy pairs. Furthermore, these and other similar studies maintained that peak 5 (and peak 4) and the 310 nm absorption band were related to higher-order clusters of the Mg^{+2}-vacancy pairs.

First Dryden and Shutter [6] and then Taylor and Lilley [14-16] demonstrated that at higher annealing temperatures the behaviour of the TL peak deviated markedly from the behaviour of the dipoles. In particular, if precipitation of the impurities can be induced the low temperature TL peak is actually seen to increase when at the same time the dipole concentration is clearly decreasing. These observations promted Taylor and Lilley to suggest that the TL peak 2 is not related to Mg at all but is in fact caused by a defect associated with Ti only. Furthermore, Townsend et al. [27], McKeever [28], and Yuan and McKeever [29] examined the emission spectra, the spectra of X-ray induced luminescence, ionic thermocurrents and optical absorption and showed that the TL peak 2 was in fact associated with a complex of a Mg-vacancy dipole/Ti while peak 5 associated with trimer/Ti complex.

The second model was developed by Kos and Nink [69] that they have experimentally identified the absorption band in TLD-100 at 310 nm and 225 nm as due to Z_2 and Z_3-centers, respectively. They have also discovered Z_1 centers, which was formed after 10 hr of F-band bleaching. Mehta et al. [83] added to this Z_2 center hypothesis that the band at 380 nm due to Z_2^- center in which Z_2 center has captured an additional electron. According to Z-center model, when the sample is heated, electron is released from the Z_2-center and yield TL peak 5, as follows

$$Z_2 \xrightarrow{\approx 220^0 \, C} Z_3 + e$$
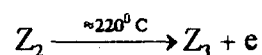
Therefore, the 310 nm band was assigned to the TL peak 5, while 380 nm band was related with peak 2. However, this model has been the subject of substantial criticisms [86-91].

In this chapter, the possible defect structure and nature of trapping centers in LiF:Mg,Ti will be studied with suitable pre-irradiation and post-irradiation heat treatment. By using these treatments, the change in the thermoluminescence glow curves will be matched with the change in the

optical absorption such that some correlation may be derived. However, the results of the post-irradiation heat treatments alone can not be used to determine the structure of the defect centers, but it can provide information about the trapping parameters.

4.2 Results

4.2.1 Curve Fitting

In order to obtain more detailed informations on the number of present bands, we have carried out computerised curve fitting of the absorption data using a non-linear least-squares fitting routine for a collection of bands. In the curve fitting routine we assumed each absorption peak to have the form of a Gaussian shape. Each band in the absorption spectra is examined by using the following expression

$$I = \frac{I_0}{\sqrt{2\pi}\sigma} \exp[-(\frac{\nu - \nu_0}{2\sigma})^2]$$

(45)

where I is the peak intensity at the wavelength, I_0 is the peak intensity at the maximum of band and

$$FWHM = 2\sqrt{2\ln 2}\sigma = 2.355\sigma$$

(46)

The TL glow curves were analysed using again a computerized glow curve deconvolution technique (CGCD). This program is capable of simultaneously deconvuluting as many as nine glow peaks from glow curve. Each peak shape is approximated from the first-order TL kinetics by the expression

$$I(T) = n_0 s \exp(-\frac{E_a}{kT}) \exp[-\frac{s}{\beta}\frac{kT^2}{E_a}\exp(-\frac{E_a}{kT})(0.9920 - 1.620\frac{kT}{E_a})]$$

(47)

80

or with the general order TL kinetics by the expression

$$I(T) = n_0 s \exp(-\frac{E_a}{kT})[1 + \frac{(b-1)s}{\beta}\frac{kT^2}{E_a}\exp(-\frac{E_a}{kT})(0.9920 - 1.620\frac{kT}{E_a})]^{\frac{b}{1-b}} \quad (48)$$

where the symbols have the usual meaning.

The optical absorption spectrum of β-irradiated TLD-100 at room temperature following a standard heat treatment noted in the caption is shown in figure 16. There are two prominent absorption bands with peak wavelength
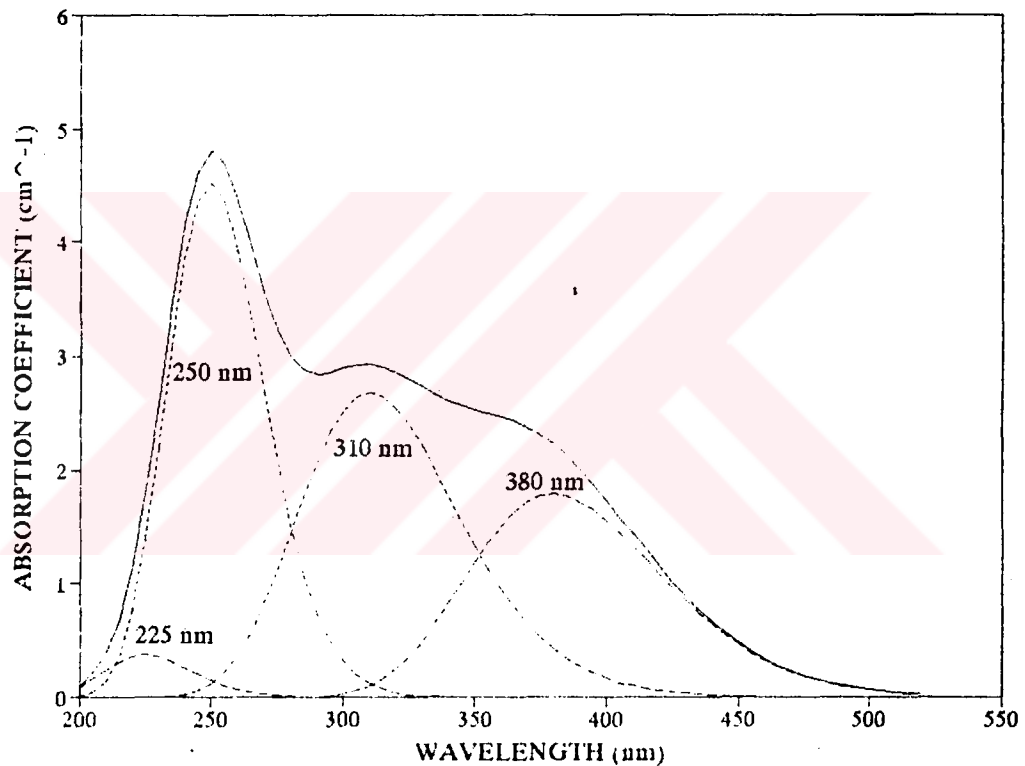
Figure 16. The deconvoluted optical absorption spectrum measured at room temperature into individual Gaussian peaks. The samples were subjected to a standart annealing at 410 ^{0}C for 30 min and rapidly cooled to room temperature. It has then been irradiated with ^{90}Sr-^{90}Y β rays for 24 hours. Dashed lines: Set of calculated Gaussian-shaped single absorption bands; solid line: theoretical spectrum as the sum of Gaussian bands. The values for the peak position are indicated in the figure.

250 nm and 310 nm. Additionally, the smaller absorption bands peaked at 380 nm and 225 nm are observed if an additional pre- and post-irradiation annealing heat treatment is not applied to the samples. The energetic positions E and the full-width at half-maximum (FWHM) are represented in table 4.

Table 4. Peak position and FWHM of β-ray induced optical absorption band in LiF:Mg,Ti (TLD-100) at room temperature.

Peak Wavelength (nm)	Peak Energy (eV)	Full-Width at Half Maximum (FWHM) (eV)
225	5.52	0.93
250	4.97	0.85
310	4.00	0.91
380	3.26	0.73

The absorption band centered at 250 nm, which is also produced in the irradiated pure LiF, is known to be due to F centers [168]. The characteristics of this band obtained from the optical absorption of irradiated LiF showed that its absorption band is somewhat asymmetric about λ_{max}=250 nm (E_m=4.97 eV), as the high-energy side of this band ($E>E_m$) was about 20 % wider than the low-energy side ($E<E_m$). However, Landreth and McKeever [98] examined the inaccuracy introduced by assuming a symmetrical Gaussian shape band for this center in a pure LiF and showed that the inaccuracies introduced by assuming a normal Gaussian shape are minor compared to the height of the peak and that the value of E_m is approximately the same in both cases.

Therefore, in view of the fact that the inaccuracy of the Gaussian fits is minor, compared with the peak heights, we proceeded to fit the complete absorption curve of figure 16 assuming a normal Gaussian shape for each peak present.

To see the inaccuracy of the Gaussian fits, firstly, we tried to fit the experimental data in figure 16 to five peaks. However, the computer curve fitting program indicated that the fifth band have always minor importance when compared with the interstitial of the other bands. The best-fit is always obtained when the experimental results are fitted with four bands.

4.2.2 Annealing Studies

The samples were subjected to the pre and post-irradiation annealing sequence at different temperatures with different times to examine the possible defect structure in LiF:Mg,Ti. When the absorption spectras are deconvoluted into their peak components, the variation in the height of the individual peaks can be seen more clearly as a function of pre-irradiation and post-irradiation annealing temperature.

Figures 17a and 17b show the effect of the pre-irradiation annealing treatment at 80 ^{0}C for six hours and 24 hours on the absorption spectra. As can be clearly seen that the Mg related absorption on the high-wavelength side of the F-band (λ=250 nm) shows a strong temperature dependence. A major change can be seen on the 380 nm band. This band highly decreased with pre-irradiation heat treatment at 80 ^{0}C for both 6 and 24 hours cases. The band at 310 nm increases with heat treatment at 80 ^{0}C for 6 hours, but a small decrease seen if the sample is held at 80 ^{0}C for 24 hours. There is no remarkable change in the band at 225 nm for both treatments. Similar effects are observable when the samples are subjected pre-irradiation heat treatment at 100 ^{0}C, except that the 310 nm band decreased for both cases as shown in figures 18a and 18b.

Figure 17. The effect of the pre-irradiation heat treatment on the optical absorption spectra of LiF:Mg,Ti at 80 ^{0}C for an annealing time a-) 6 hours b-) 24 hours. Dashed curves (a) 225 nm, (b) 250 nm, (c) 310 nm, (d) 380 nm show the resolved bands.
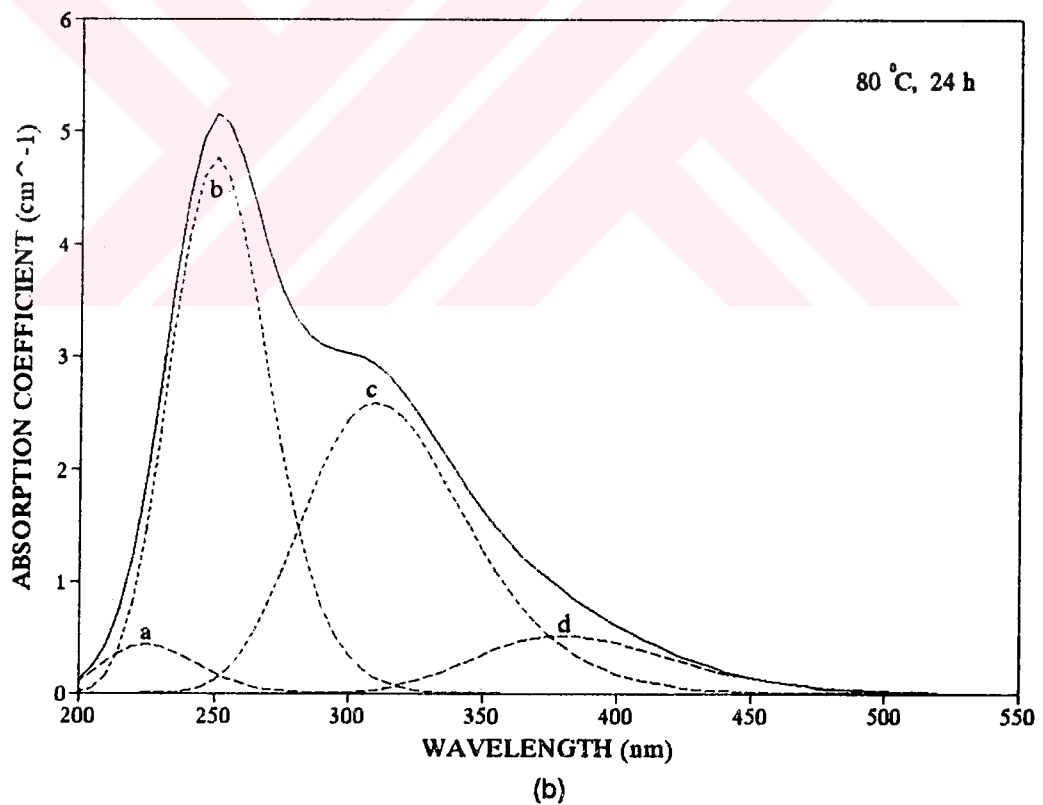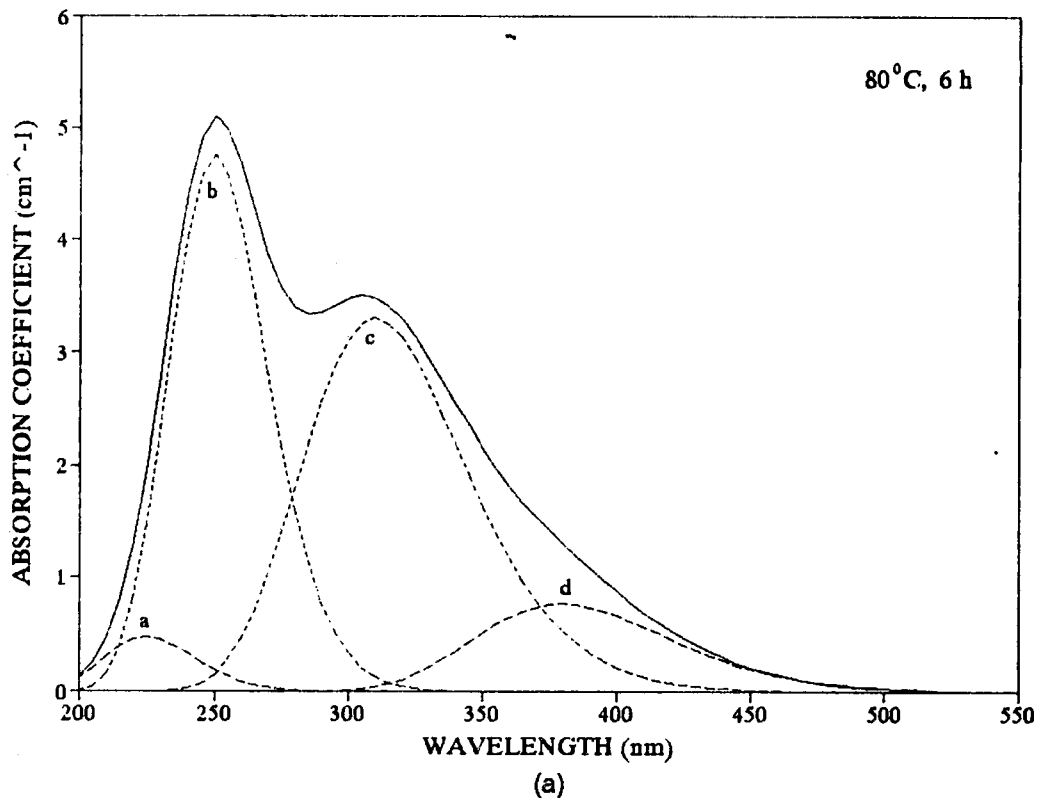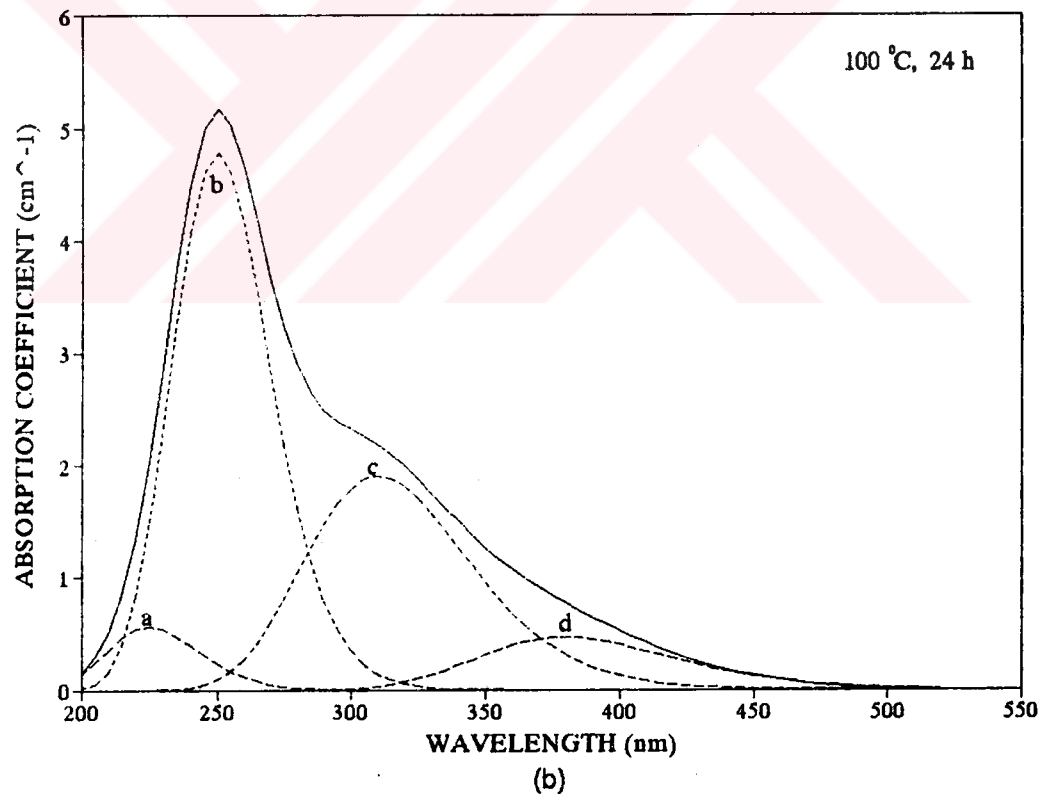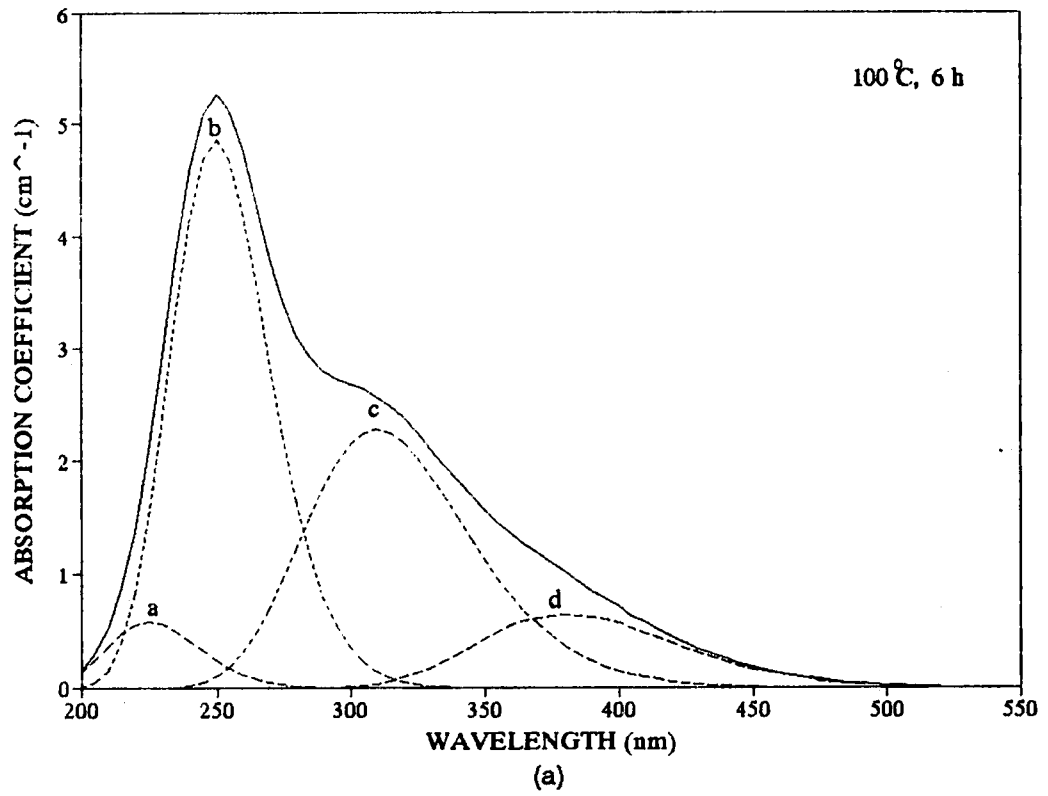
84

Figure 18. The effect of the pre-irradiation heat treatment on the optical absorption spectra of LiF:Mg,Ti at 100 ^{0}C for an annealing time a-) 6 hours b-) 24 hours. Dashed curves (a) 225 nm, (b) 250 nm, (c) 310 nm, (d) 380 nm show the resolved bands.

The drastic effects on the absorption spectras are seen when the samples are annealed at temperatures between 100 and 200 ^{0}C for six and 24 hours. The bands at the high wavelength sides of F-band are highly decreased, while the band at low wavelength side of F-band always increased with annealing time. The effect of the pre-irradiation heat treatment on the 250 nm (F-band) is not efficient. However, when the band height is normalised, it can be seen that there is a small increase in the F-band. The computer curve fitting program indicates that a new optical absorption band grows at around the 282 nm (4.4 eV) after these temperature treatments as shown in figures 19 to 22. This new band (282 nm) is always resolvable when the samples are annealed at 125 ^{0}C or higher temperatures for 24 hours before the irradiation. The height of this band is always higher for 24 hours annealing than that for 6 hours annealing at 125 ^{0}C and 175 ^{0}C. The height of this band increases with pre-irradiation heat treatment temperature up to 175 ^{0}C and then seems to decrease with further increase in the annealing temperature. It should be pointed out that this band was not resolvable when the pre-irradiation heat treatment is not applied to the samples. However, Critteden et al. [23, 64] indicate that it can be clearly resolved when the measurements are done at liquid nitrogen temperature.

Figure 19. The effect of the pre-irradiation heat treatment on the optical absorption spectra of LiF:Mg,Ti at 125 ^{0}C for annealing time **(a)** 6 hours; **(b)** 24 hours. Dashed curves **(a)** 225 nm, **(b)** 250 nm, **(c)** 310 nm, **(d)** 380 nm, **(e)** 282 nm show the resolved bands.
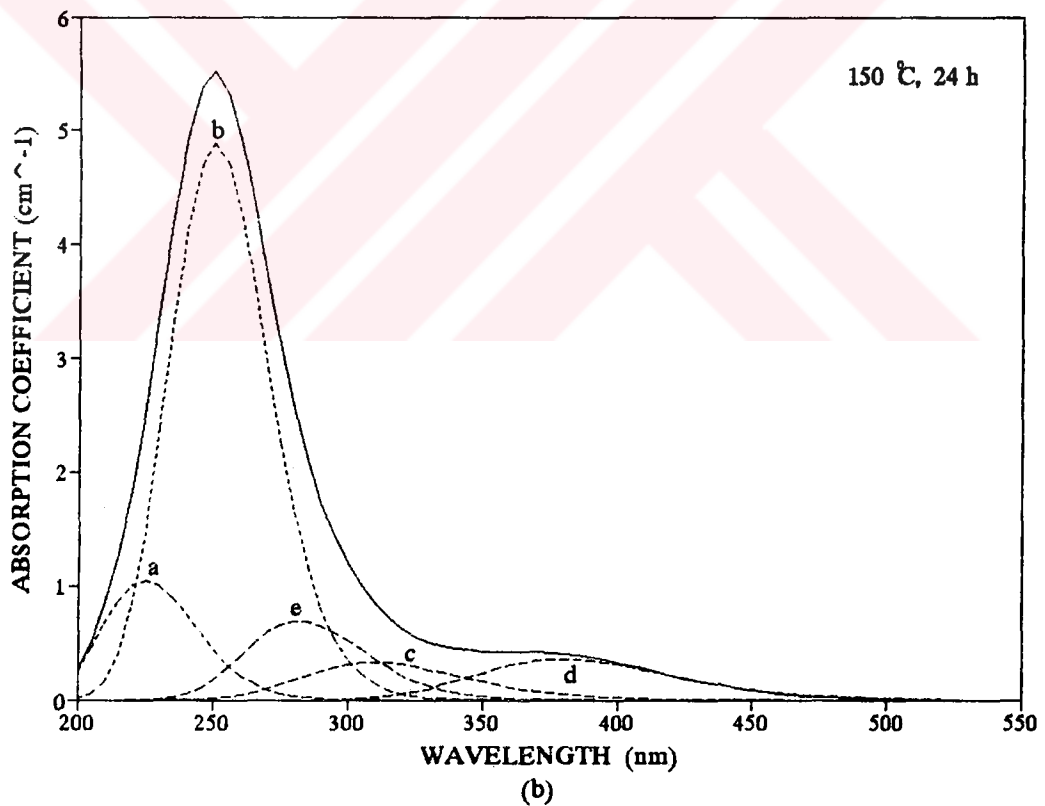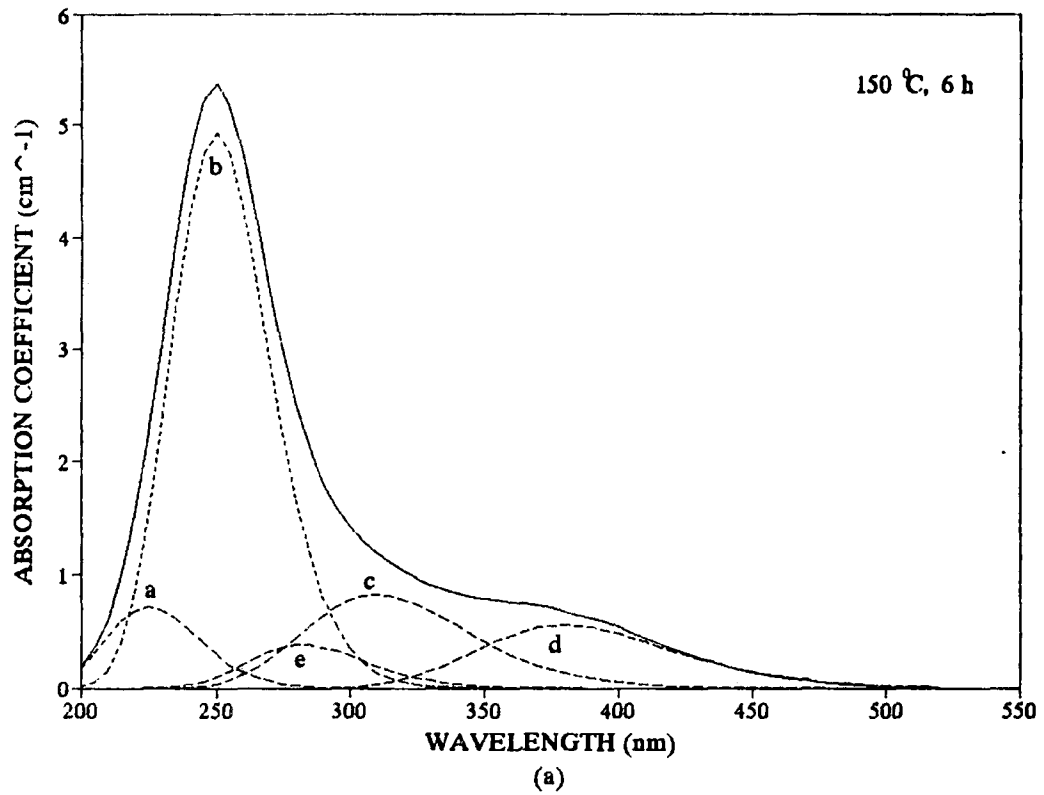
Figure 20. The effect of the pre-irradiation heat treatment on the optical absorption spectra of LiF:Mg,Ti at 150 °C for annealing time **(a)** 6 hours; **(b)** 24 hours. Dashed curves **(a)** 225 nm, **(b)** 250 nm, **(c)** 310 nm, **(d)** 380 nm, **(e)** 282 nm show the resolved bands.

Figure 21. The effect of the pre-irradiation heat treatment on the optical absorption spectra of LiF:Mg,Ti at 175 ^{0}C for annealing time **(a)** 6 hours; **(b)** 24 hours. Dashed curves (a) 225 nm, (b) 250 nm, (c) 310 nm, (d) 380 nm, (e) 282 nm show the resolved bands.
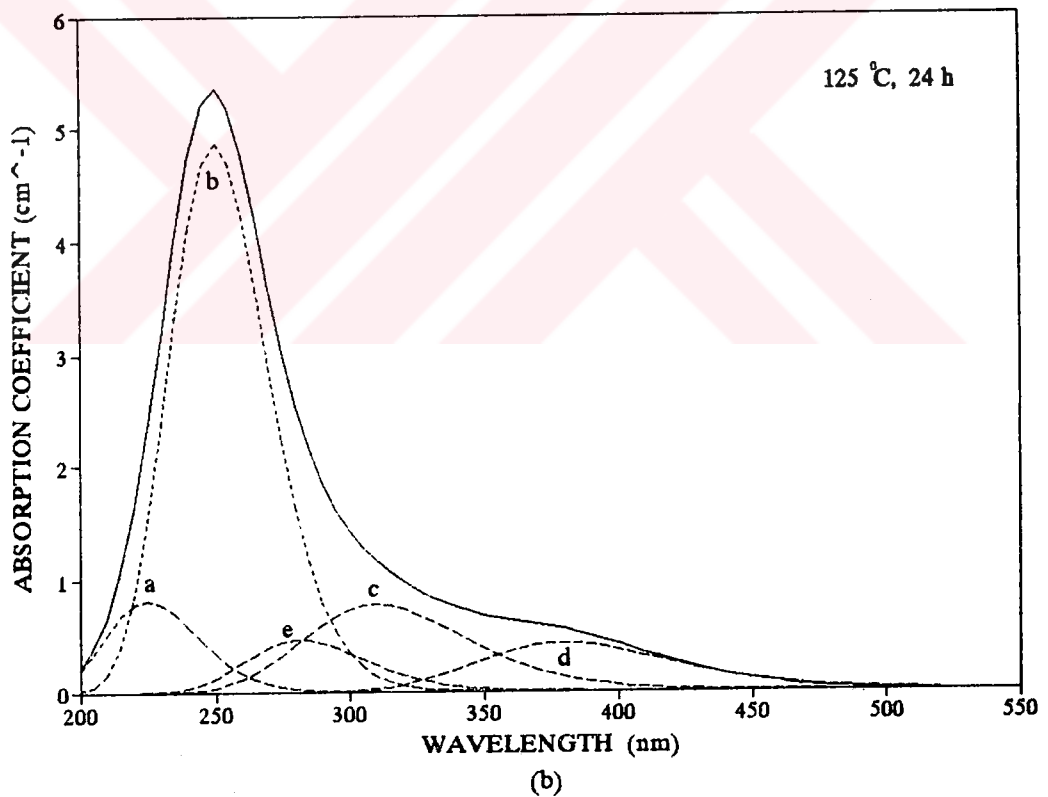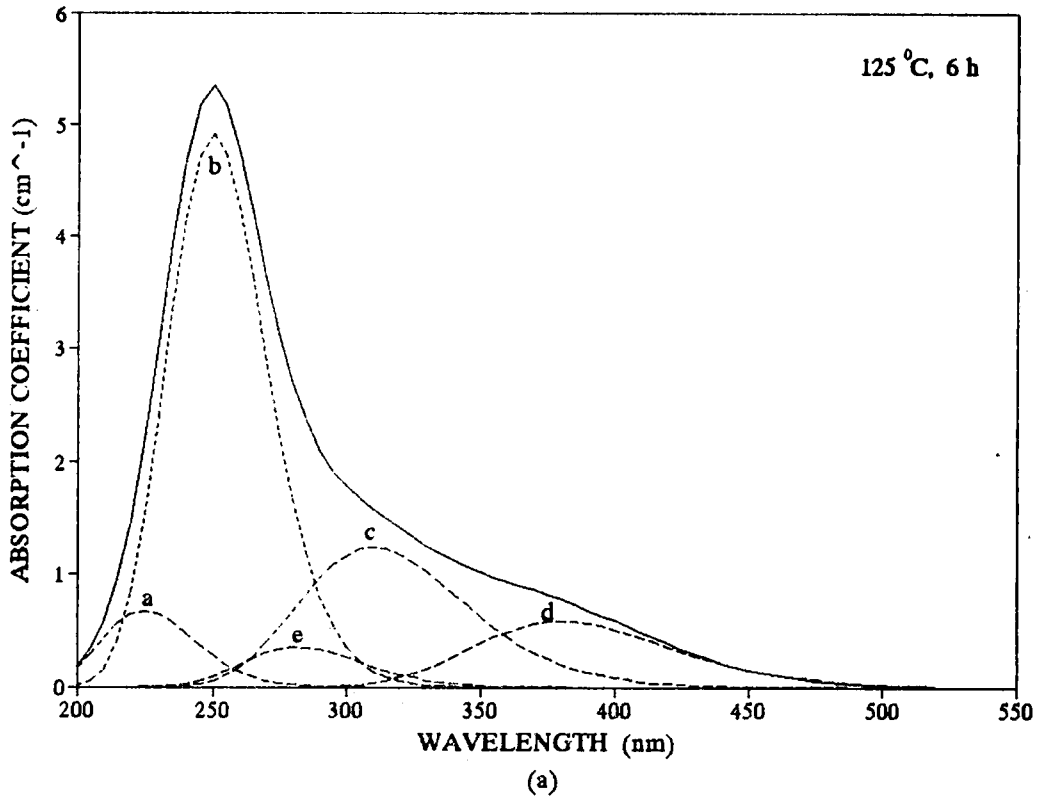
Figure 22. The effect of the pre-irradiation heat treatment on the optical absorption spectra of LiF:Mg,Ti at 200 ^{0}C for annealing time **(a)** 6 hours; **(b)** 24 hours. Dashed curves (a) 225 nm, (b) 250 nm, (c) 310 nm, (d) 380 nm, (e) 282 nm show the resolved bands.
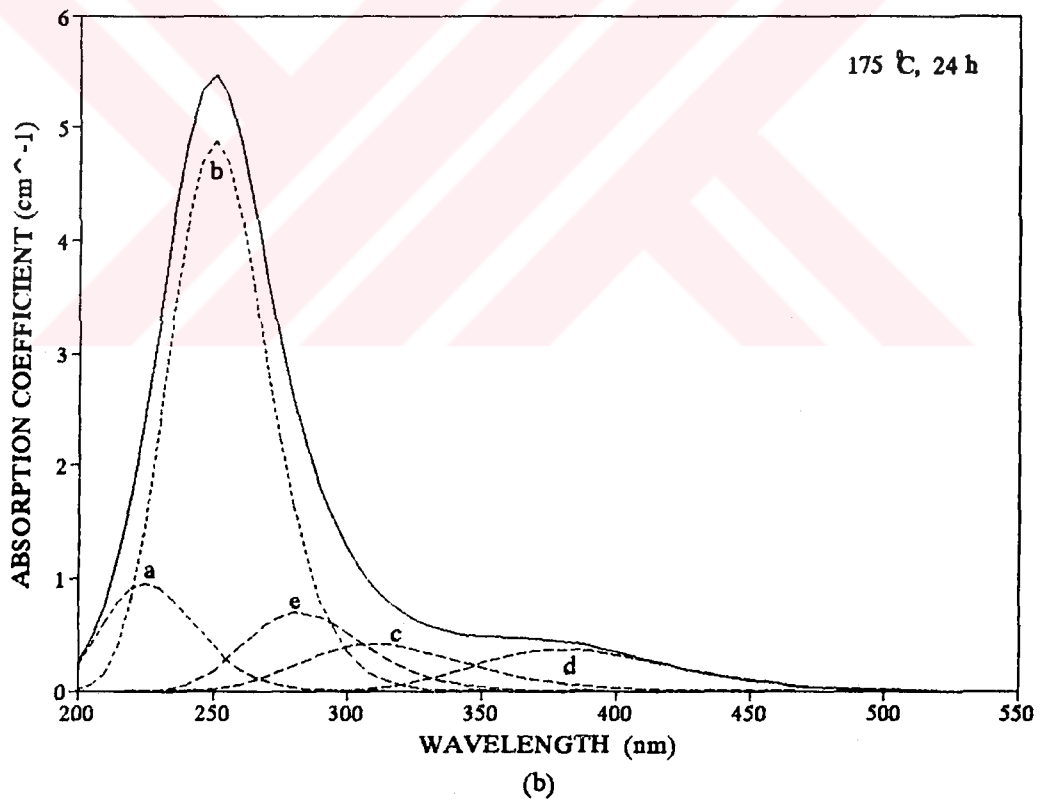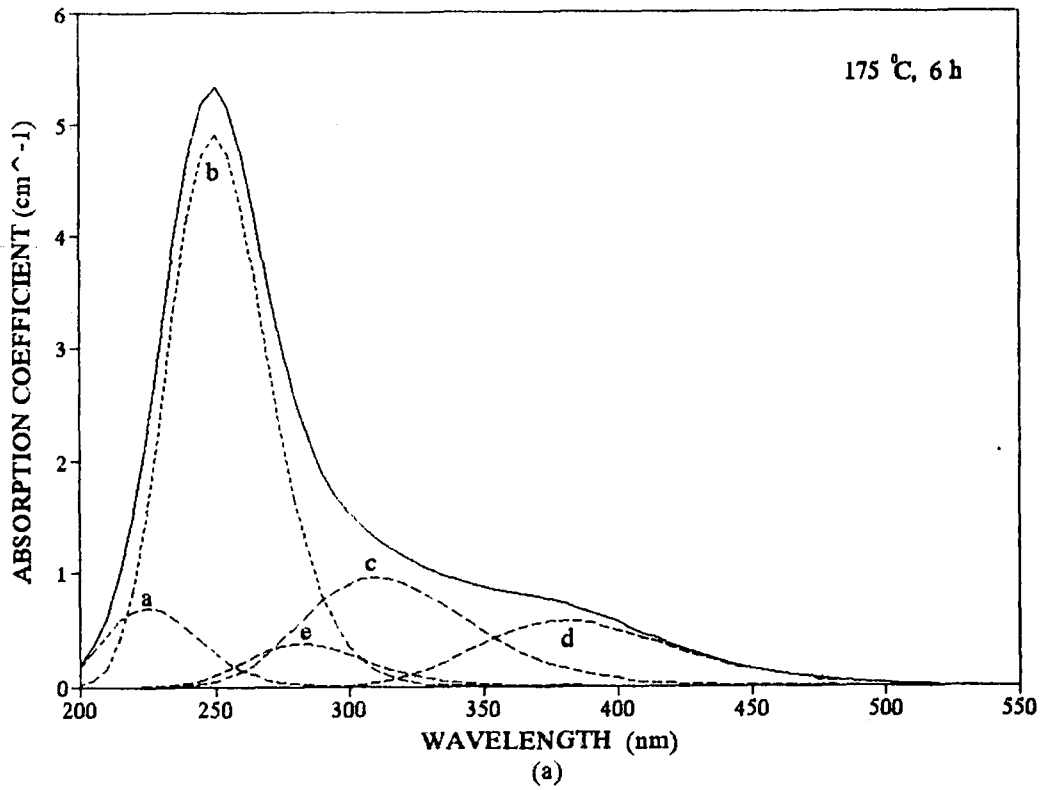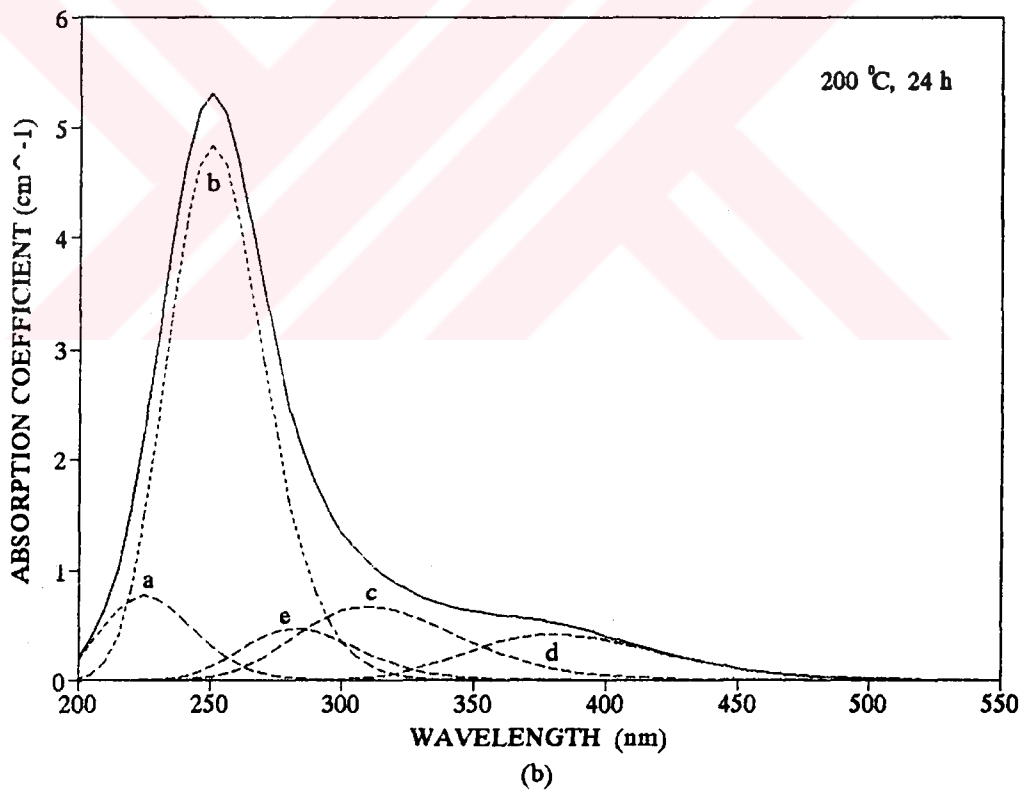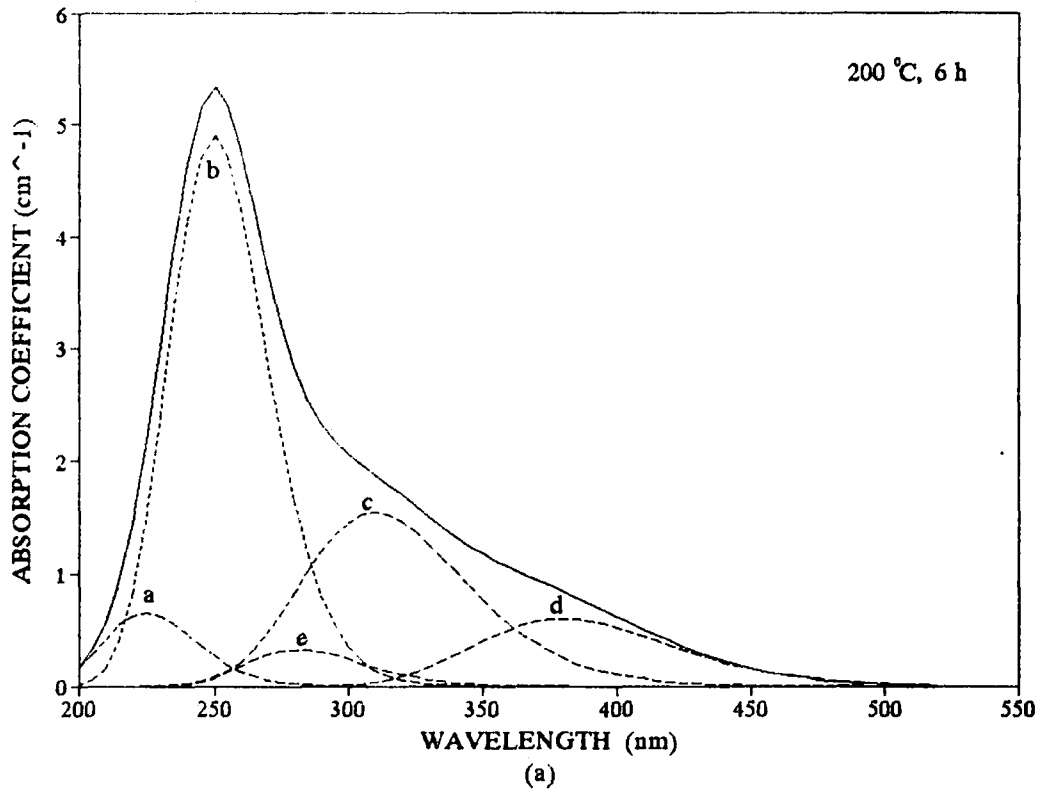
90

Figures 23a and 23b show the variation of the heights of the 380 nm , 310 nm , 282 nm, 250 nm and 225 nm bands as a function of the pre-irradiation annealing temperature for 6 and 24 hours, respectively. The new band which appears at about 125 ^{0}C increases with annealing temperatures up to 150 ^{0} C and then decreases with higher temperatures. Pre-irradiation heat treatment made very little influence on the 250 nm band. The 225 nm band first slowly increases with temperature up to 150 ^{0}C and then starts to decrease slowly for both annealing temperatures. Remarkable changes occur on the 310 and 380 nm bands. The 310 nm band first makes an initial increase at 80 ^{0}C, sharply decreases with increasing temperature up to 150 ^{0}C and then starts to return to its original height. The 380 nm band shows a similar trend. It first decreases with temperature and then starts increasing with temperature above 150 ^{0}C. These changes take place more profoundly at 6 hours than that of 24 hours annealing.

The effect of a combination of pre- and post-irradiation heat treatment on the absorption spectrum of TLD-100 samples is presented in figures 24a to 24d. The samples were first preannealed at 125 ^{0}C for 6 hours then beta irradiated and then post-annealed at different temperatures. As expected, the absorption spectra decreases with increasing post-annealing temperatures. As seen from figures 24a-24d the bands b, c, and d at the high wavelength side of F-band decreases, while the band a at the low wavelength side of F-band increases with temperature. The new band e appearing at about 282 nm shows a slow increase up to 125 ^{0}C and then steadily decreases with a further increase in temperature. The variation in the height of bands can be seen more clearly in figure 25. The bands seem to follow two different paths; the 225, 282, and 310 nm bands first increase with temperature and then decrease, while 250 nm and 380 nm band, always decrease with temperatures.
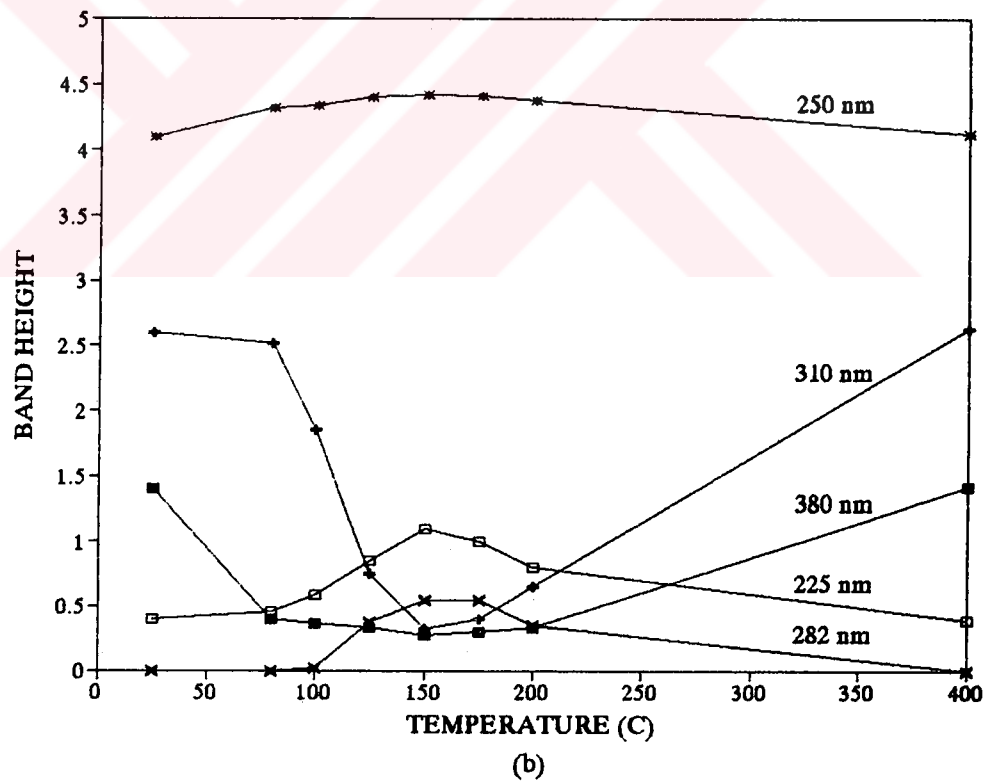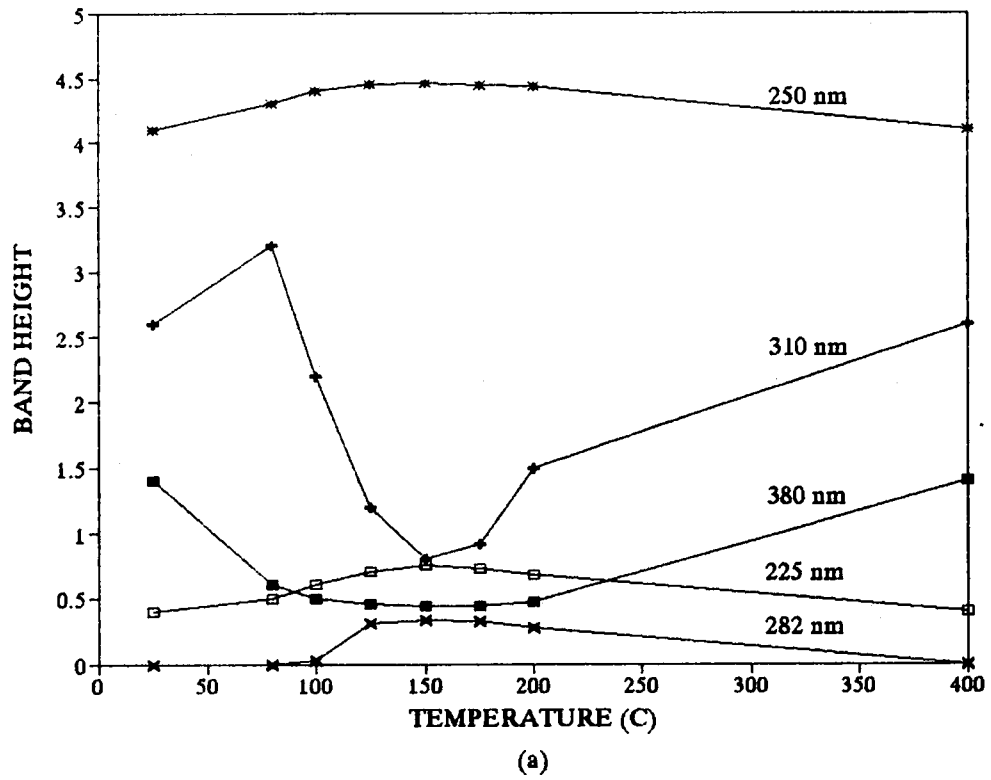
Figure 23. Variation of the optical absorption band heights with pre-irradiation annealing temperature for annealing time (a) 6 hours and (b) 24 hours.

92
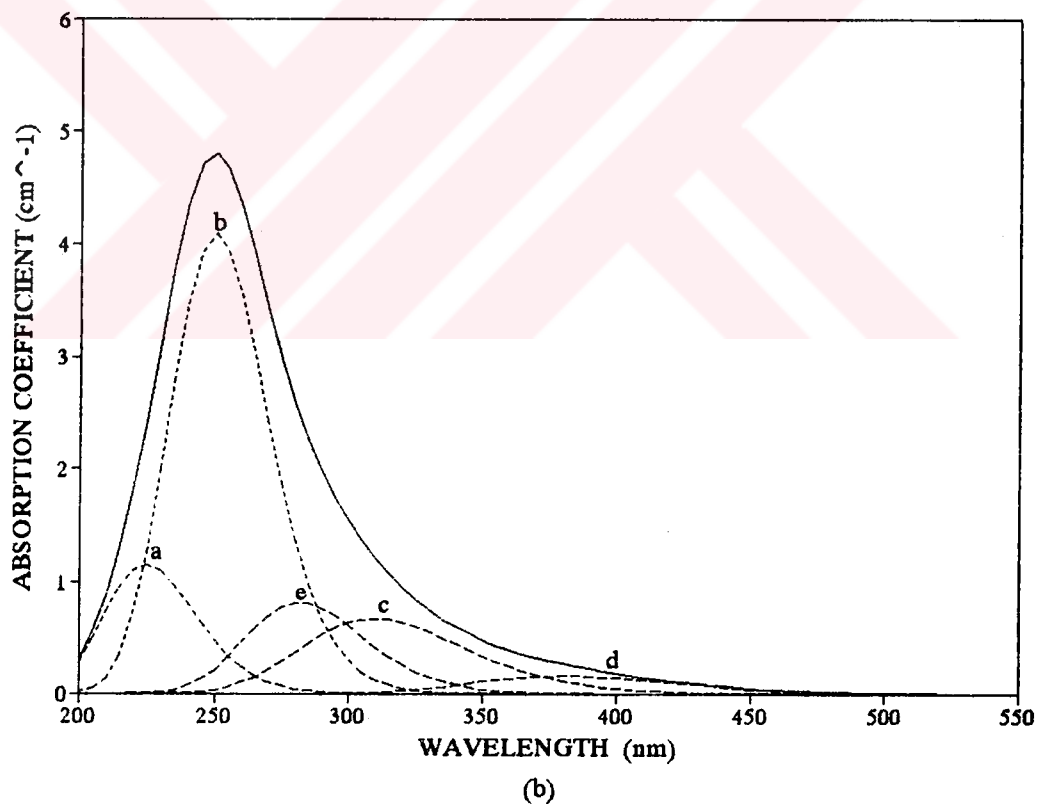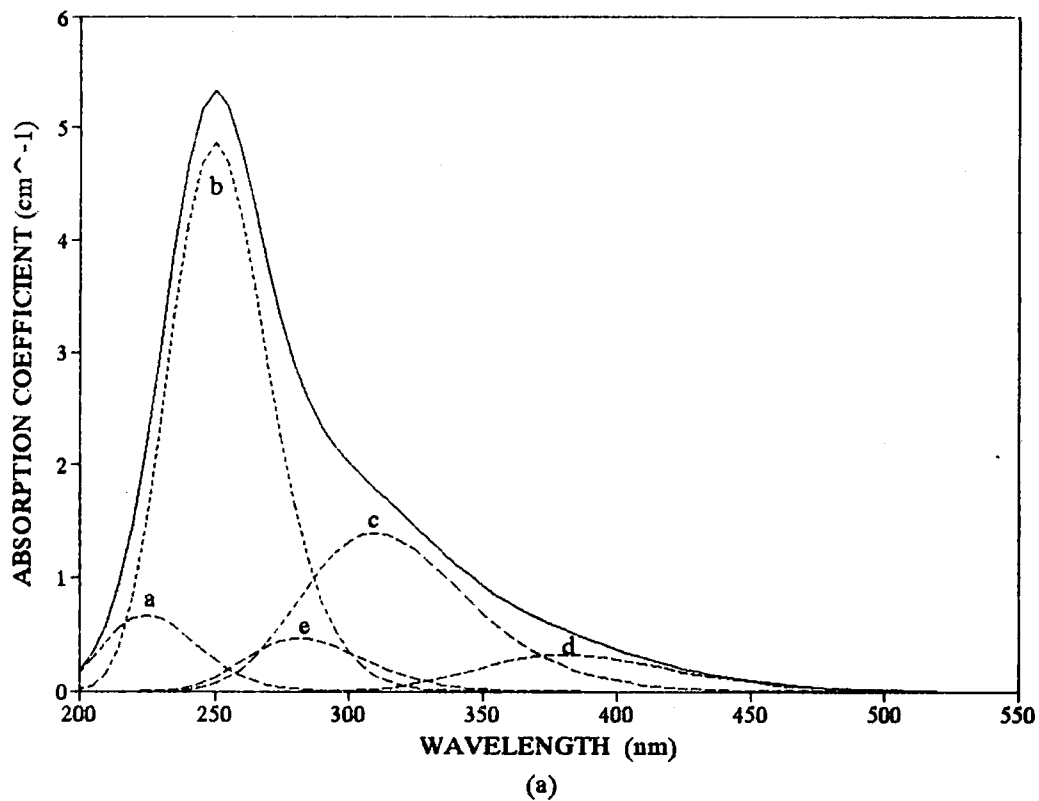
Figure 24a-24b. Optical absorption spectra of LiF:Mg,Ti after a pre-irradiation heat treatment at 125 °C for 6 hours and given subsequent post-irradiation annealing cycles for 5 min at **(a)** 80 °C and **(b)** 125 °C. Dashed curves: **(a)** 225 nm, **(b)** 250 nm, **(c)** 310 nm, **(d)** 380 nm, **(e)** 282 nm.

93
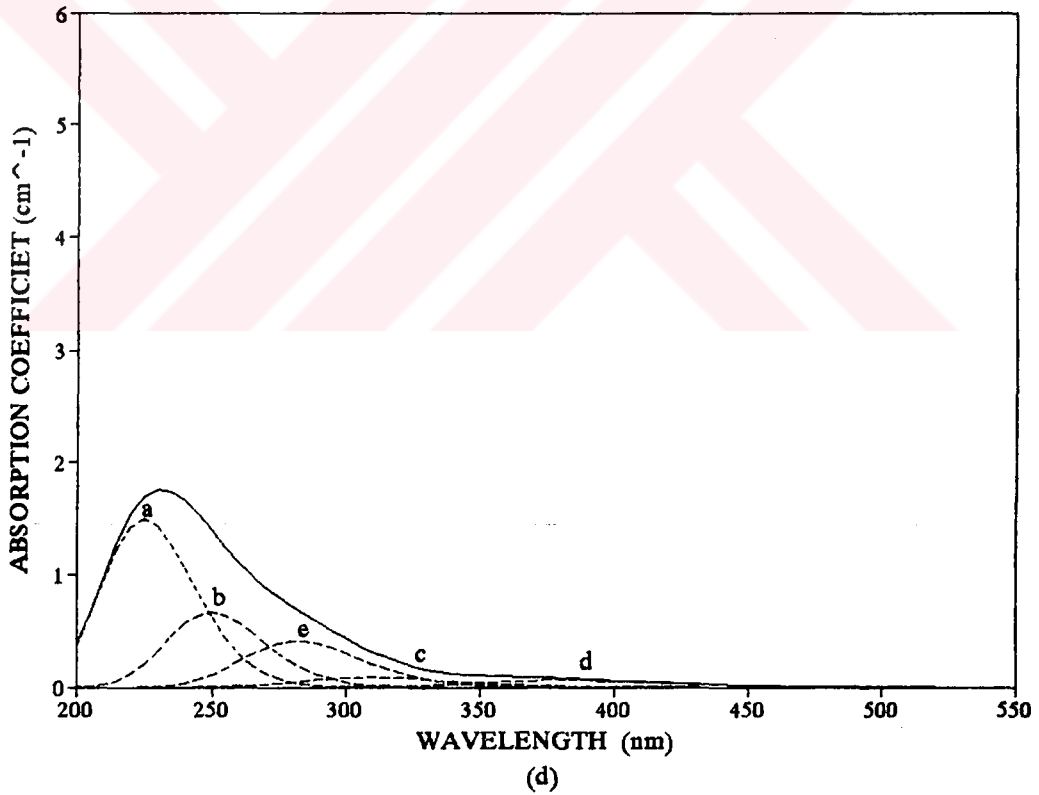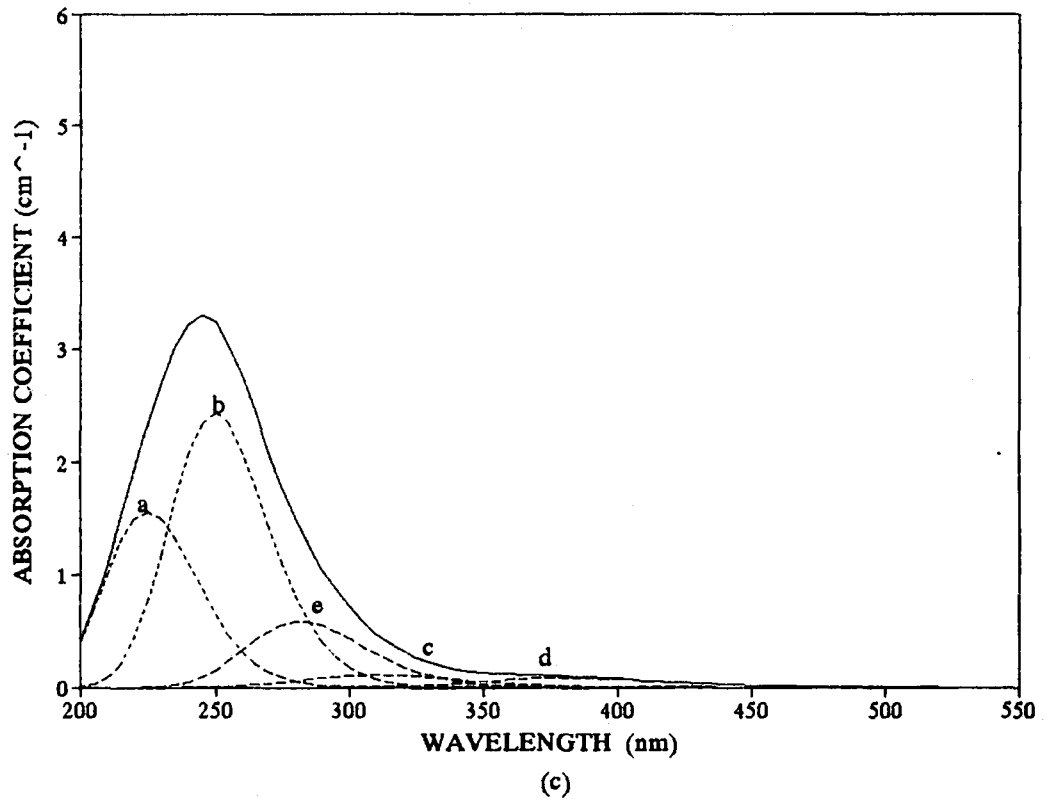
Figure 24c-24d. Optical absorption spectra of LiF:Mg,Ti after a pre-irradiation heat treatment at 125 ^{0}C for 6 hours and given subsequent post-irradiation annealing cycles for 5 min at (c) 200 ^{0}C and (d) 275 ^{0}C. Dashed curves: (a) 225 nm, (b) 250 nm, (c) 310 nm, (d) 380 nm, (e) 282 nm.
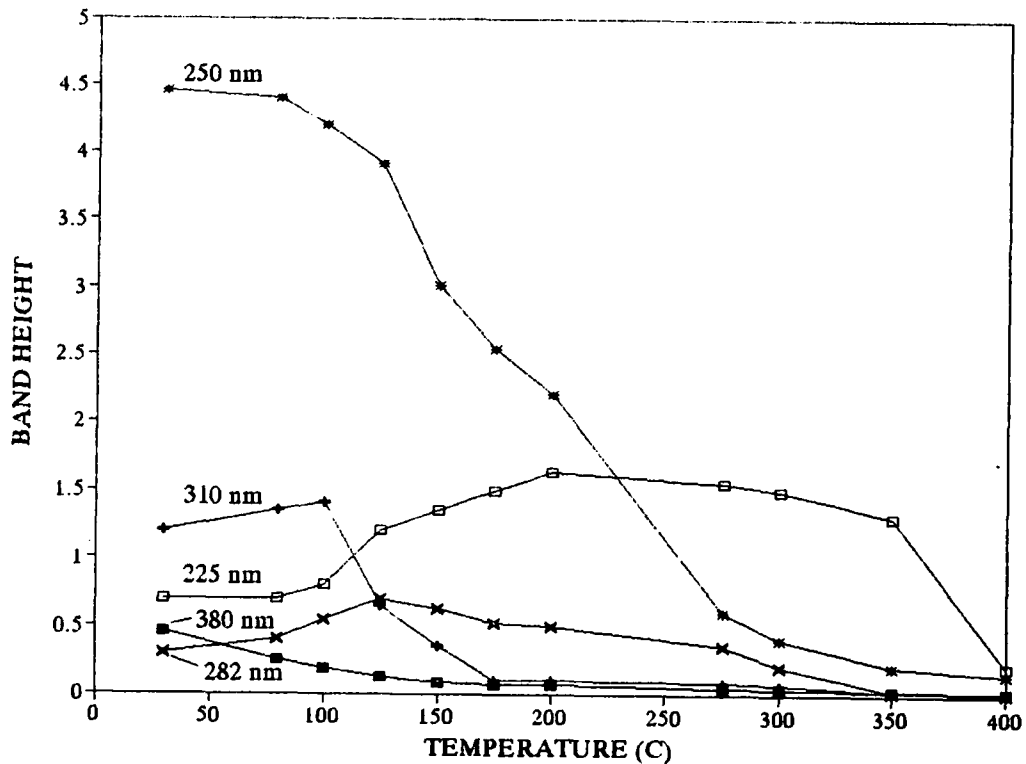
Figure 25. Variation of the optical absorption band heights with post-irradiation annealing temperature for 5 min.

A typical glow curve of a TLD-100 sample received a standard heat treatment and beta irradiation is shown in figure 26. Each peak number is illustrated on the glow curve. The observed peak temperatures depend on the heating rate. For a 2 ^{0}C/s heating rate, the peak temperatures are obtained at approximately 65 ^{0}C (Peak 1), 118 ^{0}C (Peak 2), 160 ^{0}C (Peak 3), 190 ^{0}C (Peak 4), 220 ^{0}C (Peak 5), and 287 ^{0}C (Peak 7).

The composite set of glow curves readout at the same heating rate (2 ^{0}C/sec), annealed for various times at various temperatures is shown in figures 27a-27c. During all of these measurements, an intermediate heating rate 2 ^{0}C/s was used, because, at this heating rate, the peaks are resolved by a little effort using computer curve fitting program. Additionally, at this heating rate, the height of the peaks 4 and 5 are always obtained at the maximum values [8].

95
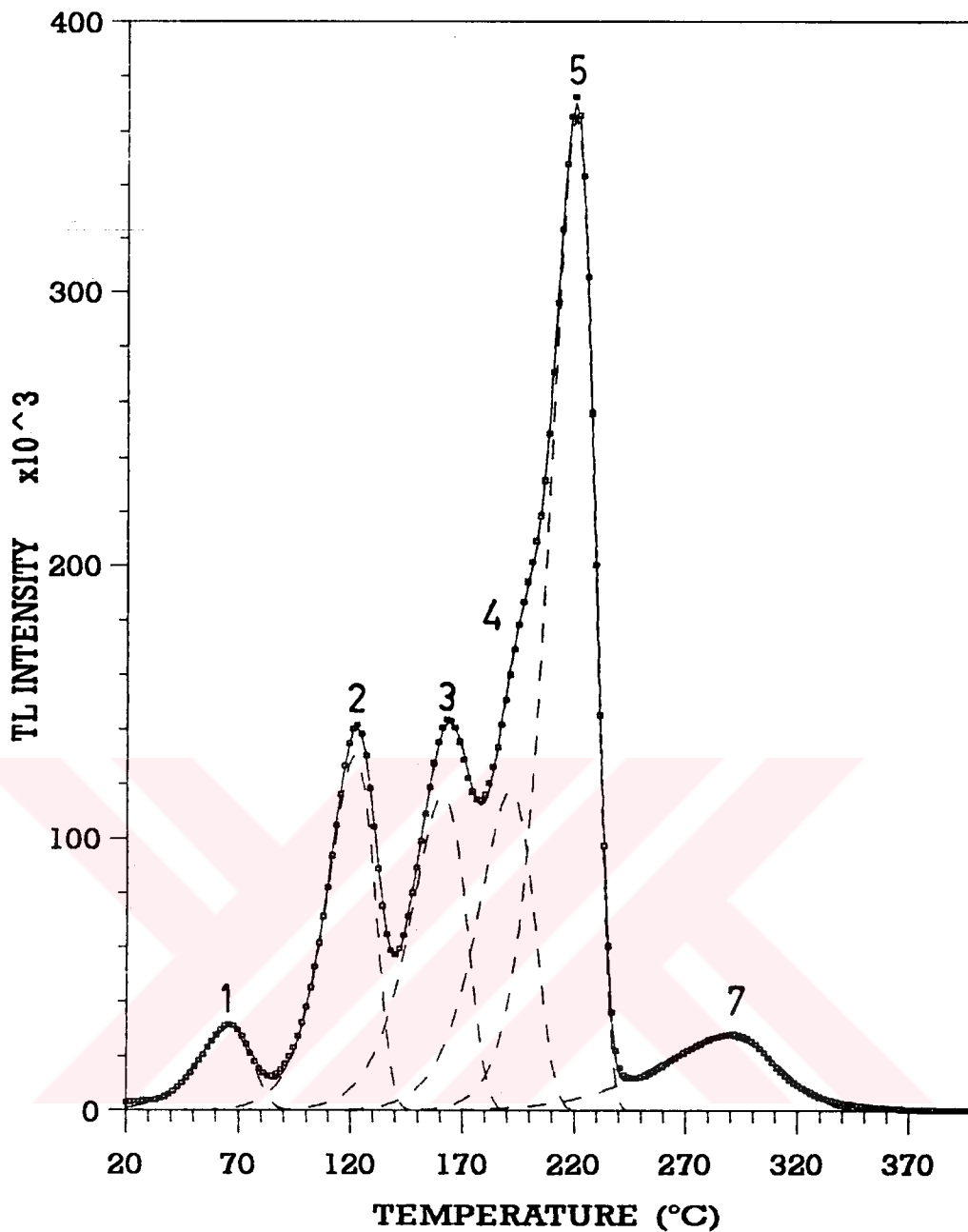
Figure 26. Glow curves of LiF:Mg,Ti (TLD-100) measured after a standart annealing procedure at 400 ^{0}C for 1 hour and rapidly cooled to room temperature. It has then been irradiated with ^{90}Sr-^{90}Y β-rays then analysed by computer glow curve fitting program. In the figures: dots represent experimental data; continues lines is the sum of the deconvoluted peaks and dashed lines are represent deconvoluted individual glow peaks.
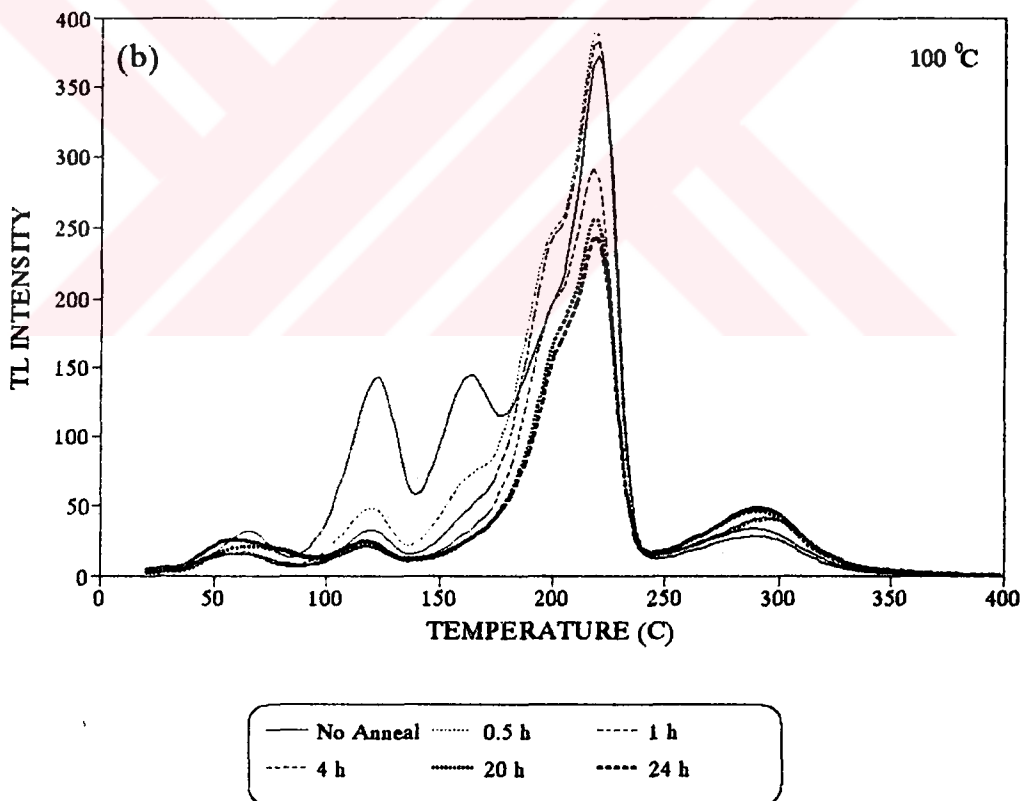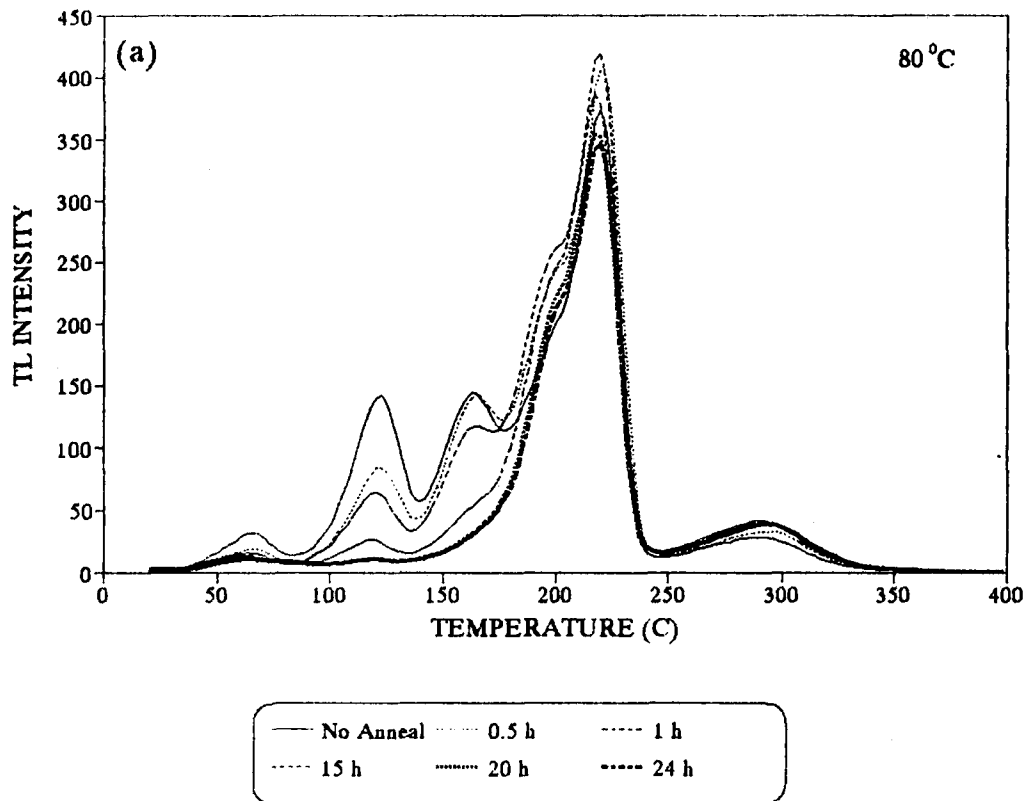
Figure 27a-b. Set of thermoluminescence glow curves for LiF:Mg,Ti (TLD-100) crystals measured after different pre-irradiation heat treatment at (a) 80 °C and (b) 100 °C. All glow curves were read out at 2 °C/sec.
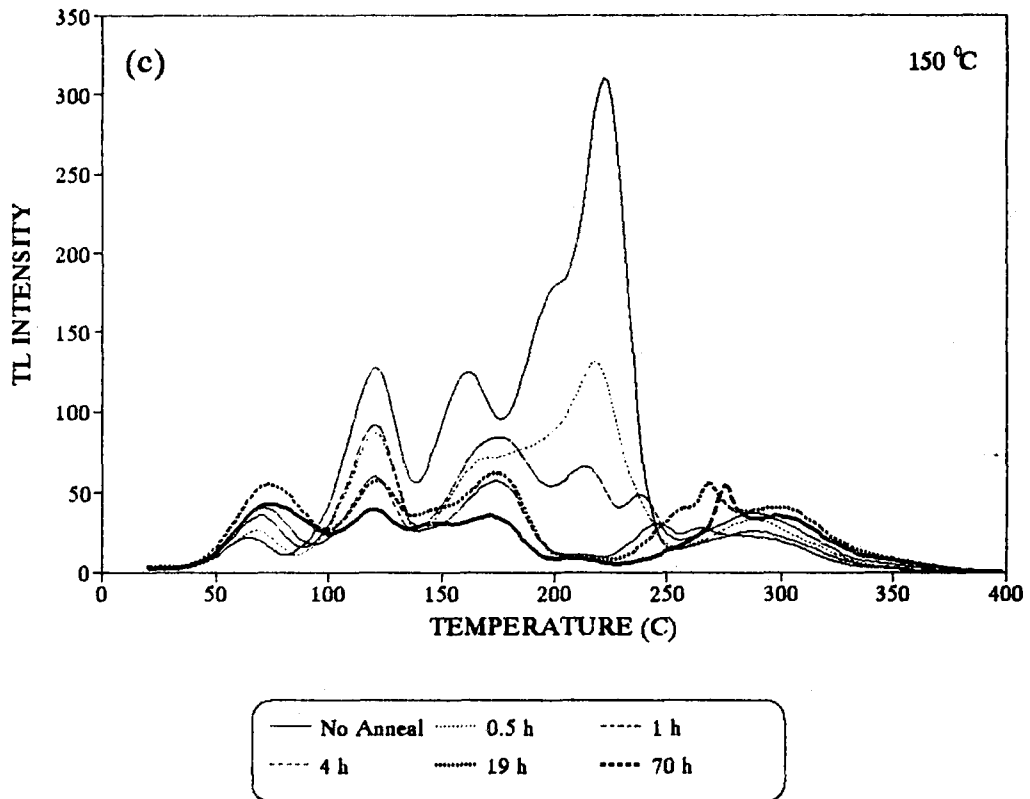
Figure 27c. Set of thermoluminescence glow curves for LiF:Mg,Ti (TLD-100) crystals measured after pre-irradiation heat treatment at 150 ^{0}C. All glow curves were read out at 2 ^{0}C/sec.

The height of each peak varies from the batch to batch of the crystals when also the same heating rate is used. Therefore, in this study, only one crystal chip is used for only one annealing temperature.

From figures 27a and 27b, it is clearly seen that at low annealing temperatures (<100 ^{0}C), the peaks 1, 2, and 3 have decreased and 4 and 5 firstly increased and then decreased with annealing time. During the annealing procedure, peak 4 exhibited very complex behaviour, with the peak becoming significantly narrower and moving towards higher temperature following pre-irradaition heat treatment at low temperature. Therefore, the seperation of peak 4 from peak 5 is very difficult and the physical interpretation of merging of the peak 4 and 5 following annealing procedure at low temperature is very difficult. In some cases, in order to overcome this

98

problem, some authors proposed that if the half-width temperature of peak 4 obtained from the unannealed glow curve is kept constant, peaks 4 and 5 can be easily separated from each other by fitting program [187].

Figure 27c shows a set of the glow curves aged for different times at intermediate temperatures 150 ^{0}C. At this temperature for long annealing times, a new peak grows around the peak 3 and 4. Therefore, the resolution of glow curves at higher annealing times becomes very difficult due to this new glow peak. The normalized peak areas of the glow peaks are presented in figures 28a-28c as a function of pre-irradiation annealing time. The peak areas of the low temperature peaks first decrease, then increase to a maximum value, and then start to decrease again with higher annealing times. However, the first decreasing period takes very long times for annealing temperatures less than 150 ^{0}C. At around 150 ^{0}C, the decaying period of low temperature peaks takes place very rapidly, therefore, it can be stated that at this temperature (150 ^{0}C), the variation of defect structure is more effective than at other temperatures.

The decrease in the intensity of peak 2 and 3 at low annealing temperatures (<80 ^{0}C) follows the same pattern of the decrease in Mg^{+2}-vacancy dipoles. Therefore, Grant and Cameron [5] thought that these peaks are related with Mg^{+2}-vacancy dipoles. At the same time, Harris and Jackson [20] examined the optical absorption band and interpreted that the band at 380 nm follows the same pattern with peaks 2 and 3. Therefore, they concluded that there is a direct relationship between 380 nm absorption band and TL peaks 2 and 3. However, our reults showed that the correlations between Mg^{+2}-vacancy dipoles, peak 2 and 3 intensity and optical absorption band at 380 nm and are not satisfied at higher annealing temperatures for the long annealing times. Examination of the optical absorption bands reveal that the 380 nm band is seen to exhibit the similar behaviour with peak 2 and 3 at low annealing temperatures, especially up to $\approx$100 ^{0}C. After passing this temperature, probably a high aggregation takes place and the band at 380
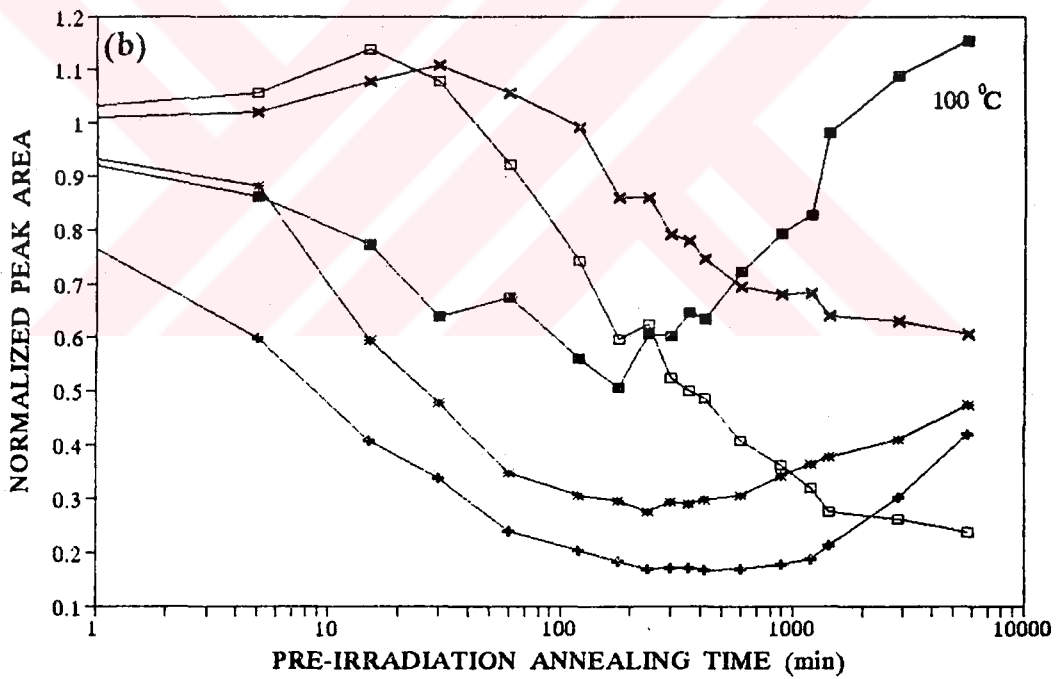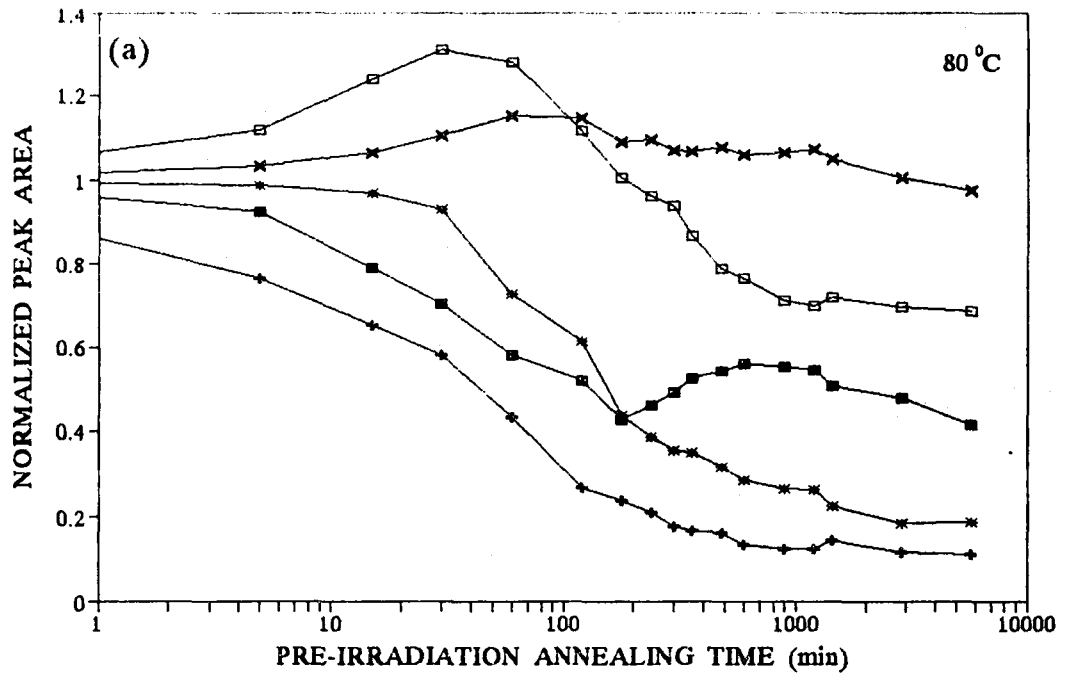
Figure 28a-b. Normalized intensity of deconvoluted glow peaks as a function
of annealig time at (a) 80 °C and (b) 100 °C.
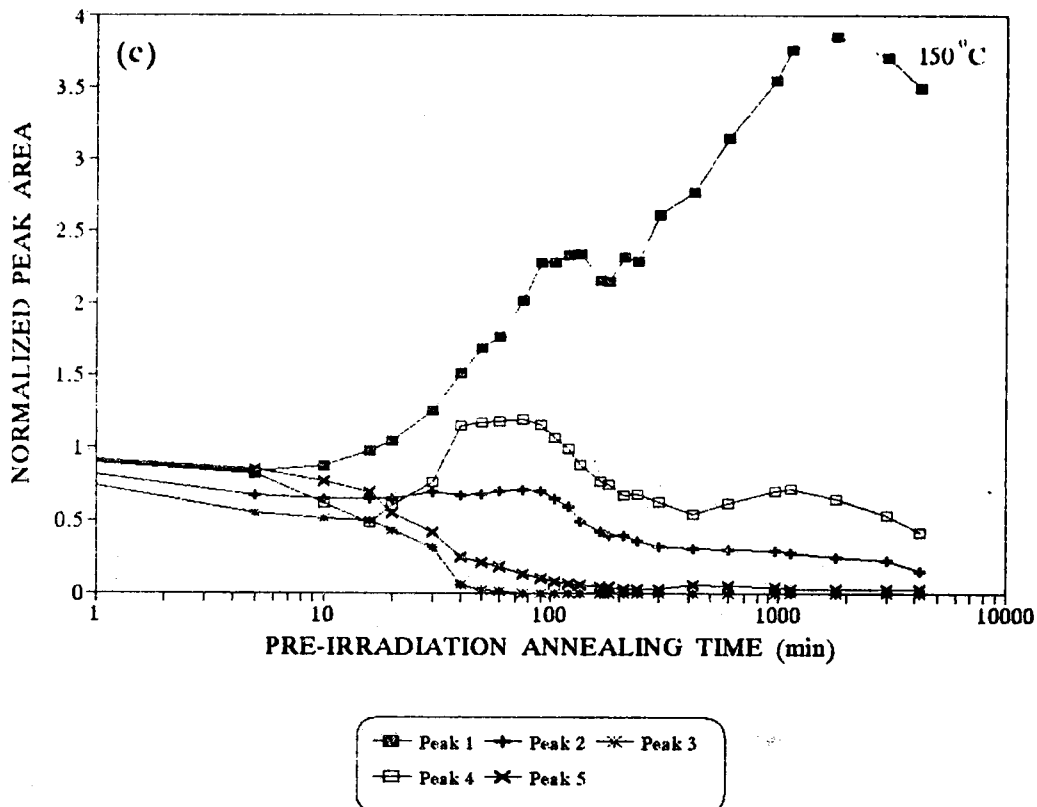
Figure 28c. Normalized intensity of deconvoluted glow peaks as a function of annealig time at 150 °C.

nm drops to its minimum value. At higher annealing temperatures (>150 °C), this band again returns back to its original value probably with trimer dissociation. These results are contrary to the TL peak 2 and 3 intensities, because, according to our results, the band at 380 nm does not follow the same pattern of peak 2 and 3 at these high annealing temperatures. In some cases, the behaviour of TL peak 2 and 3 deviated markedly from the behaviour of 380 nm band and also dipole concentrations. Generally at higher temperatures, the intensities of peak 2 and 3 are first decrease, then increase and reach to a maximum, and then again start to decrease with longer annealing times. This behaviour is not seen on the optical absorption band at 380 nm and dipole concentrations. During the annealing cycles, they always continue to decrease. Thus, it is thought that the peak 2 and 3 is not directly related with dipoles in LiF:Mg,Ti and with the band at 380 nm.

Furthermore, the similar studies maintained that peak 4 and 5 and the 310 nm absorption band are related to higher-order clusters of the Mg-vacancy pairs. If, as suggested, the 310 nm band is related to TL peak 4 and 5, then it will be instructive to examine the decay rate of the 310 nm band and compare it with the pre-irradiation annealing decay of the TL peaks.

The intensity of peak 5 slightly increases and then decreases whereas the peak 4 considerably increases and then decreases at low pre-irradiation annealing temperature. However, at high pre-irradiation annealing temperature ($\geq 125\ ^{0}C$), the intensity of peak 4 and 5 immediately decrease. In the previous paragraphs and chapters, we mentioned that optical absorptions are of the assistance in further determining the identities of specific traps. In this manner, if we again examine the behaviour of the band at 310 nm, its decaying process is similar to the decaying process of peak 5. Really, at lower annealing temperature ($\leq 100\ ^{0}C$), the peak intensity of peak 5 increases as well as the intensities of the band at 310 nm. Therefore, we can conclude that the peak 5 is probably due to the trap at 310 nm band or at least this trap contributes to the intensity of peak 4 and 5.

It is clearly seen from the optical absorption data after high-temperature annealing ($125-175\ ^{0}C$) that the initial values of the absorption band at the high-wavelength sides of the F-band (250 nm) is non-zero. Additionally, a new band always becomes evident at around 282 nm. The existence of this band is very effective after thermal annealing at $125\ ^{0}C$ and $175\ ^{0}C$ above 20 hours and at $150\ ^{0}C$ above six hours.

In the previous paragraphs, we also pointed out that for long annealing times at higher annealing temperatures a new glow peak grows between peak 2 and 4. Kathuria and Moharil (1983) [134] have employed the same thermal treatments (23 h at $150\ ^{0}C$) to measure the trapping parameters for peak 4. These authors found that this annealing procedure reverses the relative intensities of peak 4 and 5, thus producing a glow curve in which, apparently, peak 4 is preponderant. In another paper, Moharil and Kathuria (1985) [115]

worked on the TL and PTTL glow curves and they reported that peak 4 can be found in PTTL glow curves when this material is annealed for 23 h at 150 ^{0}C. However, Delgado et al. (1987-1988) [118-119], recently, pointed out that annealing treatments at 150 ^{0}C induce a new glow peak to appear at temperatures between those of peaks 2 and 4. This new peak should not be confused with peak 4, which is effectively destroyed by these thermal treatments, as is also other previously peaks 2, 3, and 5. This doubt was also supported by the relatively important difference in peak temperature between the peak 4 in unannealed TLD-100 and the peak produced by the above mentioned heavy annealing treatment. They also pointed out that this new peak is repopulated by UV light, contrary to peak 4. If it is so, it can be considered that this new peak originating with an electron-type trap.

Figure 29 presents two PTTL glow curves corresponding to unannealed and 6 h annealed LiF:Mg,Ti samples at 150 ^{0}C. The unannealed PTTL curve is formed by an intense peak 5 plus two additional very weak distributions centred at about the same temperatures as peak 2 and 3 in TL glow curve. No trace of peak 4 is found in this PTTL glow curve. Second curve, corresponding to treatment at 150 ^{0}C for 6 h, shows that a peak, at a temperature with an activation energy identical to those of new TL peak, is the main peak of the curve. Peak 5 is present but shows a considerably decreasing intensity. As in the case of the TL measurements, some additional modifications can be detected in PTTL annealed curve, such as the increase in intensity of both peak 2 and the light emission occurring at higher temperatures than peak 5.

Now, if the samples are subjected to a post-irradiation annealing sequence, as seen in figures 24a-24d, the band at 282 nm shows a marked increase at low temperatures followed by a sharp decrease up to approximately 200 ^{0}C. A region of stability is then followed by a further decrease at temperatures beyond 300 ^{0}C. The first decay process of this band follows the same pattern of the new peak between peak 2 and 4. Therefore, it can be concluded that the band at 282 nm and glow curve at 175 ^{0}C are

related to the same trap. At the same time, the intensity of the high temperature glow peak above peak 5 increases during the annealing procedure. The second decaying process of band at 282 nm can be considered to be related with high temperature glow peaks.
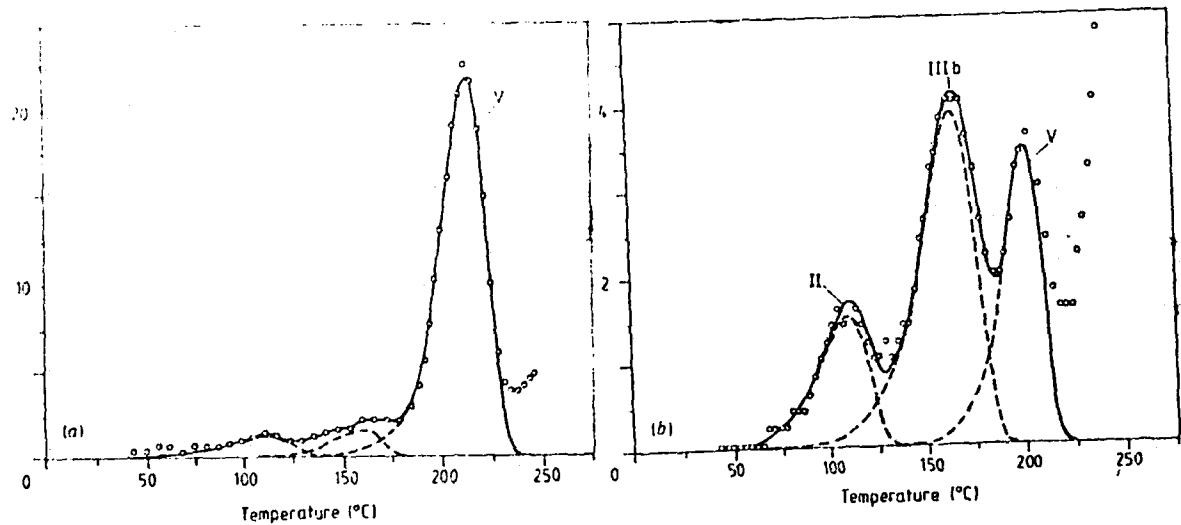
Figure 29. (a) The PTTL glow curve for unannealed TLD-100. (b) The PTTL glow curve for 360 min, 150 ^{0}C annealed samples. Open circles, experimental points; broken curves, resolved glow peaks; full curves, fitted glow curves.

4.3 Discussion

It is well-known that Z-centers are not always formed in alkali halides doped by divalent metals. Generally alkaline-earth ions (Ca^{+2}, Sr^{+2}, Ba^{+2}) and rare-earth ions (Eu^{+2}, Yb^{+2}, Sm^{+2}) do not trap electrons directly and form Z centers due to their relatively low second ionisation potentials as a first approximation. The second ionisation potential of Mg lies between the typical electron trapping and Z center forming metals (see table 5).

Table 5. Second ionisation potentials (eV) of some divalent metals.

Metals	Second Ionization Potential	Metals	Second Ionization Potential
Ba	10.00	Pb	15.03
Sr	11.03	Mg	15.04
Sm	11.07	Mn	15.64
Eu	11.25	Cd	16.91
Ca	11.87	Zn	17.96
Yb	12.17	Hg	18.76

The identification of the absorption band at 282 nm (4.4 eV) is thought to be a Z_2 center. The Mollwo-Ivey relationship for the Z_2 center is given as

$$E = 16d^{-1.84} \tag{49}$$

where E (in eV) is the maximum of the optical absorption of the Z_2 center and d is the nearest neighbour interionic distance in Angstrom. The calculated value for the Z_2 center in LiF:Mg,Ti from this equation is 4.4 eV which is consistent with the experimental results. Additionally, according to the Mollwo-Ivey relationship, the energy position of the Z_3 center in LiF:Mg,Ti is calculated to be 225 nm. This theoretical calculation is also good agreement by the experimental data.

However, the existence of a Mollwo-Ivey relationship alone does not seem to be satisfactory in a center identification, especially not in those cases when the crystal is uncontrolled for impurities like OH⁻, or Ti which seems to be very effective in many respects, even in a very low concentration. Therefore, a large number of controversy about the center identification in the alkali halide crystals exists when they contain divalent impurities. It is known that the Z-centers can be obtained only under specific conditions. In as-irradiated crystals only F centers are produced at the room temperature,

sometimes along with a small number of Z_1 center. When the crystal is warmed to 100 ^{0}C, Z_2 band is produced. Z_3 center is formed by the prolonged optical bleaching at liquid nitrogen temperature (LNT). Except Z_3 centers, the other results are consisted with our results. It can be seen that Z_2 center (282 nm band) is not produced immediately by β-irradiation in LiF:Mg,Ti (see figure 16). It can be produced only when samples are held above the 100 ^{0}C for few hours previous to the irradiation. On the other hand, the Z_3 center (225 nm) is produced immediately following irradiation. This result is not expected for the Z_3 center. However, the other behaviours of this band at 225 nm is consisted with Z-type center. We note that the increase in the defect concentration occurs over the range where F-center and 282 nm are all decreasing. Also, the 310 nm center is decreasing rapidly over the same range (see figure 25). One might speculate that F-centers are becoming mobile and associating with Mg-related band over this temperature region to form Z-type defects. Additionally, in the region 2 (125-200 ^{0}C) , the Z_2 centers convert thermally to the Z_3 center according to the following relation $Z_2 \rightarrow Z_3 + e^-$ The 225 nm band is seen to be produced only very weakly if monitored immediately after irradiation and is essentially dose independent. Also, if the sample is post-irradiation annealed beyond 250 ^{0}C it is observed to grow markedly. Figures 24a-24d show this effect clearly. The thermal stability of this center in the absence of UV illumination reaches up to 400 ^{0}C. About the center at 282 nm, we want to point out that this center is probably related with new peak growing at around 175 ^{0}C between peak 2 and 4 and also with the new peak at the high-temperature tail of peak 5 during the pre-irradiation heat treatment.

In general, there are two kinds of peaks in a glow curve, i.e., long- and short-lived peaks. If the glow curve is measured immediately after irradiation, it exhibits a multipeak structure with low and high temperature peaks. Peak 1 is one of them in the glow curve of LiF:Mg,Ti. Due to the its short-life, it has been thought to be useless in the dosimetric investigations. In the literature, there is large controversy about its decaying time [188-189]. However, it is largely expected that its decaying time following irradiation is to be 15 min.

Recent investigations on the TLD-100 represented that this sample contains OH ions as background impurities and TL glow curve shape of TLD-100 highly depends on these ions. During the irradiation, due to the irradiation effect, OH ions decompose to substitional oxygen, F and U-type centers. In the previous chapters we mentioned that there are three type U centers in the alkali halide crystals. The U_1 center belongs to interstitial H_i^- ions. It is not stable at room temperature. During the room temperature storage or readout cycle, probably, it combines with F-center and converts to U-center by the following relation

$$U_1 + F \longrightarrow U$$
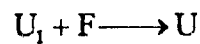
Therefore, we think that peak 1 in LiF:Mg,Ti is related with U_1 center.

The structure and nature of the trap of peaks 2, 3 , 4, and 5 is very mystery. Despite an overwhelming amount of data on this subject a satisfactory description is still lacking. Before the irradiation, the possible defect structures in LiF:Mg,Ti are Ti-OH, Mg^{+2}-vacancy type defects. After irradiation there could be a combination of the following defect types in the crystal: (I) Mg^{+2}, F center and interstitials; (ii) $(Mg^{+2}V)$-F centers-interstitial atom; (iii) Ti-related -F center-interstitial atom; (iv) Ti-related-$(Mg^{+2}V)_n$-F center-interstitial atom; (v) Mg^+-F center; (vi) Ti-related-Mg-F center etc. Some of these could give optical absorption bands, but they do not necessarily give thermoluminescence peaks.

A more satisfactory interpretation of our experiments can be made by assuming that the traps are not simply based on Mg^{+2} ions but other impurities such as Ti^{+4} , Ti^{+3}, Ti^{+2} and OH are also involved. Ti^{+4} is an essential ingredient of TLD-100 and it must be charge compensated. Ti^{+4} can be bound to three cation vacancies at near-neighbour positions, or to three OH or three O_2^- ions, or to a combination of vacancies, O_2^- and OH ions. On

the basis of ESR studies, Davies [36] proposed that three O_2^- ions were bound to the Ti^{+4} ion. Watterich et al. (1980) [40] and Wachler et al. (1980) [46] have suggested that some Mg centers contain OH^- ions.

$(Mg^{+2}-V^-)$ dipoles or trimers are neutral defects. During the irradiation, from their electrostatic considerations they would not be expected to act as traps for electrons. They could, however, be converted to other type of defects by radiation.

As seen from figure 23, during the low temperature annealing the concentration of F centers are increased. From this clue, we can understand that low temperature glow peaks (2 and 3) are related to traps that may contain F-centers. These defects are probably related with Ti-related-F center. Ti-related defect is possibly combination of V^- vacancies, OH^- or O_2^- ions at neighbouring sites of Ti impurity. During the pre-irradiation heat treatment at low temperatures, Ti related defects may be converted to other types of defects. Therefore, after the irradiation, they do not form Ti-related-F centers. The free Ti reacts with Mg-related defects which possibly give the peak 5.

Finally we want to postulate that the peak 2 trap is related with Ti-related-F centers and the peak 5 trap is a combination of Ti ions with $(Mg^{+2}-V^-)$ pairs.

Consequently we think that TL and optical absorption measurements alone are unable to explore the exact nature of defect centers in LiF:Mg,Ti crystals. Much more attention should be paid to obtaine better controlled materials especially concerning impurities, for example OH^- ions. A complex re-examination without any unproved preconceptions, including a wide range of investigation methods as e.g. ESR, ENDOR, Faraday rotation, etc, may lead to correct conclusions.

CHAPTER 5

The Effect of Pre-Irradiation Heat Treatment on the Evaluated Trapping Parameters of LiF:Mg,Ti (TLD-100)

5.1 Introduction

Lithium fluoride continues to be one of the most popular thermoluminescent materials used in radiation dosimetry [190]. In particular, LiF:Mg,Ti (TLD-100), marked by Sollon Technologies, Harshaw Inc. is so widely known that it is used as a standard material. The enriched form of this material is also available as the isotope ^{6}Li (TLD-600) or ^{7}Li (TLD-700) [191].

Although this material (TLD-100) has been successfully used over the past decades for the determination of absorbed dose by dosimetry services on a large scale, there is a lack of understanding of the thermoluminescence mechanism. The TL process is commonly described in terms of traps, mobile entities (charge carriers) and recombination centres.

When a specific lattice defect traps electrons, which are relased on heating to give rise to a glow peak, the electrons may be described by a

trapping depth (activation energy) below the conduction band E, and a frequency factor (pre-exponential factor) s which is in the order of lattice vibrations 10^8-10^{15} s^{-1} in the crystalline solids [192]. A significant part of research on LiF:Mg,Ti has involved in analysing the glow curves to obtain E and s values for peaks 2 to 5 [122-148]. There are many methods available to determine the trapping parameters from the glow curves [156-164]. For example, the trapping parameters can be determined by isothermal decay, glow curve fitting, peak shape, initial rise and heating rate methods . However, the published values of the trapping parameters calculated by these models show wide discrepancies even when the same method is used [142]. The observed variations may be attributed to the composition, the impurity concentrations of the samples used and the experimental conditions. More recently, Bos et al. [127] investigated the effects of the cooling rate and readout heating rate on the trapping parameters of the samples treated with only a high temperature annealing procedure. The results showed that the activation energies for all glow peak vary strikingly indicating that the deffect structure, which constitutes the traps for the charge carriers, is changing. Furthermore, the earlier observations demonstrated that the clustering and precipitation of defect structures during cooling and heating have a pronounced effect on the values of trapping parameters [15, 29].

In this work, the influence of the pre-irradiation heat treatment on the trapping parameters has been investigated as a function of annealing time at 125 ^{0}C by computerised glow curve analysis. In the previous investigations, the effect of the pre-irradiation heat treatment on the glow curves was investigated without deconvolution of the glow curve into its individual glow peak by computerised glow curve analysis. In some cases, small but important changes in the shape of the glow curve may not be understandable without resolving the individual glow peaks from the glow curve. In this study, these problems were overcome with computer curve fitting programs obtained from Piters and Bos [184] and modified by us. Although there are a lot of models, approximations and minimisation procedure in the computer curve fitting programs, the glow curve analysis technique has become very popular

method to evaluate trapping parameters from TL glow curves in recent years [124-131].

5.2 Results

It is well known that all the glow peaks of TLD-100 can be fitted with first-order kinetics [127]. However, in the past years, there is large controversy about the kinetic order of glow peaks , especially on the dosimetric peak 5 [148]. In this study, very good fits are obtained for the samples not subjected to the pre-irradiation heat treatment when the first-order TL kinetics is used. A set of glow curves measured immediately following irradiation after pre-irradiation heat treatment at 125 ^{0}C is shown in figure 30. It can be seen that the shape of the glow curves are highly changed as a result of the pre-irradiation heat treatment. Especially, for the prolonged annealing period, new peaks seem to be exist in the glow curves.
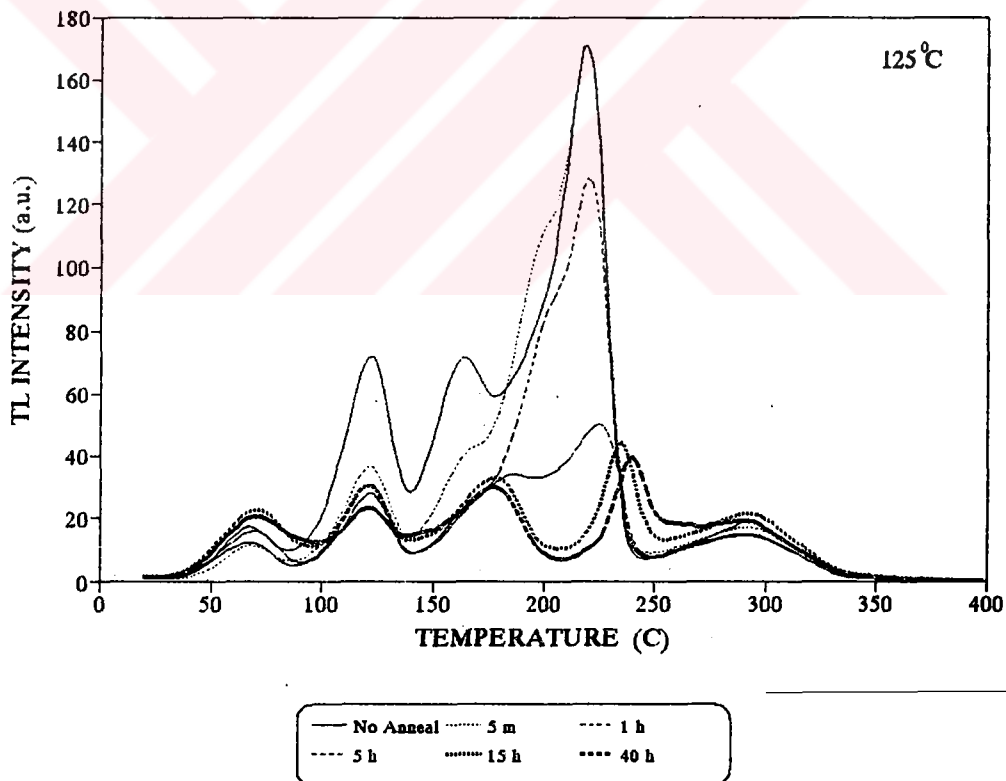
Figure 30. Set of thermoluminescence glow curves for LiF:Mg,Ti (TLD-100) crystals with pre-irradiation heat treatment time at 125 ^{0}C for different annealing time. All glow curves were read out at 2 ^{0}C/sec.

A typical deconvoluted glow curve measured at a heating rate of 2 ^{0}C/s following only the standard heat treatment at 410 ^{0}C for 30 min and rapid cooling to room temperature is shown in figure 31. In the figure 31, both the experimental points and the fitted glow peaks are presented. Best fit results have been obtained by assuming six peaks due to the first-order kinetic. The number of peaks in this study agrees well with the previous results[125-131].
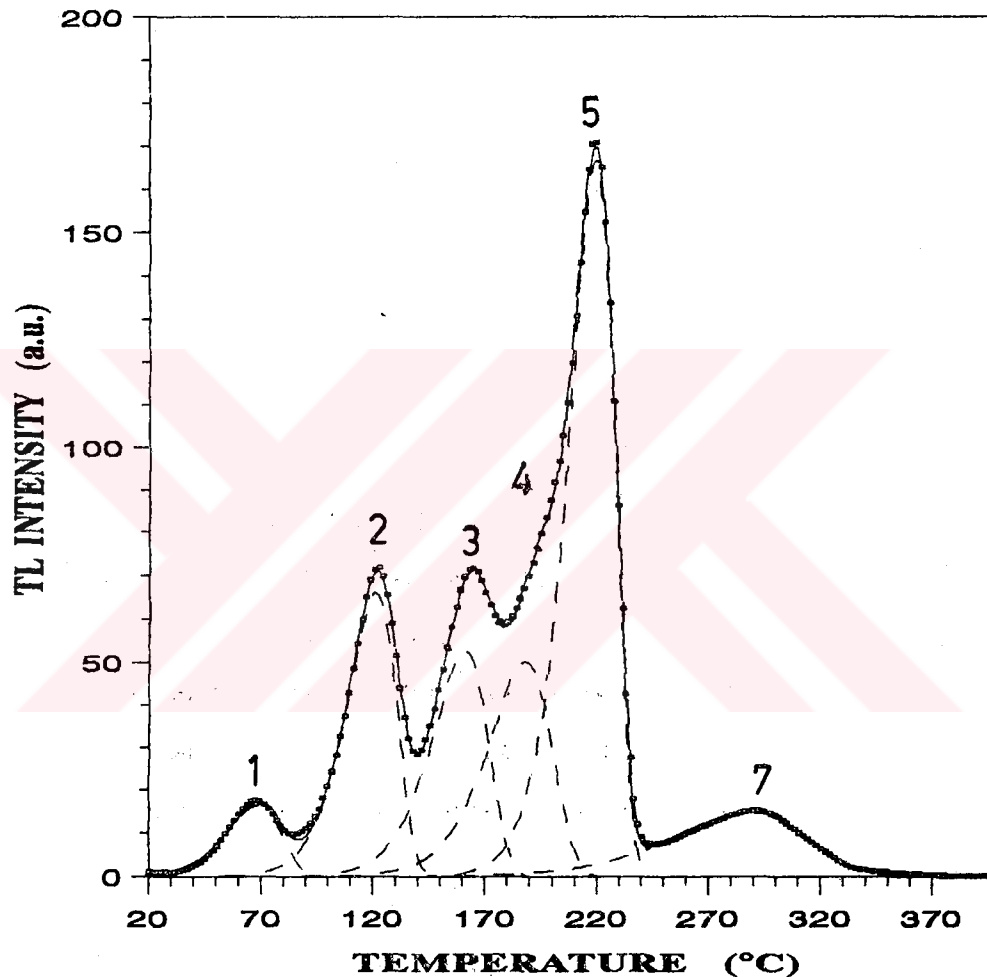
Figure 31. Fitted glow curve of LiF:Mg, Ti (TLD-100) measured after an annealing procedure of 30 min at 410 ^{0}C followed by a rapid cooling and read out at a linear heating rate β=2 ^{0}C/sec. In the figure: dots are the experimental points, the global fitting is continuous lines and the fitted peaks are represented in broken lines.

Fairchild et al. (1978) [123] and Sagastibelza and Alvarez Rivas (1981) [18] report an extra peak between peak 3 and 4, which is not found in this study, if there is no pre-irradiation heat treatment after standard annealing and rapid cooling. The evaluated peak temperatures, activation energies, frequency factor are tabulated in table 6. They are reasonably good agreement with those found in the earlier works [122-131].

Table 6. Trapping parameters for TLD-100. Obtained from computer curve fitting program.

Peak Number	n_0	E (eV)	ln(s)	T_m (^{0}C)
Peak 1	259	0.8136	25.8	69
Peak 2	947	1.210	33.89	120
Peak 3	850	1.299	32.91	160
Peak 4	914	1.293	30.60	187
Peak 5	2268	2.002	45.59	219
Peak 7	568	0.8669	15.18	288

Figure 32 presents the analysed glow curves corresponding to pre-irradiation heat treatment for 40 hours at 125 ^{0}C. This figure shows that there are important changes in the glow curves with respect to normal TL curve in Figure 31. However, the good fits can also be obtainable for the glow curves of the samples annealed at 125 ^{0}C for different time by the first-order kinetic except peak 1.

The normalised peak areas of glow peaks 1-6 with respect to annealing time at 125 ^{0}C are shown in figure 33. The trend of the peak areas are as follows; the peak intensity of peak 1, 2, and 3 immediately decreased. After approximately ten minutes, the intensity of peak 1 slightly increases up to 5 hr. Then its intensity shows a sharp increase up to a saturation point at about 20 hours. At the same time its trapping parameters, especially, kinetic order is highly varied from 1.0 to ≈2.5. On the other hand, peak 2 intensity continues
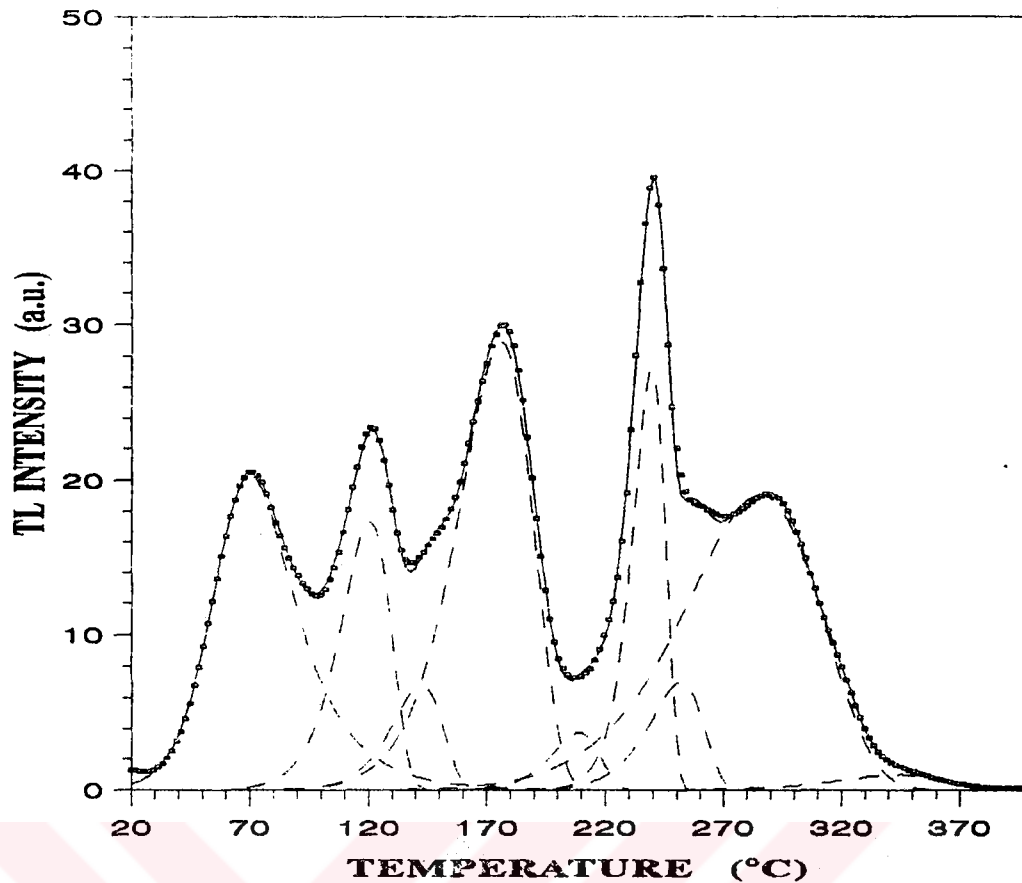
Figure 32. Glow curves of LiF:Mg,Ti (TLD-100) measured after a standart annealing procedure followed by rapid cooling and annealed additionally at $125\,^0C$ for 40 hours. $\beta=2\,^0C/sec$. Dots: experimental points. Continuous lines: global fitting. Broken lines: fitted individual peaks.

to decrease slightly. Between 4 and 16 hours, the peak 2 intensity shows a slight increase and after 16 hours a slight decrease. The peak 3 shows a similar trend as the peak 1 does. The only difference is that while the peak 1 slightly increases between 10 min and 5 hr, the peak 3 slightly decreases. Two decay stages of peak 4 intensity are seen in the figure 33. One of them is seen at around one hour and the other is at around four hours. Following a slightly initial growth up to 15 min, the main peak 5 intensity continously decrease. The behaviour of peak 7 is very interesting. Firstly its intensity slightly increases and then decreases up to 5 hr. For progressively increasing annealing time again a remarkable increase is seen as much as to the saturation point.
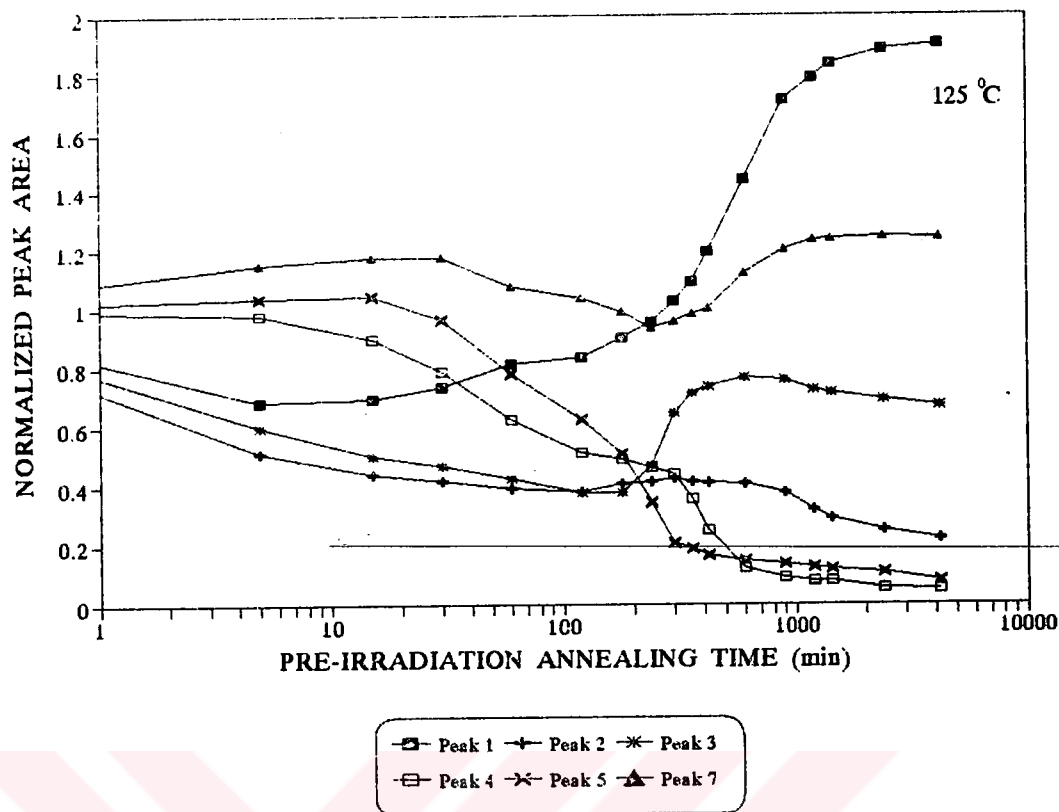
Figure 33. Normalized peak area versus log of annealing time at 125 ^{0}C for glow peaks from glow curves registered at a linear heating rate of 2 ^{0}C/sec.

The values of the activation energy E found by glow curve fitting are shown in figure 34. The values of E for the analysed glow peaks show remarkably interesting results. The dramatic changes start immediately and continue throughout the annealing period. Peaks 1 to 3 exhibit similar behaviour. In this manner, their E values first decrease to a minimum and then start increasing with time. Especially, the variation in the activation energy of peak 4 is very interesting. First it sharply increases from 1.3 eV to 1.9 eV, then sharply decreases to 1.25 eV and then starts increasing again with annealing time to 2 eV. Up to 120 min, the activation energy of peak 5 decreases very slightly and then sharply increases with time.

115
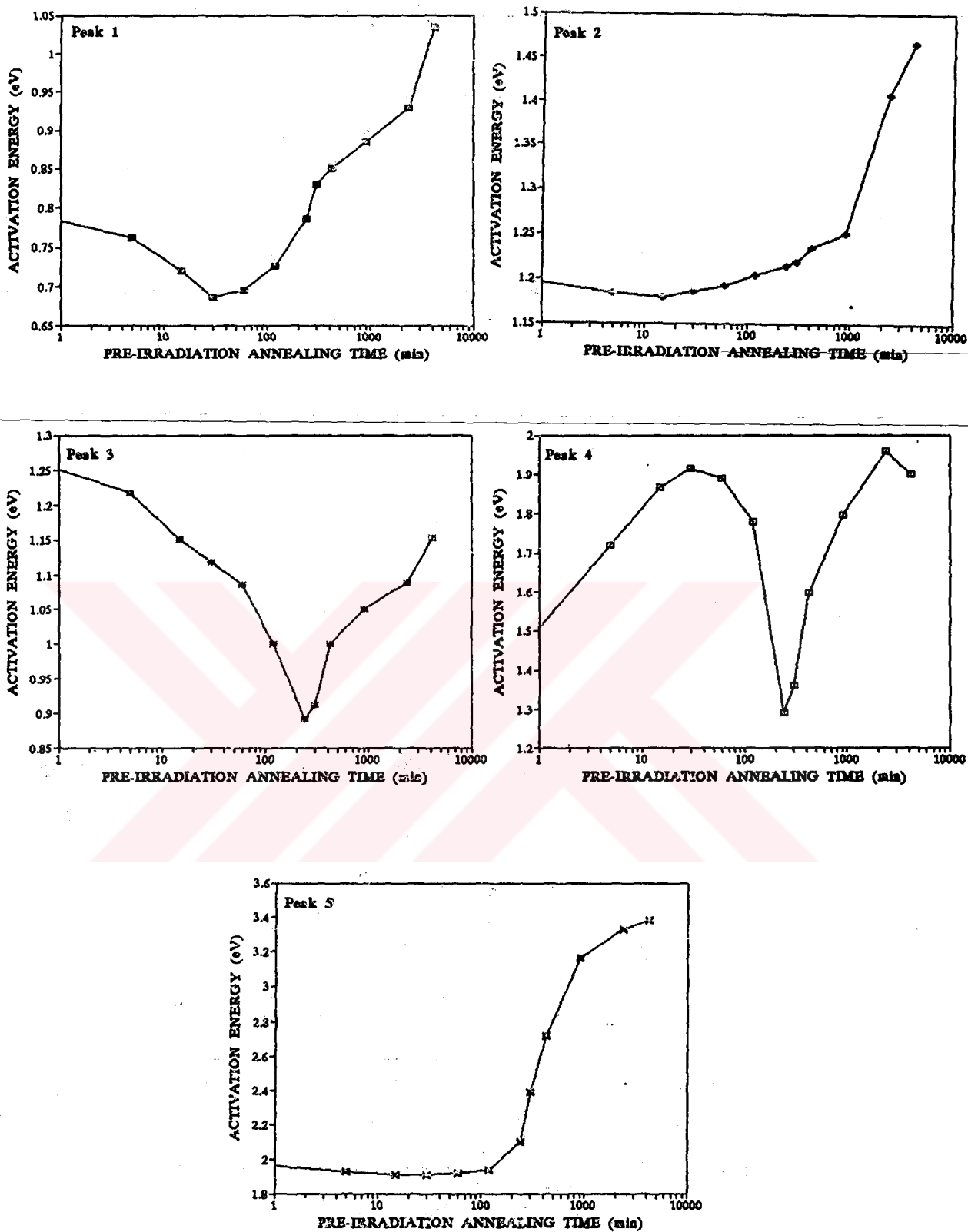
Figure 34. Activation energy determined by computerized glow curve fitting program versus pre-irradiation heat treatment time at 125 ^{0}C for glow peaks from glow curves registered at a linear heating rate 2 ^{0}C/sec.

116

In the thermoluminescence theory, for the first-order kinetic the peak temperature of the glow curve peaks are expected to change only with the heating rate. Hence for a constant heating rate, the peak maxima should not be affected by other experimental parameters and be fairly constant values in the range of experimental errors. However, this is not the case for LiF:Mg,Ti crystal. As seen from figure 35, the peak maximas of TLD-100 glow curves are shifted to higher temperatures with pre-irradiation annealing time, although a constant heating rate was applied. Peak tempeatures of peak 1 and 2 are observed to be not affected by the pre-irradiation annealing time. The behaviour of peak 3 and 4 is similar, except that peak 4 shows a mysterious decrease at about 200 minutes. Otherwise both peak temperatures slightly increase up to 200 minutes and then sharply increase to a constant value. Peak temperature of peak 5 seems to be constant up to 200 minutes. Then it increases with increasing time.
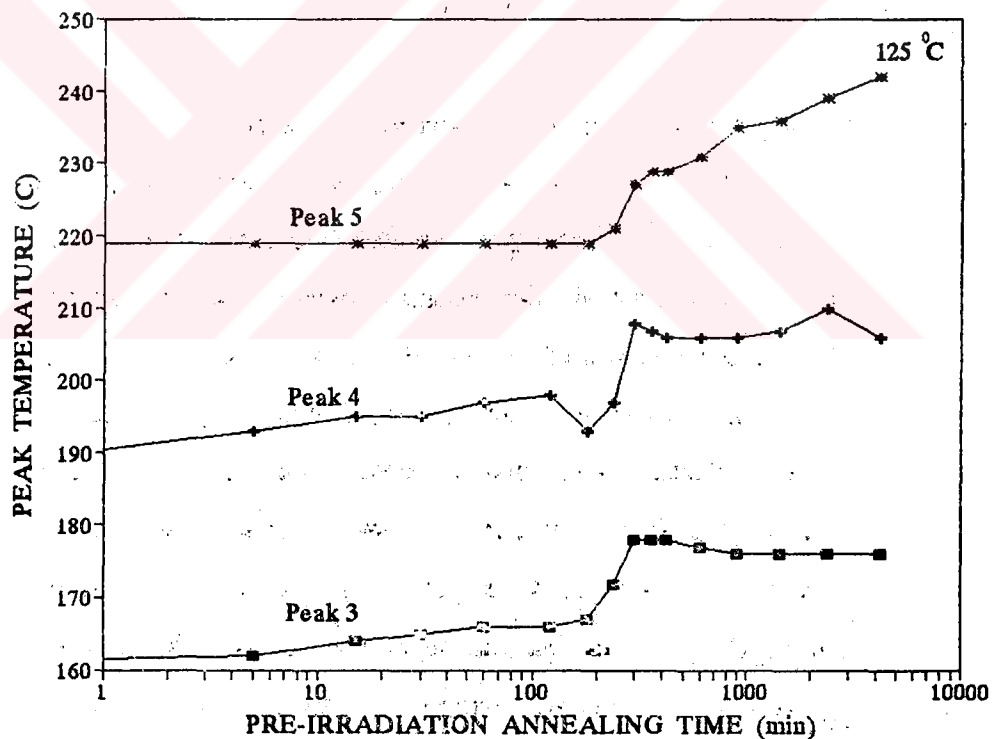
Figure 35. Variation of temperature at peak maximum for peak 3, 4, and 5 as a function of pre-irradiation heat treatment time at 125 °C.

117

As seen from the figure 31-35, the deconvolution of the glow curves to its individual glow peak reveals;

(a) considerable change in the kinetic order b and trapping parameters n_0, E and s of the peak 1.

(b) an important decrease in the peak 4 and 5 area.

(c) a presence of a new peak as a shoulder on the low temperature side of peak 3 which we label this as 2a. This peak seems to appear after approximately seven hours pre irradiation heat treatment at 125 ^{0}C.

(d) important variations in the trapping parameters of all the glow peaks.

(e) an important shift of the peak maxima of peak 3, 4, and 5 to the higher temperatures.

(f) also creation of a new peak at the high temperature tail of peak 5.

5.3 Discussions

In earlier studies, the glow curve deconvolution analysis was not applied to separete the glow peaks. Instead of this technique, because of easily separation of the glow peaks 2 and 5 from the glow curves, researchers paid attention especially on these glow peaks and responsible defects with these peaks. However, the deconvolution analysis of the glow curves as a function of annealing times, gives us clear pictures of the alteration in not only the shape and relative intensities of glow peak 2 and 5 but also all glow peaks with the pre-irradiation heat treatment. The following two factors might be used to explain the alterations in the glow curve shapes. The first is that during the pre-irradiation heat treatment, cooling and heating cycle the important defect reactions occur between the defects and second is that the trap structures themselves are undergoing important trap modifications. Therefore, defect reactions highly influence the TL mechanism.

118

The peak areas can be considered to be related to the concentration of defects in TLD-100. Therefore, during the heat treatment, the peak areas are changed due to the defect reactions. Our results indicate that the defect reactions not only exist between the defects that give rise to peak 2 and 5 but also between all of the defects in TLD-100 during the heat treatment. Although there is almost a total lack of consensus regarding to the responsible specific defects of glow peaks, in principles, it is accepted that peak 2 is related with $Mg^{2+}-V_c^-$ dipoles and peak 5 with $Mg^{2+}-V_c^-$ trimers. During the heat treatment the dipoles can change their position in the lattice and associate with other dipoles which give rise to clusters of dipoles or other defect types which in turn, give rise to defect complexes.

The alteration in the activation energies and peak temperature with annealing treatment is not expected to occur for some alkali halide crystals. However, defect clusters and precipitate phase in impurity doped alkali halide crystals affect lattice orientations of the crystals. The small change in the lattice orientations and lattice constant of the crystal causes the change in the band gap energies of the crystals and also the change in the trapping parameters of the traps. In the present experiments during the annealing cycle, the Mg and Ti related defects interact with each other and form defect complexes in the crystal. Most perhaps these defect complexes affect the band gap and consequently due to the change in the lattice, the perturbations in the activation energies of all glow peak in TLD-100 can be expected.

Recently, Piters and Bos (1993) [193] report a model in which defect reactions are incorporated, such as the interacting defect model which may help us to get more insight into the TL process. According to interactive defect model, the dependence of trapping parameters on annealing procedure and impurity concentration is possible and the change in the concentration of defects means a change in the rate of defect reactions and, therefore, this influence the shape of the glow peak. The glow peak is still fitted by the first-order TL kinetics, however, the trapping parameters are affected by annealing procedure and impurity concentrations.

In conclusion, it has been shown that the pre-irradiation heat treatment strongly influences the values of trapping parameters of all glow peaks in TLD-100 as determined by computerised glow curve analysis. These influence can be understood qualitatively in terms of defect interactions in the crystals.
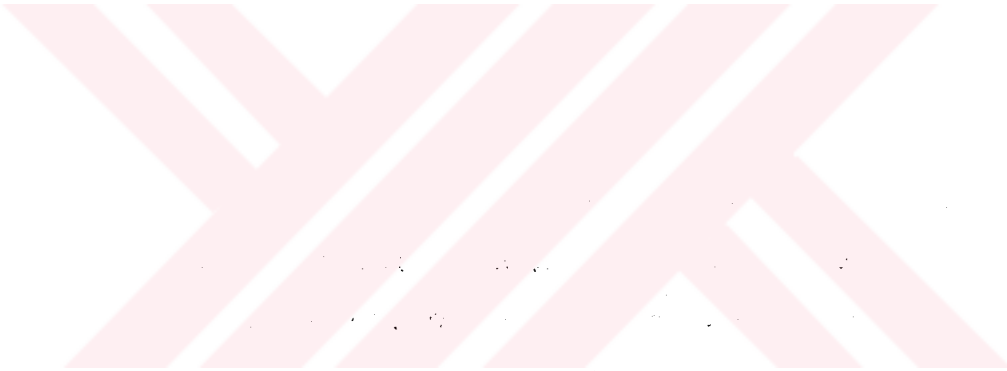
CHAPTER 6

A New Simple Model for the Shape of Thermoluminescence Emission Bands: Application to LiF:Mg,Ti (TLD-100)

6.1 Introduction

Knowledge of the mechanism of thermoluminescence (TL) is of great importance for the development of thermoluminescent materials. The basic model for the mechanism of thermoluminescence comprises three steps: (1) the trapping of charge carriers during irradiation with ionization radiation, (2) the release of charge carriers out of traps due to thermal heating, and (3) the capture of charged particles in luminescent centers under photon emission.

The simultaneous measurement of the light emission during heating of the TL materials as a function of sample temperature and in terms of emitted photon energy gives information on the TL mechanism, kinetic parameters for the individual defect and the influence on the defect reactions. In addition, it gives the structure of defects within the insulator and semiconductor when this type of measurement has been supplemented by many other techniques such as optical absorption, electron spin resonance measurements [194].

However, both glow curve and emission spectrum obtained from TL sample are the summation of many overlapping bands. The separation of individual bands from each other is very difficult. There are many methods to distinguish these bands. The famous one is the computerized curve-fitting procedure which constructs a glow curve or emission band using the initial values of the parameters and compares the computed curve with the experimental curve [148].

In this study, we developed a new simple model to describe the emission band based on a classical treatment of the lattice vibrations and the Franck-Condon principle. In order to see the success of developed model, we also measured the emitted light as a function of both temperature and wavelength from LiF:Mg,Ti (TLD-100) sample.

6.2 Theory

The simplest band model in crystalline solids for the TL emission is shown in figure 9. According to this model there are at least two distinct localized energy levels, one acts as a trap (T) and the other acts as a recombination (luminescent) center (R) [195].

In general, there are several types of electron transitions between the traps and recombination centers that have been reviewed by Chen and Kirsh in their excellent text book [196]. Some of transitions were represented in figure 9.

In order to observe TL luminescence, the electron in the trap must be excited to the excited state of trap and/or to the conduction band (CB) (transitions 1 and 2). These electrons then migrate in the CB (3) and recombine with a hole in the luminescent center by the emission of a photon (transition 4 and 5).

122

The transition 4, based on the transfer of the extra energy of electron to the lattice via phonons, is called as multi-phonon emission. This process has been renewed by Pässler using a slightly different set of approximations [197]. According to this process, there is a strong coupling between the electron and the lattice vibrations. If an electron approaches to the luminescent center, the electron settles down to this center due to the vibration of the lattice around the luminescent center. The electron is still in the excited state of luminescent center after the transition 4. The second recombination process is the direct transition of electron from the conduction band to the ground state of luminescent centers and/or is the transition from the excited state to the ground state of luminescent center via emitting a photon. If the emission of light takes place between the excited and ground state, a characteristic time is required in the excited state around 10^{-8} s [198].

The excited and ground state configuration of a luminescent center in crystalline solid are shown in figure 36 for one-dimension. The potential

(a)   (b)
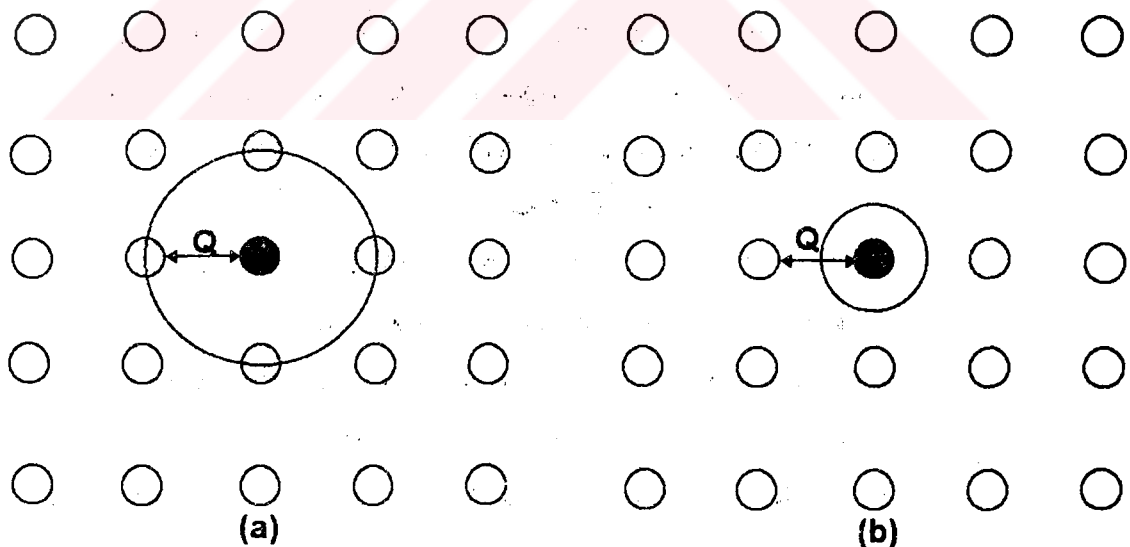
Figure 36. The excited and ground state configuration of a luminescent center in crystalline solid for one-dimension. (a) in the excited state, (b) in the ground state.

energy of a luminescent center in the excited state and also in the ground state interacts with its neighbours atoms (ligand) in the lattice, which means that when the center is excited, its electron moves to the outermost orbits. These orbits can overlap with the electron orbits of the ligand. The big and small circles around the center in Fig.36 represent the approximate effect of the electron wave functions in the excited and ground state of the center, respectively. The difference between the excited state and ground state depends upon the strong electron-lattice interaction. The distance Q between the luminescent center and its nearest neighbour atom is often used to characterize the configuration coordinate (CC) diagram.

The shape of an emission band of a luminescent center in the crystalline solid can be explained by the use of a CC model. Additionally, the electron transitions between an excited state and ground state within the same center and the potential energy of interaction of the center is the best instructive from a CC diagram. The CC representation is also used to depict the coupling between the vibration lattice energy and the electron lattice interaction energy.

A CC scheme is represented in figure 37. The horizontal axis shows the CC distance (Q) and vertical axis shows the total energy levels of the luminescent center, i.e., the electronic (E_e) plus the vibration excitation energy (E_m). In this model each energy state of a center is represented by a wavefunction that consists of product of an electronic wavefunction and a vibrational wavefunction. The electronic wavefunctions are expressed in terms of electrons of the center, whereas the vibrational wavefunctions are the wavefunctions of the center in a potential due to the presence of the ligand atom.

The first assumption in this work is that as the electron approaches to the luminescent center, it behaves as a simple harmonic oscillator. In a simple harmonic oscillator, the lattice energy can be explained by the vibrating

124
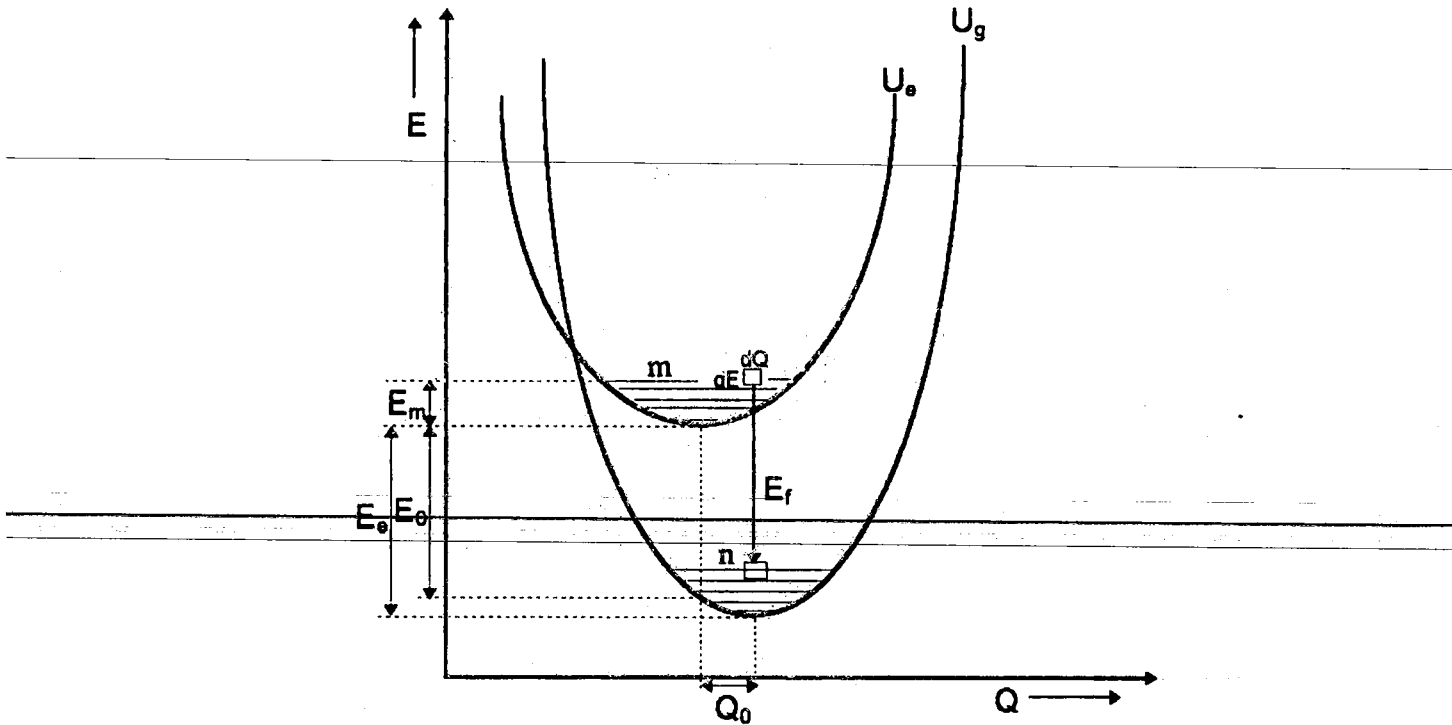
Figure 37. The configuration coordinate diagram of the luminescent center with potential energy curves as function of the configuration coordinate Q for the excited state U_e and ground state U_g.

configuration of a luminescent center. The potential energy of the excited state(U_e) and the ground state (U_g) of a harmonic oscillator is quadratic and its curves can be expressed with configuration coordinate Q as;

$$U_e(Q) = \frac{1}{2}k_e Q^2 + E_e$$

$$U_g(Q) = \frac{1}{2}k_g(Q-Q_0)^2$$

(50)

where k_e and k_g are the force constants in the excited state and in the ground state, respectively. E_e is the energy difference between the excited and ground states and Q_0 is the minimum potential energy in the ground state equilibrium of luminescent center. It is noted that in the CC diagram the minima of the ground and excited states occurs at different values of the coordinates.

According to the Franck-Condon principle the transitions between the excited and ground states are vertical. During these transitions, the CC position does not change and also the kinetic energy K_e of the configuration is preserved.

In principle, it can be considered that during the radiative transition the emitted light photon energy is equal to the energy difference between the excited and ground states. The non-radiative transitions only occur between the vibrational levels (n) in the ground state or vibrational levels (m) in the excited states. The number of non-radiative transitions between the vibrational levels in the ground state or excited state are assumed to be much higher than that of the radiative transitions between the excited and ground state. The distribution of vibrational levels in both state is assumed to be equal to each other.

The shape of emission band of a luminescent center has a Gaussian line shape and depends on the distribution of the number of emitted photons with different energies E_f. The number of emitted photons with an energy between E_f and $E_f + dE_f$ is proportional to the probability $A(E_f)dE_f$ of photon emission. $A(E_f)dE_f$ is the sum of the total emitted photon with an energy between E_f and $E_f + dE_f$. In order to obtain $A(E_f)dE$, it is required to find firstly all transitions with a photon energy between E_f and $E_f + dE_f$ and secondly the probabilities $P(E,Q)dEdQ$ of these transitions.

If the potential energy curves in the ground and excited state are reasonably parabolic functions of the CC, so the difference between the potential energy is also a parabolic function. The difference between the potential energy of the excited and ground state can be used to find the emitted photon energy during the light emission process.

$$E_f = U_e(Q) - U_g(Q) \qquad (51)$$

If we insert Eq.(50) into Eq.(51), we obtain

$$E_f = (\frac{1}{2}k_e - \frac{1}{2}k_g)Q^2 + 2\frac{1}{2}k_g QQ_0 + E_e - \frac{1}{2}k_g Q_0^2 \qquad (52)$$

Following the assumptions $(1/2)k_e=F_e$, $(1/2)k_g=F_g$ and $E_0=E_e-(1/2)k_gQ_0^2$, the above equation becomes

$$E_f = (F_e - F_g)Q^2 + 2F_g QQ_0 + E_0 \qquad (53)$$

where E_0 is the central emitted photon energy of the emission band.

In general, it can be accepted that the force constant F_e and F_g is equal to each other ($F_e=F_g=F$). Then;

$$E_f = 2FQQ_0 + E_0 \qquad (54)$$

It can be seen from the CC diagram, there is only one unique coordinate for a certain photon energy during the transition and by using the above equation, this coordinate can be written as

$$Q = \frac{E_f - E_0}{2FQ_0} \qquad (55)$$

When we take the integral over all vibrational levels at a certain coordinates, the sum of all probabilities of transition with photon energy E_f can be found

$$A(E_f)dE_f = \int_{U_e(Q)}^{\infty} P(E, Q)dEdQ \qquad (56)$$

where $P(E,Q)dEdQ$ is the probability of finding the configuration in the interval $dEdQ$ at coordinate Q and energy level E.

127

In order to calculate the probability P(E,Q), the integral in the above equation can be separated into two parts; P(E) and P(E,Q)|$_E$, where P(E) is the probability of finding the luminescent center at a certain vibration level and P(E,Q)|$_E$ is the probability of finding the luminescent center at a certain CC when the vibration level is fixed at a specified energy E. The product of these two probability gives us P(E,Q)

$$P(E,Q) = P(E)P(E,Q)\big|_E \qquad (57)$$

P(E) can be determined by using the Boltzmann statistics as in the form

$$P(E)dE = \frac{Exp(-\frac{E}{kT})}{\int_{E_e}^{\infty} Exp(-\frac{E}{kT})dE} dE \qquad (58)$$

The above equation gives the probability of finding the luminescent center in an energy interval dE at a vibration level E.

P(E,Q)|$_E$ can be calculated using the theory of harmonic oscillator as

$$Q(E,t) = \sqrt{\frac{E_m}{w_e^2 m}} \sin(w_e t)$$

$$\frac{dQ}{dt} = \sqrt{\frac{E_m}{m}} \cos(w_e t) \qquad (59)$$

$$T_p = \frac{2\pi}{w_e}$$

where $w_e = \sqrt{(F_e/m)}$, m is the effective mass of the configuration, T_p is the time required for one period of the oscillation cycle and E_m is the vibration energy in the excited state which is equal to

$$E_m = E - E_e \qquad (60)$$

The probability of finding the configuration between Q and Q+dQ is equal to the time configuration in this interval during one cycle divided by T_p

$$P(E,Q)|_E dQ = \frac{dt}{T_p} \qquad (61)$$

The time dt that the configuration is in the interval dQ is equal to the number of times the configuration passes Q two times the length of the interval dQ divided by the absolute value of the velocity v of the configuration in Q

$$dt = \frac{2dQ}{v(Q,E)} \qquad (62)$$

where

$$\frac{dQ}{dt} = \frac{v(Q,E)}{2} \qquad (63)$$

From Eq.59, one obtain

$$\sin^2(w_e t) = \frac{Q^2(E,t)}{\frac{E_m}{w_e^2 m}}$$

$$\cos^2(w_e t) = \frac{(\frac{dQ}{dt})^2}{\frac{E_m}{m}} \qquad (64)$$

If we substitute these equations into the below equation,

$$\sin^2(w_e t) + \cos^2(w_e t) = 1 \qquad (65)$$

again one can obtained the value of dQ/dt

$$\frac{dQ}{dt} = \sqrt{\frac{E_m}{m} - Q^2 \frac{F_e}{m}} \qquad (66)$$

If the expressions of T_p and dt from Eq.59 and Eq.62 are substituted into Eq.61, we obtain

$$P(E,Q)|_E \, dQ = \frac{dt}{T_p} = \frac{\frac{W_e}{2}}{\pi \frac{dQ}{dt}} dQ \qquad (67)$$

Consequently, if Eq.66 is substituted into Eq.67, the expression of $P(E,Q)|_E$ can be obtained as

$$P(E,Q)|_E = \frac{1}{2\pi \sqrt{\frac{E_m}{F_e} - Q^2}} \qquad (68)$$

Intruducing Eq.68 and Eq.58 into Eq.57 yields

$$P(E,Q) = \frac{Exp(-\frac{E}{kT})}{2\pi \sqrt{\frac{E_m}{F_e} - Q^2} \int\limits_{E_o}^{\infty} Exp(-\frac{E}{kT}) dE} \qquad (69)$$

The shape of emission band depends on the number of vibrational energy levels in the excited state. Thus by integrating $P(E,Q)$ over all energy levels in the excited state it can be determined as

$$\int\limits_{v_e(Q)}^{\infty} P(E,Q) dE = \int\limits_{v_e(Q)}^{\infty} [\frac{\frac{Exp(-\frac{E}{kT})}{2\pi \sqrt{\frac{E_m}{F_e} - Q^2}}}{\int\limits_{E_o}^{\infty} Exp(-\frac{E}{kT}) dE}] dE \qquad (70)$$

130

The integral in the denominator of the above expression is computed by using a computer program. The solution is given by

$$\int_{E_*}^{\infty} Exp(-\frac{E}{kT}) dE = \frac{kT}{Exp(\frac{E_*}{kT})} \tag{71}$$

If Eq.60 and Eq.71 are substituted into Eq.70 and then by changing the boundaries of integral, the simple expression can be obtained as

$$\int_{U_*(Q)}^{\infty} P(E,Q) dE = \frac{1}{kT} \int_{U_*(Q)-E_*}^{\infty} \frac{Exp(-\frac{E_m}{kT})}{2\pi \sqrt{\frac{E_m}{F_e} - Q^2}} dE_m \tag{72}$$

In order to evaluate the above integral, the best appropriate substitution of E_m can be expressed as

$$E_m = kTx + F_e Q^2 \tag{73}$$

Then the substitution of Eq.73 and Eq.50 into Eq.72 and by adjusting the limit of integral one can obtain

$$\int_{U_*(Q)}^{\infty} P(E,Q) dE = \frac{Exp(-\frac{F_e Q^2}{kT})}{2\pi \sqrt{\frac{kT}{F_e}}} \int_{0}^{\infty} \frac{Exp(-x)}{\sqrt{x}} dx \tag{74}$$

The solution of integral in the above equation can be given as

$$\int_{0}^{\infty} \frac{Exp(-x)}{\sqrt{x}} dx = \sqrt{\pi} \tag{75}$$

Then Eq.74 becomes

131

$$\int_{U_e(Q)}^{\infty} P(E,Q)dE = \frac{Exp(-\dfrac{F_e Q^2}{kT})}{2\sqrt{\dfrac{\pi kT}{F_e}}} \qquad (76)$$

According to this equation, the shape of the emission spectrum appears to be a Gaussian function of Q. If we take the derivative of Eq.55 with respect to E_f and then substitute this and Eq.55 into Eq.56 we obtain $A(E_f)$

$$A(E_f) = \frac{1}{2U\sqrt{\pi}} Exp(-\frac{(E_f - E_0)^2}{U^2}) \qquad (77)$$

where

$$E_0 = E_e - FQ_0^2$$
$$U^2 = 4FQ_0^2 kT \qquad (78)$$
$$C = FQ_0^2$$

The emission band generally measures the number of emitted photon I as a function of energy. Thus the product of $A(E_f)$ by the number of emitted photon at the peak maximum gives the expression of a TL emission band

$$I(E_f) = \frac{I_0(E_0)}{2U\sqrt{\pi}} Exp(-\frac{(E_f - E_0)^2}{U^2}) \qquad (79)$$

According to this expression, the shape of the emission band is also in Gaussian form and it depends on just two parameters, E_0 and U.

6.3 Results

The glow curves constructed from LiF:Mg,Ti at different wavelengths are shown in figure 38. The usual peak labeling is employed in this figure. It is
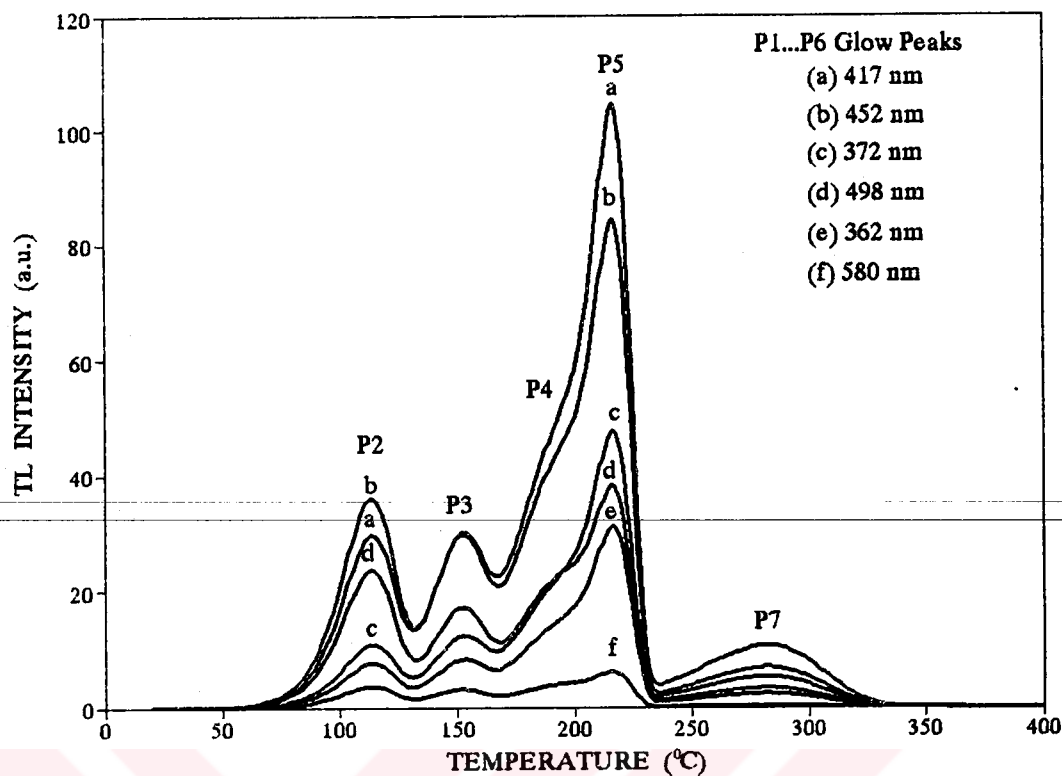
Figure 38. The glow curves from LiF:Mg,Ti at different wavelengths.

obviously seen from this figure that relative TL peak intensities are highly changed with emitted photon wavelength. The peak temperatures obtained from the most intense glow curve are; peak 2 (113 ^{0}C), peak 3 (151 ^{0}C), peak 4 (190 ^{0}C), peak 5 (217 ^{0}C), peak 6 (282 ^{0}C).

The emission spectra of glow peaks that have been recorded as a function of emitted photon energy at their peak temperatures is represented in figure 39. The relative values of emission spectrum intensity have been obtained from their individual glow curves peak height by using a computer glow curve deconvolution program. The kinetic value of the computed glow curve is the first order kinetic. The main emission is seen to be the peak at ≈420 nm and this is in general agreement with the similar spectra recorded by previous authors [26-27]. From the shape of curves it is clear that there are in fact several emission components in the spectra. These bands have been
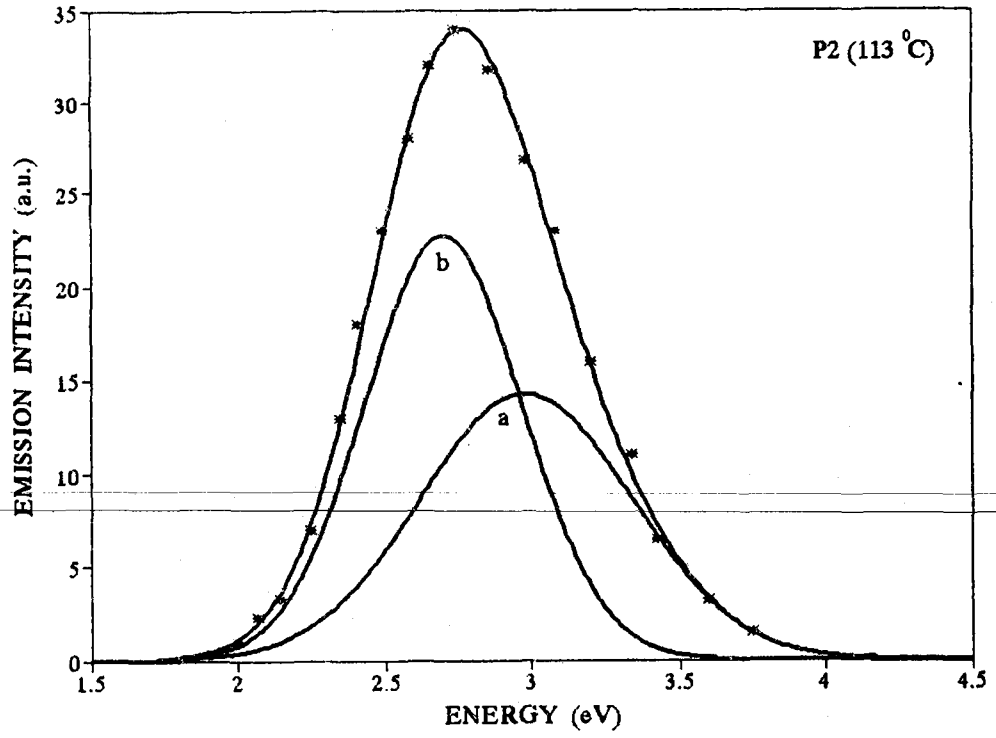
Figure 39a
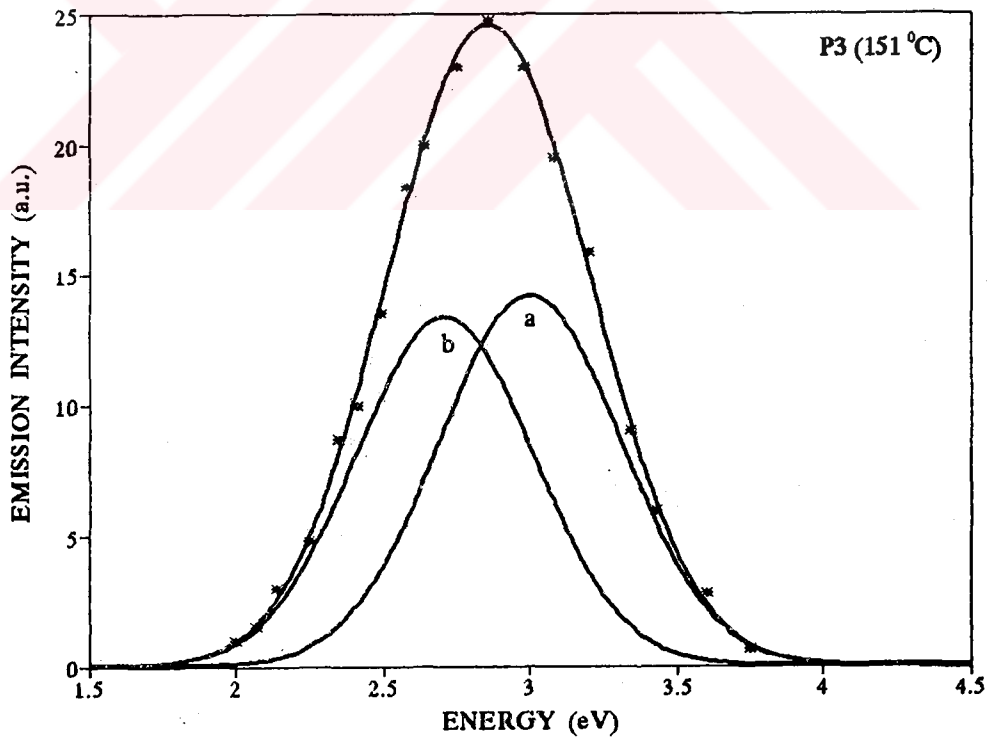
Figure 39b

Figure 39c

Figure 39d

The figure shows emission intensity (a.u.) versus energy (eV) with curves labeled a, b. Label P6 (282 °C).
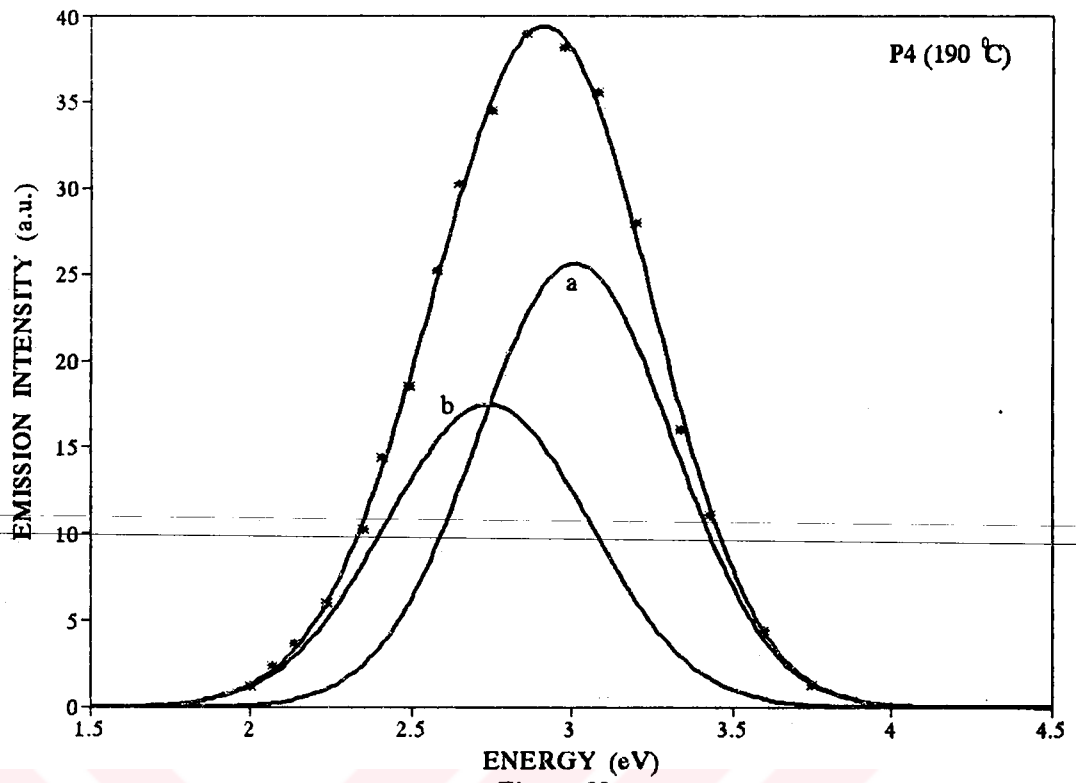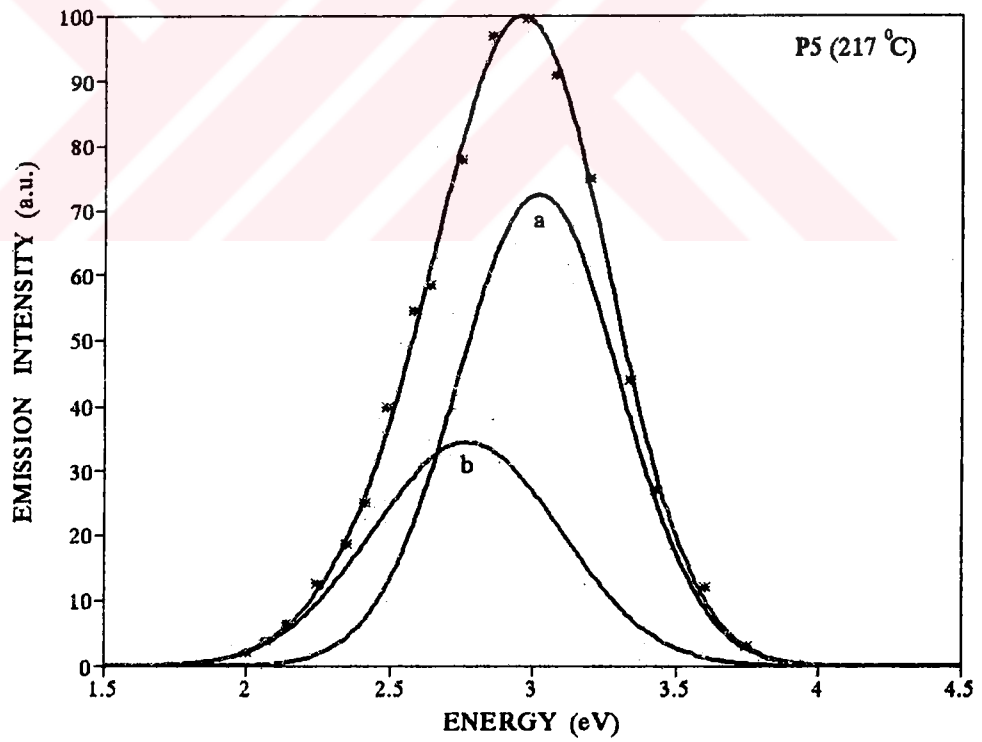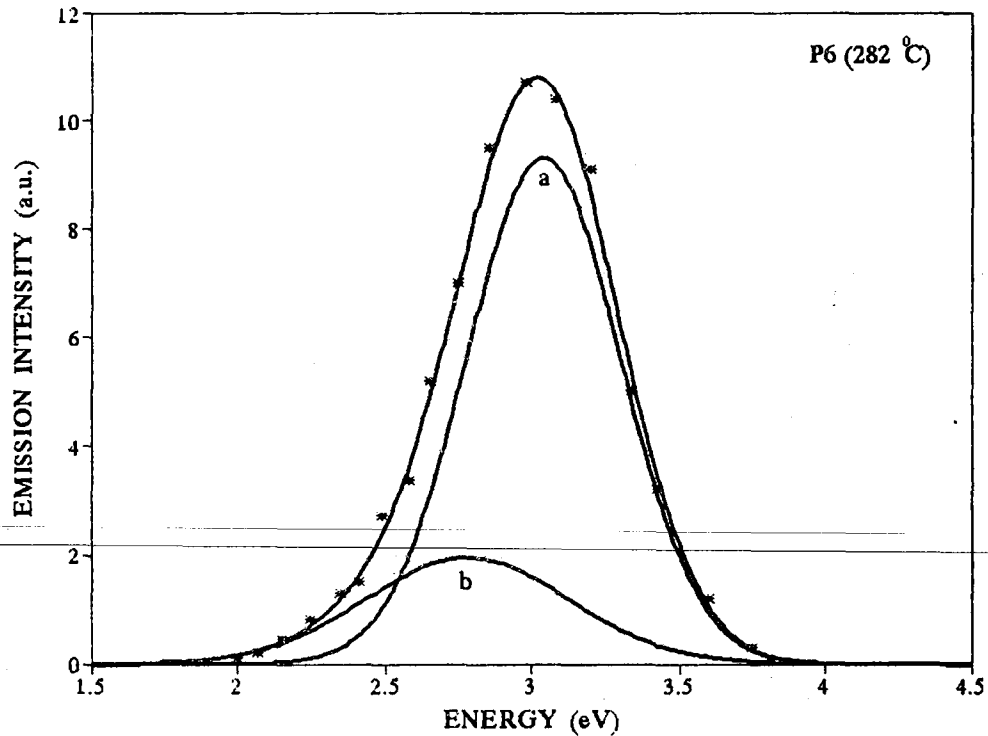
Figure 39. TL emission spectra measured at the maxima of different glow peaks from LiF:Mg,Ti. (a) Glow peak 2, (b) Glow peak 3, (c) Glow peak 4, (d) Glow peak 5, (e) Glow peak 6.

resolved by using the developed simple expression (Eq.79). However, the previously recorded emission band around 620 nm is not present in this study. Probably this band appears at higher irradiation doses. The separation procedures have been performed by means of a computerized curve-fitting program. The best-fit program was modified by us according to our developed expression.

The emission spectrum of whole glow peaks was successfully fitted with two emission bands. But there is a small systematic shift in the central photon energy and relative intensity of emission band as the peak temperature increases. At 113 ^{0}C (peak 2) the 2.7 eV component is dominant.

With increasing temperature, this band broadens and its intensity decreases. Therefore, at 217 ^{0}C (peak 5) the 3.02 eV is the main component. This behaviour is in general agreement with the results of previous studies [15-16]. We observed that the peaks and their emission maxima are peak 2 at ≈450 nm, peak 3 at ≈434 nm, peak 4 at ≈426 nm, peak 5 at ≈419 nm, peak 6 at ≈410 nm. The kinetic parameters of emission bands obtained from the emission spectrum of glow peak 2 and peak 5 are shown in table 7 which also contains some kinetic parameters of emission bands recorded in the previous publications.

Table 7. Kinetic parameters of TL emission spectrum of LiF:Mg,Ti (TLD-100).

Authors	Peak No	Band No	E_0 (eV)	U (eV)	C_1 (eV)	C_2 (eV)	C (eV)
Fairchild and et al.[a]	5	1	3.01	0.90[*]	3.07	0.04	-
		2	2.90	0.72[*]	2.94	0.04	-
		3	2.71	0.96[*]	2.75	0.04	-
Delgado and et al.[b]	5	1	3.01	-	-	-	-
		2	2.88	-	-	-	-
		3	2.70	-	-	-	-
Yazici[c]					-		
	2	1	2.98	0.51[**]	-	-	1.95
		2	2.70	0.38[**]		-	1.08
					-		
	5	1	3.02	0.40[**]	-	-	0.95
		2	2.77	0.46[**]		-	1.21

[a]Ref.[26]

[b]Ref.[43]

[c]This Work

[*]U=FWHM

[**]FWHM=2√(ln(2))U

137

6.4 Discussion

Earlier investigations of the emission spectra of LiF:Mg,Ti have been made by several authors [4, 20, 23, 25 -27]. Especially four emission band regions have been observed at approximately 300 nm, 420 nm, 520 nm and 620 nm. All of them found out a broad line emission at approximately 420 nm. Additionally, Townsend et. al. (1983) [27] have observed a gradual shift in the emission maximum to lower wavelength with increasing peak temperature. The experimental measurements at low temperatures represented that the principal emission is also in the region of 400-420 nm [31]. The other peculiar properties such as the effect of the ageing period duration and heating rate on the emission bands have been investigated previously [43,199-200]. Delgado and Delgado (1984) showed that there are no changes in the emission spectrum but Piters and Bos (1993) observed only very small changes with heating rate. However, in most of these studies, the emission spectra were recorded at large dose levels on the order of 10^3 Gy (at least 10^2 Gy). But it is well known that at these high dose levels, the shape of glow curves alter and some new peaks appear at the higher side temperature [18]. In the previous studies, the TL emission spectra has been fitted to a single Gaussian components. The exact form of this expression can be given by equation 32. In this equation, E_0 and U are depend on the temperature. This equation predicts that the emission band maximum should decrease slowly and monotonically with increasing temperature and the full-width at half maximum should increase monotonically with increasing temperature.

Fairchild et al.[26] point out that the emission spectrum of TLD-100 can not be explained with the well known above expressions. They also criticized the number of bands in the emission spectra and they suggested that two bands are more plausible than three bands. However, they have obtained three bands because of the Eq.32 from their fitting program.

Therefore, firstly we tried to fit the experimental results with three emission bands according to the developed model to obtain best-fit results. However, third band always drifts away from the region of experimental data points or the computer program indicates that the additional band was minor importance when compared with the intensities of the other two bands. Secondly, the emission spectra is tried to fit with one band. However, there were large differences between experimental and computed spectra in both cases. When we tried to fit the experimental results with two bands instead of one or three bands, a best-fit was always obtained.

Although there is a controversy in the number of fitting bands between our and previous results, there is a high agreement in the parameters of the most intense band between the results which have been represented in the table 7. We think that these incompatibles probably arise from the different behaviour of the temperature dependency of E_0 and U or from the different irradiation dose levels.

We point out that the developed simple model in this study gives better results than the results obtained previously developed models to explain the emission spectra of an associated pair trap model in the solids. According to this trap model, the trap and luminescent center are the same center. During heating, the electron in the ground state raises to the excited state of luminescent centers from which it may either be retrapped or, alternatively, emit photon by returning to the ground state of the luminescent centers. Finally, in our opinion this model is the better model to explain the emission spectra than previous models particularly for LiF:Mg,Ti.

CHAPTER 7

Conclusion

The highly complex nature of the optical absorption and TL glow curves in LiF doped with Mg and Ti makes the identification of the individual peaks and their related defects extremely difficult. There are four important trap centers in an irradiated LiF:Mg,Ti (see Fig.16) with peak absorbance at 380 nm, 310 nm, 250 nm, and 225 nm and five glow peaks in the glow curves. When the optical absorption spectra and also glow curve are deconvoluted into their absorption bands and glow peak components, the height of the individual bands and areas of the individual peaks can be seen more clearly.

Thermal depletion of these bands and glow curves occur at different temperatures. The usual pre-irradiation heat treatment of TLD-100 at and above 400 ^{0}C for 1 h disperses all of the Mg-impurity in dipole form. Subsequent annealing at lower temperatures (<100 ^{0}C) results in the clustering of dipoles into trimers and even in the formation of some Mg-precipitates. Under this pre-annealing treatment, the 380 nm band decays, whereas the height of the optical absorption band at 310 nm increases as well as peaks 4 and 5 in the glow curves. When the samples are subjected to the

heat treatment above 100 ^{0}C before the irradiation, the height of the optical absorption bands at the higher wavelength side of the F-band and area of peaks 4 and 5 are considerably decreased. The band at 380 nm continuously decays in the region between approximately 70 ^{0}C and 150 ^{0}C, whereas the 310 nm band at first increases (perhaps due to Mg-dipole clustering) and decays in the region approximately between 100 ^{0}C and 150 ^{0}C. Above 150 ^{0}C, they start to return to their original heights. Over the same temperature regions, the decaying periods of peaks 4 and 5 are similar to the decaying period of 310 nm. Therefore, it can be thought that the band at 310 nm and glow peaks 4 and 5 are probably belong to the same trap, namely Mg-trimer/Ti-complex. However, the lack of correspondence between the peak 2, Mg-dipoles and 380 nm band led us conclude that peak 2 is not related to Mg, but it is possibly Ti-related/F-center combinations.

Before irradiation, when the crystals are subjected to heat treatment above the 125 ^{0}C for long times, a new optical absorption band is clearly resolved at around 282 nm. Furthermore, when a composite heat treatment (before irradiation at 125 ^{0}C for 6 hours and after irradiation at different annealing temperatures) applied to the samples, the band at 282 nm firstly shows an increase at low temperatures (<125 ^{0}C). The thermal depletion of this band occurs over two different temperature regions. The first depletion region is between 150 ^{0}C and 200 ^{0}C and second region is between 275 ^{0}C and 300 ^{0}C. Under the same heat treatments, a new glow peak appears between the peak 3 ($\approx$160 ^{0}C) and peak 4 ($\approx$190 ^{0}C). The similar thermal decaying properties of this glow peak and optical absorption band at 282 nm leads to a conclusion that they may be belong to the same trap center. The Mollwo-Ivey relationship and other thermal and optical properties indicate that the behaviour of this center is consisted with Z-type center.

The hydroxyl impurities (OH$^-$) enter to crystal as background impurities during the crystal growth cycles. Therefore, in this study, it is considered that all samples contain OH$^-$ ions. Before irradiation, these OH$^-$ ions are probably connected with Ti-impurities and may form Ti-OH$^-$ defects. During irradiation,

141

this bond breaks due to the irradiation effects and forms U-centers in the crystals. These centers are not stable at room-temperature and decay rapidly. The peak 1 also rapidly decays at room temperature. Therefore, the peak 1 can be considered to be related with U-type centers.

Trapping parameters of LiF:Mg,Ti (TLD-100) determined by glow curve analysis are strongly dependent on the thermal history of the samples before and after irradiations.

It has been shown that annealing stages before irradiation strongly influence the values of the trapping parameters of the glow peaks 1 to 7 in LiF:Mg,Ti as determined by computerized glow curve analysis. These observation can be understood qualitatively in terms of clustering and precipitation of defects involved in the production of thermally stimulated luminescence. When TLD-100 crystals are pre-annealed for some time at low temperature (after annealing at 410 ^{0}C for 30 min followed by a rapid cooling at 50 ^{0}C/sec) the trap concentration of the peaks 2 and 3 decreases. The peaks 4 and 5 initially increase due to clustering and decrease at longer annealing times due to precipitation.

The results showed that the activation energies (trapth depth) E and frequency factor s for all glow peaks vary strinkly indicating that the defect structure, which constitutes the traps for charge carriers, is changing. It has been suggested that the variation in the activation energy at the trapping centers could be caused by the band gap narrowing near precipitates. Band gap narrowing influences all electron energy levels regardless to the type of trapping centers or luminescent centers.

The Mg precipitate phases in LiF will undoubtedly have a different band gap to that of LiF. Additionally, the region surrounding the precipitate surfaces will exhibit substantial strain caused by the mismatch between crystal structures. As a result, at these places one should expect a perturbation in the crystal potential and a distortion of the band gap (band

bending) in the vicinity of the precipitate particles extending over several lattice constants. Thus, both the static and dynamic disorder within solids can alter trapping parameters (E and s). In the present work we are altering both the static and dynamic disorder by varying the annealing time before irradiation at different temperature and thus perturbations in the trapping parameters of the various TL peaks can be expected.

As a result, the process described in this thesis clarify to some extent the wide variation in the published trapping parameters and fading properties of different TL samples. The present data reveals that the trapping parameters highly depend upon the experimental conditions such as cooling rate, heating rate, pre-irradiation and also post-irradiation heat treatment. Furthermore, even under the same cooling and heating rates, if annealing procedures were dissimilar then different E and s values would still result. These features may go someway to explain why there are wide variation in the published trapping parameters values and calculated fading rates (determined from E and s values) and actual fading rates measured in the laboratory.

In chapter 6, a new simple model for the shape of thermoluminescence emission band is described. According to this model, the lattice vibrations are classically treated and the electronic transitions are assumed to occur directly (Franck-Condon principle). To see the success of the developed model, we measured TL emission spectra of LiF:Mg,Ti. At low dose levels (≈ 1 Gy) the measured emission spectra of LiF:Mg,Ti shows one main emission band around 420 nm. This is in agreement with previous studies. The emission spectra of all glow peaks was successfully fitted with two emission bands by the developed expression. However, for high dose levels the extra emission bands would also be expected at different wavelengths, which were not observed in our measurements. Additionally, at high dose levels extra peaks in the glow curves of LiF:Mg,Ti also appear. Probably at high dose levels luminescent centers and trapping centers are coupled or at least one type of defect centers is converted to the other type centers. In chapter 5, we represented that pre-irradiation heat treatment affects the shape of the glow

curves due to the defect reactions during the annealing procedure. In this manner, the defect reaction between the luminescent centers would be expected

Although the measurements of emission spectra provide more informations about the defects and TL mechanism in the alkali halide crystals, the interpretation of the results of these measurements are not enough unless they are not supplemented with other type of measurements.

LIST OF REFERENCES

[1]- Daniels F., Boyd C.A. and Saunders D.F. (1953) Science **117 343**.

[2]- Patent Specification (1967) No.1059518 (London:Pattent Office).

[3]- Cameron J.R., Suntharalingam N. and Kenney G.N. (1968) Thermoluminescence Dosimetry, The University Of Wisconsin Press, Madison.

[4]- Stobe T.G. and Watanable S., (1975). "Thermoluminescence and Lattice Defects in LiF", Phys.Stat.Sol.(a), **29**, pp. 11-29.

[5]- Grant R.M. and Cameron J.R. (1966) "Effect of the pre-irradiation annealing on the thermoluminescence and dielectric loss of LiF:Mg", Journal of Applied Phys., **37**, pp. 3791-3795.

[6]- Dryden J.S. and Shuter B. (1973) "The dependence of the thermoluminescence of $LiF:Mg^{2+}$ crystals on the state of aggregation of the Mg^{2+} ions", J.Phys.D:Appl.Phys., **6**, pp. 123-130.

[7]- Bradbury M.H. and Lilley E. (1976). "Effect of deformation on the thermoluminescence properties of LiF and TLD 100 dosimeter crystals", J.Mat.Sci., **11**, pp. 1849-1856.

145

[8]- Bradbury M.H., Nwosu B.C.E., and Lilley E. (1976). "The effect of cooling rate on the performance of thermoluminescence dosimeter crystals (TLD-100) and LiF crystals", J.Phys.D:Appl.Phys., **9**, pp. 1009-1016.

[9]- Bradbury M.H. and Lilley E. (1977a). "Precipitation reactions in thermoluminescent dosimetry crystals (TLD-100)", J.Phys.D:Appl.Phys., **10**, pp. 1261-1266.

[10]- Bradbury M.H. and Lilley E. (1977b). "Effect of solution treatment temperature and ageing on TLD-100 crystals", J.Phys.D:Appl.Phys., **10**, pp. 1267-1274.

[11]- Barsis E., Lilley E., and Taylor A., (1967), Proc.Br.Ceram. Soc., **9**, pp. 203.

[12]- Rao S.M.D. (1974). "The Role of Magnesium in the Thermoluminescence of Lithium Fluoride", Phys.Stat.Sol.(a), **24**, pp. 519-524.

[13]- Gavartin J.L., Shidlovskaya E.K., Shluger A.L., and Varaksin A.N. (1991). " Structure and interaction of impurity-vacancy (Mg^{2+}-V_c^-) dipoles in crystalline LiF",J.Phys.:Condens. Matter, **3**, pp. 2237-2245.

[14]- Taylor G.C. and Lilley E. (1982a). "Clustering and Precipitation in LiF (TLD-100) crystals:I", J.Phys.D:Appl.Phys., **15**, pp.1243-1251.

[15]- Taylor G.C. and Lilley E. (1982b). "Effect of clustering and precipitation on thermoluminescence in LiF (TLD-100) crystals:II", J.Phys.D:Appl.Phys., **15**, pp. 1253-1263.

[16]- Taylor G.C. and Lilley E. (1982c). "Rapid readout rate studies of thermoluminescence in LiF (TLD-100) crystals:III", J.Phys.D:Appl.Phys., **15**, pp. 2053-2065.

[17]- Mieke S. and Nink R. (1980). "On the TL mechanism of LiF:Ti", Nuclear Instrument and Methods, **175**, pp. 10-11.

[18]- Sagastibelza F. and Alvarez Rivas J.L. (1981). "Thermoluminescence in LiF (TLD-100) and LiF crystals irradiated at room temperature", J.Phys.C:Solid State Phys., **14**, pp.1873-1889.

[19]- Miller L.D. and Bube R.H., (1970). "Luminescence, Trapping, and F Centres in Lithium Fluoride Crystals", Journal of Applied Physics, **Vol.41, No:9**, pp. 3687-3697.

[20]- Harris A.M. and Jackson J.H. (1970). "The emission spectrum of thermoluminescence dosimetry grade lithium fluoride",J.Phys.D: Appl.Phys., **3**, pp. 624-627.

[21]- Podgorsak E.B, Moran P.R., and Cameron J.R., (1971). "Thermoluminescent Behaviour of LiF (TLD-100) from 77^0 to 500^0 K", Journal of Applied Physics, **Vol.12, No:7**, pp. 2761-2767.

[22]- Jain V.K., Bapat V.N., and Kathuria S.P., (1973). J.Phys.C: Solid State Phys., **6**, pp. L343-344.

[23]- Crittenden G.C., Townsend P.D., Gilkes J., and Wintersgill, (1974), "LiF dosimetry:II. The effects of Mg and Ti on the thermoluminescent emission spectra of LiF", J.Phys.D: Appl.Phys., **7**, pp. 2410-2421.

[24]- Cook D.W. and Rhodes J.F., (1981). "Thermoluminescence of LiF (TLD-100) in the temperature interval 10-300 K", Journal of Applied Physics, **Vol.52, No:6**, pp. 4244-4247.

147

[25]- Cooke D.W., (1978). "The thermoluminescence mechanism in LiF (TLD-100): Extension of the Mayhugh-Christy model", Journal of Applied Physics, Vol.47, No:7, pp. 4206-4215.

[26]- Fairchild R.G., Mattern P.L., Lengweiler K., and Levy P.W., (1978a). "Thermoluminescence of Lif TLD-100:Emission-spectra measurements", Journal of Applied Physics, Vol.49, No:8, pp. 4512-4522.

[27]- Townsend P.D., Ahmed K., Chandler P.J., McKeever S.W.S., and Whitlow H.J., (1983). "Measurements of the emission spectra of LiF during thermoluminescence", Radiation Effects, 72, pp.245-257.

[28]- McKeever S.W.S., (1984). "Optical absorption and luminescence in lithium fluoride TLD-100", Journal of Applied Physics, Vol.56, No:10, pp. 2883-2889.

[29]- Yuan X.L. and McKeever S.W.S., (1988). "Impurity Clustering Effects in Magnesium-Doped Lithium Fluoride", Phys.Stat.Sol.(a), 108, pp. 545-551.

[30]- Jain V.K., (1986). "Thermoluminescence mechanism in LiF (TLD-100) from 90 to 300 K", J.Phys.D:Appl.Phys., 19, pp. 1791-1807.

[31]- Jain V.K., (1987). "Defect Complexes and Thermoluminescence spectra in Lithium Fluoride at Low Temperatues", Radiation Effects, 102, pp. 95-102.

[32]- Kos H.J. and Nink R., (1980). "Dipole ® Z Centre Conversion in Mg-Doped Lithium Fluoride", Phys.Stat.Sol.(a), 57, pp.203-207.

[33]- Sootha G.D., (1970). "Transition Metal Impurities in Alkali Halides: I. Optical Absorption of 3d Transition Metal Ions", Phys.Stat.Sol.(a), 1, pp. 363-373.

[34]- Rositter M.J., Rees-Evans D.B., Ellis S.C., and Griffiths J.M., (1971). "Titanium as a luminescence center in thermoluminecence lithium fluoride", J.Phys.D:Appl.Phys., 4, pp. 1245-1251.

[35]- Rossiter M.J., Rees-Evans D.B., and Ellis S.C. (1972). "Thermoluminescence in lithium fluoride:apperent activation by manganese", J.Phys.D:Appl.Phys., 5, pp. 1164-1168.

[36]- Davies J.J., (1974). "EPR and ENDOR of titanium-doped lithium fluoride", J.Phys.C:Solid State Phys., 7, pp. 599-609.

[37]- Stobe T.G., Wolfenstine J.B., and Las W.C., (1980). "Titanium-related defects in LiF:Mg,Ti", Journal de Physique, C6, pp. 265-268.

[38]- Cappelletto R., Mora C., Prato S., Calestani G., Földvári I., Kovács L., and Watterich A., (1991). "A New Phase Growth in LiF:Ti and LiF:Mg,Ti", Radiation Effects and Defects in Solids, Vols.119-121, pp.159-164.

[39]- Wintersgill M.C., Townsend P.D., and Cusso-Perez F., (1980). "The Role of Oxygen and Titanium in the Luminescence of LiF:Mg,Ti", Journal de Physique, C7, pp. 123-126.

[40]- Watterich A., Kovács L., Földvári I., and Cravero I., (1983). "Ti Related Defects in LiF:Ti and LiF:Mg,Ti Crystals", Radiation Effects, 75, pp.253-261.

[41]- Vergara I., Diéguez E., Bausá L.E., and Garcia Solé J., (1991). "Growth and optical characterization of titanium-doped LiF", J.Phys.D:Appl.Phys., 24, pp. 622-625.

[42]- He S.S., Merklin J.F., Qiang Sun, Qian Wang, (1994), "Deep Traps in LiF:Mg,Ti", Phys.Stat.Sol.(a), 145, pp. K1-K4.

[43]- Delgado L. and Delgado A., (1984). "Photoluminescence and thermoluminescence of Ti centers in LiF (TLD-100)", Journal of Applied Physics, Vol.55, No:2, pp. 515-518.

[44]- Vora H., Jones J.H., and Stobe T.G., (1975). "Hydroxyl ions and the 200 nm absorption band in Mg- and Ti-doped thermoluminescence LiF single crystals", Journal of Applied Physics, Vol.46, No:1, pp. 71-77.

[45]- Jain S.C. and Sootha G.D., (1967). Phys.Stat.Sol.(a), 22, pp. 505.

[46]- Wachter W., Vana N.J., and Aiginger H., (1980), "The Influence of Hydroxyl Ions on the Thermoluminescence Properties of LiF:Mg,Ti", Nuclear Instruments and Methods, 175, pp. 21-23.

[47]- Wachter W., (1982). "New method for the optimization of thermoluminescence sensitivity in liF:Mg,Ti", Journal of Applied Physics, Vol.53, No:7, pp. 5210-5215.

[48]- Kamikawa T., (1975). Phys.Stat.Sol.(b), 68, pp. 639.

[49]- Stobe T.G and DeWerd L.A., (1985). "Role of hydroxide impurities in the thermoluminescence behavior of lithium fluoride", Journal of Applied Physics, Vol.57, No:6, pp. 2217-2220.

[50]- Watterich A., Földvári I., and Voszka R., (1980). "Colour centres in LiF:Mg crystals", Journal de Physique, C6, pp. 159-162.

[51]- Okhura H., (1964). "Z_2 and Z_3 Color Centers in KCl and KBr", Physical Review, Vol.136, No:2A, pp. A446-A451.

[52]- Radhakrishna S. and Chowdari B.V.R., (1972). "Z-Centers in Rare-Earth Doped Alkali Halides", Phys.Stat.Sol.(a), 12, pp. 557-562.

[53]- Radhakrishna S. and Chowdari B.V.R., (1972). "Z Centers in Impurity-Doped Alkali Halides", Phys.Stat.Sol.(a), 14, pp.11-39.

[54]- Radhakrishna S. and Chowdari B.V.R., (1972), "Thermoluminescence of Z_1-Centers in Rare Earth Doped Alkali Halides", Phys.Stat.Sol.(a), 14, pp. K73-K76.

[55]- Gartia R.K., (1976). "Thermoluminescence Studies of Z_1 Centers in X-Irradiated Ca-Doped NaCl Crystals",Phys.Stat.Sol. (a), 37, pp. 571-578.

[56]- Jackson J.H. and Harris A.M., (1970). "Annealing effects and optical absorption of thermoluminescence lithium fluoride", J.Phys.C:Solid State Phys., 3, pp. 1967-1977.

[57]- Nakajima T., (1971). "Thermoluminescence and colour centres in LiF crystals irradiated at room temperature", J.Phys.C: Solid State Phys., 4, pp. 1060-1068.

[58]- McLaughlin W.L., Miller A., Ellis S.C., Lucas A.C., and Kapsar B.M., (1980). "Radiation-Induced Color Centers in LiF for Dosimetry at High Absorbed Dose Rates", Nuclear Instruments and Methods, 175, pp. 17-18.

[59]- Mort J., (1965). Solid State Communucation, 3, pp. 263.

[60]- Mort J., (1966). Physical Letters, 21, pp. 124.

[61]- Christy R.W., Johnson N.M., and Wilbarg R.R., (1967). "Thermoluminescence and color centers in LiF", Journal of Applied Physics, 38, pp. 2099-2106.

[62]- Klick C.C., Claffy E.W., Gorbics S.G., Attix F.H., Schulman J.H., and Allard J.G., (1967). "Thermoluminescence and Color Centers in LiF:Mg", Journal of Applied Physics, Vol.38, No:10, pp. 3867-3874.

[63] Claffy E.W., (1967). "Preceeding of International conference on Luminescence Dosimetry", AEC Symposium Series, No.8., Stanford University.

[64]- Crittenden G.C., Townsend P.D., and Townshend S.E., (1974). "LiF dosimetry:I.Optical absorption studies of LiF:Mg", J.Phys.D: Appl.Phys., 7, pp. 2397-2409.

[65]- Mayhugh M.R., Christy R.W., and Johson N.M., (1970). "Thermoluminescence and Color Center Correleations in Dosimetry LiF", Journal of Applied Physics, Vol.41, No:7, pp. 2968-2976.

[66]- Mayhugh M.R., (1970). "Color Centers and the Thermoluminescence Mechanism in LiF", Journal of Applied Physics, Vol.41, No:12, pp. 4776-4782.

[67]- Mayhugh M.R. and Christy R.W., (1970). "V$_3$ Band in LiF", Physical Review B, Vol.2, No:8, pp. 3330-3332.

[68]- Christy R.W. and Mayhugh M.R., (1972), Journal of Applied Physics, Vol.43, pp.3216.

[69]- Nink R. and Kos H.J., (1976). "On the Role of Z Centers in the Trapping Mechanism of Thermoluminescence Lithium Fluoride", Phys.Stat.Sol.(a), 35, pp. 121-129.

[70]- Nink R. and Kos H.J., (1976). "An Improved Lithium Fluoride Material for Thermoluminescence Dosimetry", Journal de Physique, C7, pp. 127-131.

[71]- Nink R. and Kos H.J., (1980). "Lithium Fluoride Dosimetry", Nuclear Instruments and Methods, 175, pp.15-16.

[72]- Kos H.J. and Nink R., (1977), "Z_1 Centers in Mg-Doped Lithium Fluoride", Phys.Stat.Sol.(a), 41, pp.K157-K161.

[73]- Kos H.J. and Nink R., (1977). "Mechanism of Restored Thermoluminescence in Lithium Fluoride", Phys.Stat.Sol.(a), 44, pp. 505-510.

[74]- Rao S.M.D., (1980). "Identification of Z_2- and associated Z-centres in LiF Through a correlation of electrical conductivity, ITC and optical absorption measurements", Journal de Physique, C6, pp. 123-125.

[75]- Battaglia C., Bonora S., Cevolani M., Degli Esposti G.C., and Petralia S., (1982). "Thermoluminescence Sensitization in LiF (TLD-100) at Different Post-Annealing Temperatures", Phys.Stat.Sol.(a), 73, pp. K169-K173.

[76]- Gartia R.K., (1977). "Thermoluminescence of Z_3 Centers in X-Irradiated Mg-Doped LiF Crystal", Phys.Stat.Sol.(a), pp. K21-K24.

[77]- Kos H.J. and Nink R., (1979). "Correlation of Thermoluminescence and Optical Absorption of Z_3 Centers in LiF:Mg,Ti Crystals", Phys.Stat.Sol.(a), 56, pp. 593-596.

[78]- Jain V.K. and Kathuria S.P., (1978). "Z_3 Centre Thermoluminescence in LiF TLD Phosphor", Phys.Stat.Sol.(a), 50, pp. 329-333.

[79]- Jain V.K., (1980). "Radiation-Induced Sensitization and UV Effects in Lithium Fluoride TLD Phosphor", Phys.Stat.Sol.(a), 60, pp. 351-356.

[80]- Jain V.K., (1981). "Z_3 Centre Thermoluminescence and Sensitization Mechanism in Lithium Fluoride", Phys.Stat.Sol.(a), 66, pp. 341-346.

[81]- Bapat V.N. and Kathuria S.P., (1981). "Correlation of Optical Absorption and Thermoluminescence in LiF:TLD-100", Phys.Stat.Sol.(a), **66**, pp. K67-K70.

[82]- Jain V.K., Kathuria S.P., and Gaguly A.K., (1974). J.Phys.C: Solid State Phys., **7**, pp. 3810.

[83]- Mehta S.K., and Merklin J.F., and Donnert H.J., (1977). "Thermoluminescence Related Z Centers in LiF:Mg,Ti", Phys.Stat.Sol.(a), **44**, pp. 679-685.

[84]- Jen L.C. and Merklin J.F., (1978). "Optically Induced Dichroism of Z_2-Centers in LiF:Mg,Ti (TLD-100)", Phys.Stat.Sol. (a), **50**, pp. 469-474.

[85]- Merklin J.F., (1978). "Optical Bleaching of Defect Centers in TLD-100 (LiF:Mg,Ti)", Nuclear Instruments and Methods, **157**, pp. 519-523.

[86]- Moharil S.V., (1980). "On the Trapping Centers in LiF TLD-100", Solid State Commun., **33**, pp. 697-700.

[87]- Agulló López F., López F.L., and Jaque F., (1982).Cryst. Lattice Defects Amorph.Mat., **9**, pp. 227.

[88]- Paus H.J. and Strohm K.M., (1980). J.Phys.C:Solid State Phys., **13**, pp. 57.

[89]- Kos H.J. and Takeuchi N., (1980). "On the Radiation Induced Sensitization Mechanism in Lithium Fluoride", Phys.Stat.Sol.(a), **57**, pp. K171-K174.

[90]- Kos H.J., Nink R., and Takeuchi N., (1980). "Growth of Z centers in X-irradiated LiF:Mg", Journal of Materials Science Letters, **15**, pp. 2933-2935.

[91]- Horowitz Y.S., (1982). "Criticism of the Z-Center Model in LiF-TLD", Phys.Stat.Sol.(a), **69**, pp. K29-K32.

[92]- Parfianovich I.A., (1976). Opt.Spectrosc., **41**, pp. 40.

[93]- Lakshmanan A.R., (1984). "Modified Z Centre Model for Thermoluminescence in LiF TLD Phosphor", Radiation Protection Dosimetry, **6**, pp. 52-54.

[94]- Watterich A., Földvári I., Corradi G., and Opyrchal H., (1984). "Comment on the Identification of Z Centres in LiF:Mg and LiF:Mg,Ti Single Crystals", **121**, pp. 117-125.

[95]- Nepomnyashchikh A.I. and Radzhabov E.A., (1980). "Magnesium electron color centers in LiF-Mg crystals" Opt.Spectrosc., **48**, pp. 154-156.

[96]- Radyabov E.A. and Nepomnyachikh A.I., (1981). "Neutral Magnesium Atoms on Anion Sites in LiF", Phys.Stat.Sol.(b), **108**, pp. K75-K78.

[97]- Radyabov E.A. and Nepomnyachikh A.I., (1981). "Magnesium Color Centers at 3.5 amd 5.0 eV in Lithium Fluoride", Phys.Stat. Sol.(a), **68**, pp. 77-81.

[98]- Landreth J.L. and McKeever S.W.S., (1985). "Some observation on the optical absorption bands in LiF:Mg,Ti", J.Phys.D:Appl.Phys., **18**, pp. 1919-1933.

[99]- Caldas L.V.E., Mayhugh M.R., and Stobe T.G., (1983). "Optical absorption and thermoluminescence in LiF TLD-100", Journal of Applied Physics, **Vol.54, No:6**, pp. 3431-3437.

[100]- McKeever S.W.S., (1990), "5.5 eV optical absorption, supralinearity, and sensitization of thermoluminescence in LiF TLD-100", Journal of Applied Physics, **Vol.68, No:2**, pp. 724-731.

[101]- Kathuria S.P., Moharil S.V., and Sunta C.M., (1985). "Some Interesting Observation on the Optical Absorption Spectra, Thermoluminescence and Order of Kinetics of Lithium Fluoride", Nucl.Tracks., **Vol.10, Nos.1/2**, pp. 61-69.

[102]- Lakshmanan A.R. and Bhatt R.C., (1980). "Re-Investigation of the Sensitization Mechanism in LiF TLD-100 Phosphor", Phys. Stat.Sol.(a), **57**, pp. 323-329.

[103]- Chandra B., Lakshmanan A.R., and Bhatt R.C., (1980). "Effect of Deep Traps on the Sensitization in LiF (TLD-100) Phosphor", Phys.Stat.Sol.(a), **60**, pp. 593-598.

[104]- Lakshmanan A.R., Chandra B., and Bhatt R.C., (1982). "On the role Z centres and competing nonluminescent centres in the sensitisation and supralinearity mechanism of LiF TLD-100 phosphor", J.Phys.D:Appl.Phys., **15**, pp. 1501-1517.

[105]- Chandra B., Lakshmanan A.R., and Bhatt R.C., (1982). "Dependence of thermoluminescence sensitivity on temperature of irradiation in LiF (TLD-100) phosphor", J.Phys.D:Appl.Phys., **15**, pp. 1803-1816.

[106]- Lakshmanan A.R., Chandra B., and Bhatt R.C., (1983). "Thermoluminescence of Z Centres in LiF (TLD-100) at Elevated Irradiation Temperature", Phys.Stat.Sol.(a), **75**, pp. 263-272.

[107]- Lakshmanan A.R. and Madhusoodanan, (1993). "Optical Absorption and Thermoluminescence Studies in LiF:Mg,Ti (TLD-100) Single Crystals as a Function of Irradiation Temperature", Phys.Stat.Sol.(a), 139, pp. 229-240.

[108]- Lakshmanan A.R., (1994). "Optical Absoption and Thermoluminescence in LiF:Mg,Ti", Phys.Stat.Sol.(a), 142, pp. 225-236.

[109]- He S.S., (1994). "Mg^{2+} Related Defect Centers in LiF:Mg,Ti", Phys.Stat.Sol.(a), 144, pp. K83-K86.

[110]- Ausin V. and Alvarez Rivas J.L., (1977). "Optically induced F-centre-interstitial recombination in g-irradiated KCl", J.Phys.C:Solid State Phys., 10, pp. 1089-1096.

[111]- Rascón A. and Alvarez Rivas J.L., (1977). "Thermoluminescence and colour centre thermal stability in KCl:Ca and KCl:Sr irradiated ar room temperature", J.Phys.C:Solid State Phys., 10, pp. 1239-1251.

[112]- Moharil S.V. and Kathuria S.P., (1982). "Role of peak IV in the sensitisation of LiF TLD-100", J.Phys.C:Solid State Phys., 15, pp. L997-L1000.

[113]- Moharil S.V., (1984). "On the mobile interstitial model for TL in LiF-TLD 100", J.Phys.C:Solid State Phys., 17, pp. 531-536.

[114]- Sunta C.M. and Watanable S., (1976). "Thermoluminescence of LiF TLD-100 by phototransfer", J.Phys.D:Appl.Phys., 9, pp. 1271-1278.

[115]- Moharil S.V. and Kathuria S.P., (1985). "Evolution of TL and PTTL glow curves in LiF TLD-100", J.Phys.D:Appl.Phys., 18, pp. 691-701.

[116]- Bhasin B.D., Kathuria S.P., and Moharil S.V., (1988). "Some Peculiarities of Photo-Transfer Thermoluminescence in LiF TLD-100", Phys.Stat.Sol.(a), 106, pp. 271-276.

[117]- Kathuria S.P., Bhasin B.D., and Moharil S.V., (1988). "On the mechanism of phototransfer thermoluminescence in LiF TLD-100", J.Phys.D:Appl.Phys., 21, pp. 647-651.

[118]- Delgado A. and Portillo J.C., (1987). "On the presence of the peak IV in the TL and PTTL glow curves of heavily annealed LiF TLD-100", J.Phys.D:Appl.Phys., 20, pp. 661-663.

[119]- Delgado A., Gomez Ros J.M., and Portillo J.C., (1988). "New evidence against the presence of peak IV in the TL and PTTL glow curves of heavily annealed TLD-100", J.Phys.D:Appl.Phys., 21, pp. 1015-1018.

[120]- Delgado A., (1992). "On the hole character of LiF TLD-100 peak IV", J.Phys.D:Appl.Phys., 25, pp.295-296.

[121]- Delgado A., Muñiz J.L., and Gómez Ros J.M., (1994). "On the peculiarities of peak 4 in LiF TLD-100", Radiation Measurements, Vol.23, No:4, pp. 693-701.

[122]- Taylor G.C. and Lilley E., (1978). "The analysis of thermoluminescence glow peaks in LiF (TLD-100)", J.Phys.D:Appl. Phys., 11, pp. 567-581.

[123]- Fairchild R.G., Mattern P.L., Lengweiler K., and Levy P.W., (1978). "Thermoluminescence of LiF TLD-100: Glow-curve kinetics[a]", Journal of Applied Physics, Vol.49, No:8, pp. 4523-4533.

[124]- de Vries W., Hoogenboom J.E., Dielhof J.B., and Bos A.J.J., (1988). "Proc. Symp. Thermoluminescence Dosimetry " Eds Aalbers A.H.L., Bos A.J.J., and Mijnheer B.J., (Bilthoven: NCS) p.31.

[125]- Ben Shachar B. and Horowitz Y.S., (1993). "Long-term Fading of peak 5 in TLD-100 using Computerixed Glow Curve Deconvolution (CGCD) and Thermal Peak Isolation Techniques" Radiation Protection Dosimetry, 47, No:1/4, pp. 181-185.

[126]- Bos A.J.J., Piters T.M., de Vries W., and Hoogenboom J.E., (1990). "Comparative study of trapping parameters of LiF (TLD-100) from different production batches", Radiation Protection Dosimetry, 33, pp.7.

[127]- Bos A.J.J., Vijverberg R.N.M., Piters T.M., and McKeever S.W.S., (1992). "Effect of cooling and heating rate on the trapping parameters in LiF:Mg,Ti crystals", J.Phys.D:Appl.Phys., 25, pp. 1249-1257.

[128]- Bos A.J.J. and Piters T.M., (1993). "Study of Aging Effects in LiF:Mg,Ti by Analysis of Thermoluminescence Glow Curves", Nucl. Tracks Radiat. Meas., Vol.21, No:1, pp. 163-167.

[129]- Yossian D., Mahajna S., Ben Shachar B., and Horowitz Y.S., (1993). "Re-investigation of the Kinetic Trapping Parameters of Peak 5 in TLD-100 via 'Prompt' and 'Residual' Isothermal Decay", Radiation Protection Dosimetry, 47, pp. 129-133.

[130]- Horowitz Y.S., Ben Shachar B., and Yossian D., (1993). "Study of the long-term stability of peaks 4 and 5 in TLD-100: correlation with isothermal decay measurements at elevated temperatures", J.Phys.D:Appl.Phys., 26, pp. 1475-1481.

[131]- McKeever S.W.S., (1980). "Thermoluminescence in LiF: Analysis of the Glow-Curves", <u>Nuvlear Instruments and Methods</u>, **175**, pp. 19-20.

[132]- Kathuria S.P. and Sunta C.M., (1979). "Kinetics and trapping parameters of thermoluminescence in LiF TLD-100-dependence on dose", <u>J.Phys.D:Appl.Phys.</u>, **12**, pp. 1573-1587.

[133]- Kathuria S.P. and Sunta C.M., (1982). "Order of kinetics for thermoluminescence in LiF TLD-100", <u>J.Phys.D:Appl.Phys.</u>, **15**, pp. 497-505.

[134]- Kathuria S.P. and Moharil S.V., (1983). "Trapping parameters for peak IV in LiF TLD-100", <u>J.Phys.D:Appl.Phys.</u>, **16**, pp. 1331-1341.

[135]- Kathuria S.P. and Moharil S.V., (1983). "Trapping parameters for peak XII in LiF TLD-100", <u>J.Phys.D:Appl.Phys.</u>, **16**, pp. 2011-2016.

[136]- Sunta C.M. and Kathuria S.P., (1983). "Order of kinetics for thermoluminescence in LiF (TLD-100)", <u>J.Phys.D:Appl.Phys.</u>, **16**, pp. L163-L164.

[137]- Lilley E. and and Taylor G.C., (1981). "Order of Kinetics for Thermoluminescence in LiF TLD-100", <u>J.Phys.D:Appl.Phys.</u>, **14**, pp. L13-L15.

[138]- Lilley E. and McKeever S.W.S., (1983). "On the order of kinetics for thermoluminescence in LiF TLD-100", <u>J.Phys.D:Appl. Phys.</u>, **16**, pp. L39-L44.

[139]- Delgado A. and Gomez Ros J.M., (1988). "An interpretation of the isothermal decay associated with peaks IV and V in the TL of LiF TLD-100", <u>J.Phys.D:Appl.Phys.</u>, **21**, pp. 652-656.

[140]- Delgado A. and Gomez Ros J.M., (1990). "Evolution of TLD-100 glow peaks IV and V at elevated ambient temperatures", J.Phys.D:Appl.Phys., 23, pp. 571-574.

[141]- Delgado A., Gómez Ros J.M., and Muñiz J.L., (1991). "High ambient temperature effects in LiF TLD-100", J.Phys.D:Appl.Phys., 24, pp. 1126-1130.

[142]- Gartia R.K. and Dorendrajit Singh S., (1993). "Analysis of Peak V of LiF TLD-100 by Curve Fitting", Phys.Stat.Sol.(a), 135, pp. K83-K86.

[143]- Dorendrajit Singh S. and Gartia R.K., (1993), "A new interpretation of the thermoluminescence and isothermal decay of LiF TLD-100", J.Phys.D:Appl.Phys., 26, pp. 119-123.

[144]- Randall J.T. and Wilkins M.H.F., (1945). "Phosphorescence and Electron Traps I. The Study Of Trap Distributions", Proc.R. Soc.A, A184, pp. 366-389.

[145]- Chen. R., (1969). "Glow-Curves with General Order Kinetics", J.Electro.Soc., Vol.116, No:9, pp. 1254.

[146]- Chen R., (1969). "On the Calculation of the Activation Energies and Frequency Factors from Glow-Curves", Journal of applied Physics. Vol.40, pp.570.

[147]- Delgado A. and Barreiro J.C., (1986). Radiation Protection Dosimetry, 16, pp. 295-300.

[148]- Yossian D. and Horowitz Y.S., (1995), "Computerized glow curve deconvolution applied to the analysis of the kinetics of peak 5 in LiF:Mg,Ti (TLD-100)", J.Phys.D:Appl.Phys., 28, pp. 1495-1508.

[149]- Chen R., McKeever S.W.S. and Durrani S.A., (1981)., Phys.Rev. B, **24**, pp. 4931.

[150]- Adirovitch E.I., (1956), J.Phys.Rad., **17**, pp. 705.

[151]- Haering R.R. and Adams E.N., (1960), Phys.Rev., **117**, pp. 451.

[152]- Halperin A. and Braner A.A., (1960), "Evaluation of Thermal Activation Energies from Glow Curves", Phys.Rev., **117**,pp. 405-415.

[153]- Bull R.K., McKeever S.W.S., Chen R., Mathur V.K., Rhodes J.F. and Brown M.D., (1986), "Thermoluminescence kinetics for multipeak glow curves produced by the release of electrons and holes", J.Phys.D:Appl.Phys., **19**, pp.1321-1334.

[154]- Dharamsi A.N. and Joshi R.P., (1991), "An approximate rate equation analysis for bleaching and excitation of thermoluminescence", J.Phys.D:Appl. Phys., **24**, pp.982-987.

[155]- Sakurai T., (1995), "New method for numerical analysis of thermoluminescence glow curves", J.Phys.D:Appl.Phys., **28**, pp.2139-2143.

[156]- Randall J.T. and Wilkins M.H.F., (1945), "Phosphorescence and electron traps II. The interpretarion of long-period phosphorescence", Proc.R. Soc.A, **A184**, pp. 390-407.

[157]- Garlick G.F.J. and Gibson A.F., (1948), "The electron trap mechanism of luminescence in sulphide and silicate phospors" Proc.Phys.Soc., **60**, pp.574-590.

[158]- May C.E. and Partridge J.A., (1964), "Thermoluminescent kinetics of alpha irradiated alkali halides", J.Chem.Phys., **40**, pp. 1401.

[159]- Bohun A., (1954), "Thermoemission and photoemission of NaCl", Czech.J.Phys., **4**, pp. 91-93.

[160]- Booth A.H., (1954), "Calculation of electron trap depths from thermoluminescence maxima", Can.J.Chem., **32**, pp- 214-215.

[161]-Hoogenstraaten W., (1958), "Electron traps in zinc-sulpide", Philips Res.Rep. **13**, pp- 515-523.

[162]- Chen R. and Winer A., (1970), "Effects of various heatinh rates on glow-curves", Journal of Applied Physics **41**, pp- 5227-5232.

[163]- Grossweiner L.I., (1953) " A note on the analysis of first-order glow curves", Journal of Applied Physics, **24**, pp- 1306-1307.

[164]- Lushchik C.B., (1956), "The investigation of trapping centers in crystals by the method of thermal bleaching", Sov.Phys. JEPT, **3**, pp- 390-395.

[165]- Oberhofer M. and Scharmann A., (1981), Applid Thermoluminescence Dosimetry, Adam Hilger Press, Bristol.

[166]- Aitken M.J., (1988), Thermoluminescence Dating, Acadamic Press, London.

[167]- Lax M., (1952), "The Franck-Condon Principle and its application to crystals", J.Chem.Phys.,**20**, pp.1752-1760.

[168]- Schulman J.H. and Compton W.D., (1962). Color center in Solids, Pergamon press, Oxford.

[169]- Dawson R.K. and Pooley D., (1969), Phys.Stat.Sol. (a), **35**, p.95.

[170]- 9010 Optical Dating System User Manual, Dec.1993.

[171]- Model 3500 Manual TLD Reader User's Manual, July 30 1994, Publication No 3500-0-U-0793-005.

[172]- Model 7800 Spectrophotometer Instruction Manual, Japan Spectroscopic Co.,LTD. July 1987.

[173]- Mohan N.S. and Chen R., (1970). "Numerical Curve Fitting for calculating Glow Parameters", J.Phys.D:Appl.Phys., 3, pp. 243-247.

[174]- Shenker D. and Chen R., (1971). "Numerical Curve Fitting of General Order Kinetics Glow Peaks", J.Phys.D:Appl.Phys., 4, pp. 287-291.

[175]- Shenker D. and Chen R., (1972). "Numerical Solution of the Glow Curve Differential Equations", J.Comp.Phys., 10, pp. 272-283.

[176]- Hoogenboom J.E.,de Vries W., Dielhof J.B., and Bos A.J.J., (1988), "Computerized Analysis of Glow Curves from Thermally Activated Processes", Journal of Applied Physics, Vol.64, No:6, pp. 3193-3200.

[177]- Vana N. and Ritzinger G., (1984). "Analysis of TL Glow Curves in differently doped LiF:Mg,Ti", Radiation Protection Dosimetry, Vol.6, No:1-4, pp. 29-32.

[178]- Moscovitch M., Horowitz Y.S., and Oduka J., (1984). "LiF Thermoluminescence Dosimetry First Order Kinetics Glow Curve Analysis", Radiation Protection Dosimetry, Vol.6, No:1-4, pp. 157-159.

[179]- Horowitz Y.S. and Moscovitch M., (1986). "Computerized Glow Curve Deconvolution applied to High Dose (10^2-10^5 Gy) Dosimetry", Nucl.Instrum.Methods, A243, pp. 207-214.

[180]- Horowitz Y.S., Moscovitch M., and Wilt M., (1986). "Computerized Glow Curve Deconvolution applied to Ultralow Dose LiF Dosimetry", Nucl.Instrum.Methods, A244, pp. 556-564.

[181]- Bacci C., Bernardini P., Di Domenico A., Furetta C., and Rispoli B., (1990). "Analysis of Thermoluminescence Kinetics of $CaF_2(Tm)$ Peaks with Glow Curve Deconvolution", Nucl.Instrum.Methods, A286, pp. 295-300.

[182]- Borchi E., Bruzzi M., and Furretta C., (1991). "Deconvolution of $BaSO_4$:Eu TL Glow Curve", IEEE Trans.Nucl.Sc., Vol.38, No:2, pp. 877-882.

[183]- Perks C.A. and Marshall M., (1991). "Techniques for Thermoluminescence Glow Curve Analysis", Radiation Protection Dosimetry, Vol.38, No:4, pp.261-269.

[184]- Bos A.J.J., Piters T.M., Gómez Ros J.M., and Delgado A., (1993). "GLOCANIN, an Intercomparision of Glow Curve Analysis Computer Programs", IRI-CIEMAT Report 131-93-005 (IRI, Delft).

[185]- Balian H.G. and Eddy N.W., (1977). "Figure-of-Merit (FOM), an Improved Criterion over the Normalized Chi-Squared Test for Assessing Goodness-of-Fit of Gamma-Ray Spectra Peaks", Nucl. Instrum.Methods, 145, pp. 389-395.

[186]- Misra S.K. and Eddy N.W., (1979). "IFOM, a Formula for Universal Assessment of Goodness-of-Fit of Gamma Ray Spectra", Nucl.Instrum.Methods, 166, pp. 537-540.

[187]- Ben Shachar B. and Horowitz Y.S., (1991). "Anomalous thermally induced fading of annealed and unannealed LiF:Mg,Ti (TLD-100, Harshaw) using computerized glow curve deconvolution", J.Phys.D:Appl.Phys., 24, pp. 1649-1657.

[188]- Grant R.M. Stowe W.S. and Correll I., (1968). Proc.2nd Int. Conf. Luminescence Dosimetry, pp.613-622.

[189]- Mason E.W., McKinlay A.F. and Clark I., (1976), Phys.Med.Biol., **21**, pp.60-66.

[190]- Horowitz Y.S., (1984), Thermoluminescence and Thermoluminescence Dosimetry , Vol.1, ed. Horowitz Y.S. (Boca Raton, FL-CRC Press) Ch.3, p.89.

[191]- Azorin J., Furretta C. and Scacco A., (1993), "Preparation and properties of thermoluminescence materials", Phys.Stat.Sol. (a), **138**, pp.9-45.

[192]- McKeever S.W.S., (1985), Thermoluminescence of Solids, Cambridge University Press, Cambridge.

[193]- Piters T.M. and Bos A.J.J., (1993), "A model for the influence of defect interactions during heatinh on thermoluminescence in LiF:Mg,Ti (TLD-100)", J.Phys.D: Appl.Phys., **26**, pp.2255-2265.

[194]- Townsend P.D. and Kirsh Y., (1989), Contempt.Phys., **30**, p.337.

[195]- McKeever S.W.S., (1990), "Thermoluminescence in the alkali halides", Radiat.Prot.Dosim., **33**, pp.83-105.

[196]-Chen R. and Kirsh Y., (1981), Analysis of Thermally Stimulated Processes, Pregamon press, Oxford.

[197]-Passler R., (1978), Phys.Stat.Sol. (b), **85**, p.203.

[198]-Mahesh K. Weng P.S. and Furetta C., (1989), Thermoluminescence in Solids and its Applications, Nuclear Technology Publishing, Ashford.

[199]- Piters T.M. Meulemans W.H., and Bos A.J.J., (1993), "An automated research facility for measuring thermoluminescence emission spectra using an optical multichannel analyzer", Rev.Sci.Instrum., 64, pp.109-117.

[200]- Piters T.M. and Bos A.J.J., (1993), "Thermoluminescence emission spectra of LiF (TLD-100) after different thermal treatments", Radiation Protection Dosimetry, 47, pp.91-94.

CURRICULUM VITAE

The author was born in Agin/ELAZIG, in December, 1966. He graduated from the primary, secondary and high schools in Agin, in 1978, 1981 and 1984, respectively. He received the B.S. degree from Middle East Technical University, Gaziantep Extension Campus, Faculty of Engineering, Department of Physics Engineering in 1990. He started to work as research assistant in the Department of Engineering Physics, University of Gaziantep in the same year. He also received the M.S. degree from the Department of Engineering Physics, University of Gaziantep in 1993. In 1993, he was accepted to the Ph.D. program in the Department of Engineering Physics, University of Gaziantep.

He married in November, 1990 by Hatice and he has still two beautiful girls Busra and Beyza.